Avalanche statistics, nonlinear dynamics, and self-affine roughening of ferroelectric domain walls during polarisation switching

Patrycja Paruch
DQMP, University of Geneva

ferro.unige.ch

UNIVERSITÉ DE GENÈVE
FACULTÉ DES SCIENCES
Département de physique de la matière quantique

Elasticity + disorder : simple ingredients…

ferroelectric domain walls

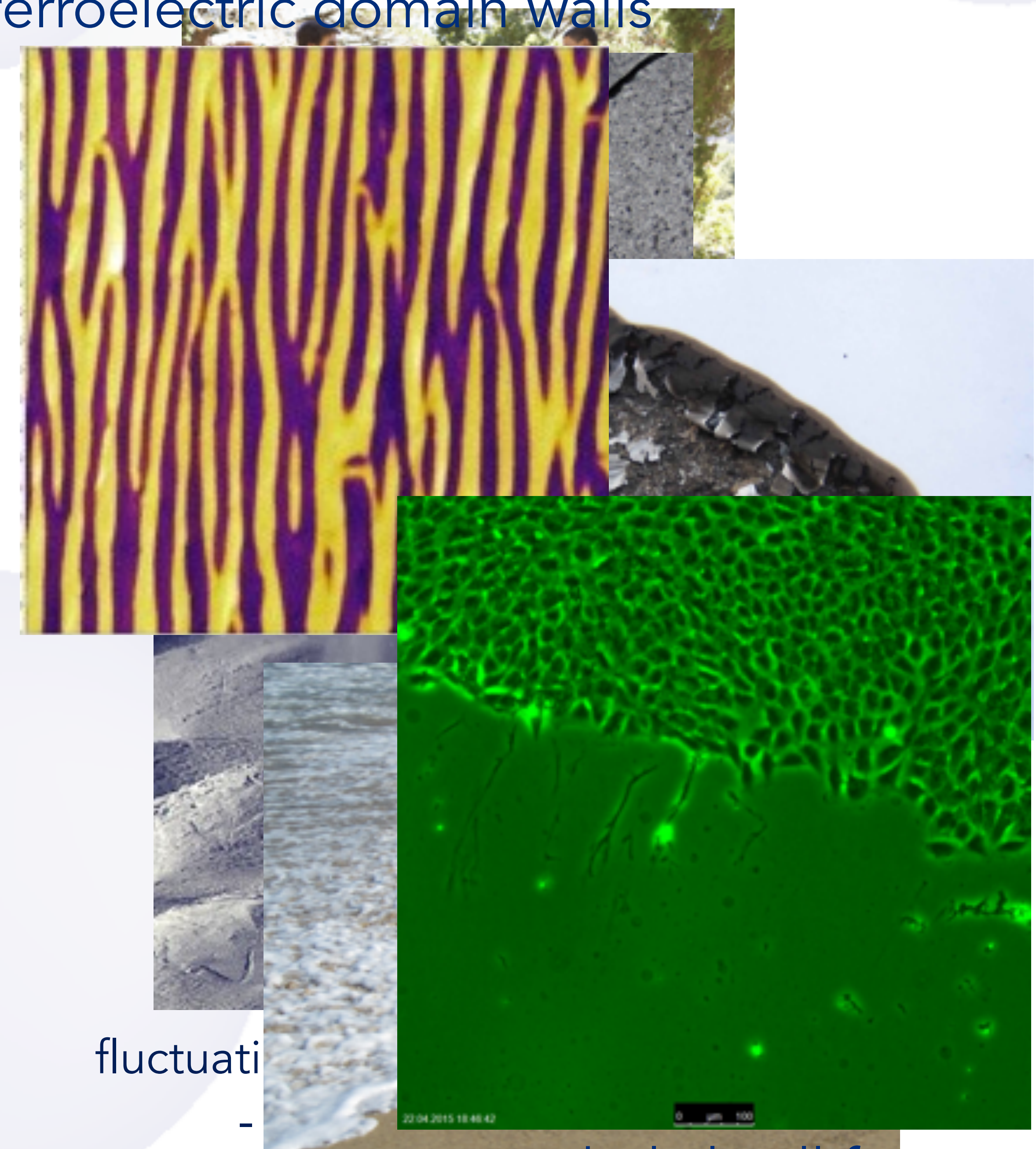

fluctuati

-

epithelial cell fronts

many metastable states, glassy behaviour

statics: self-similarity, scaling laws

dynamics: universality, scaling laws, nonlinear

out-of-equilibrium, ageing, thermal effects

… of complex physics

interfaces separate regions with different properties

diverse interfaces show common dynamics and geometric properties

Ferroelectrics - late to the party

"dawn of humanity"
Louis Néel 1948
Ferromagnetism

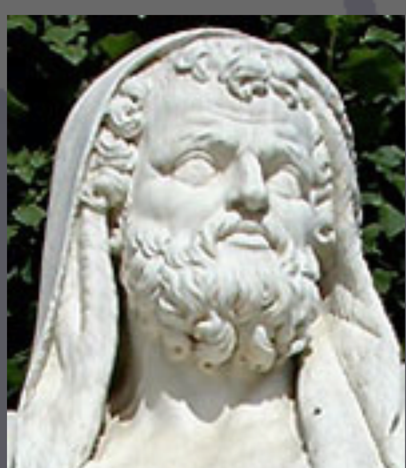

Theoprastus 314 BC
Carl Linnaeus 1747
Pyroelectricity
heat - electricity

Pierre Seignette 1675, La Rochelle

Pierre Curie 1880s

Piezoelectricity
strain - electricity

Joseph Valasek 1920

Ferroelectricity

spontaneous
switchable
electric polarization

Ferroelectrics - late to the party

ABO_3

$P = 10 \mu C/cm^2 = 6.2 \times 10^{13}$ charges/cm^2

$KNaC_4H_4O_6 \cdot 4H_2O$

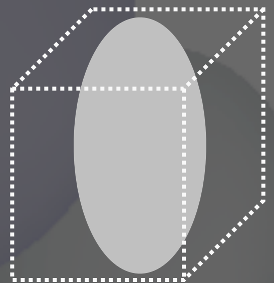

paraelectric

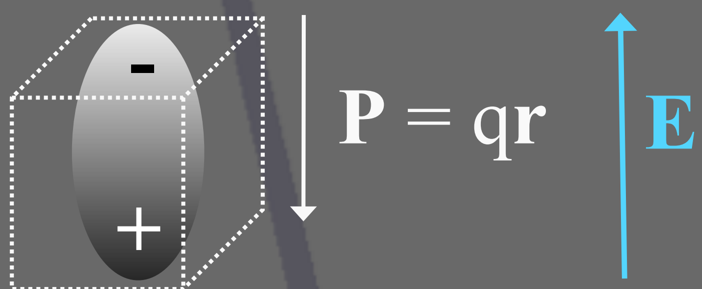

Pyroelectricity

heat - electricity

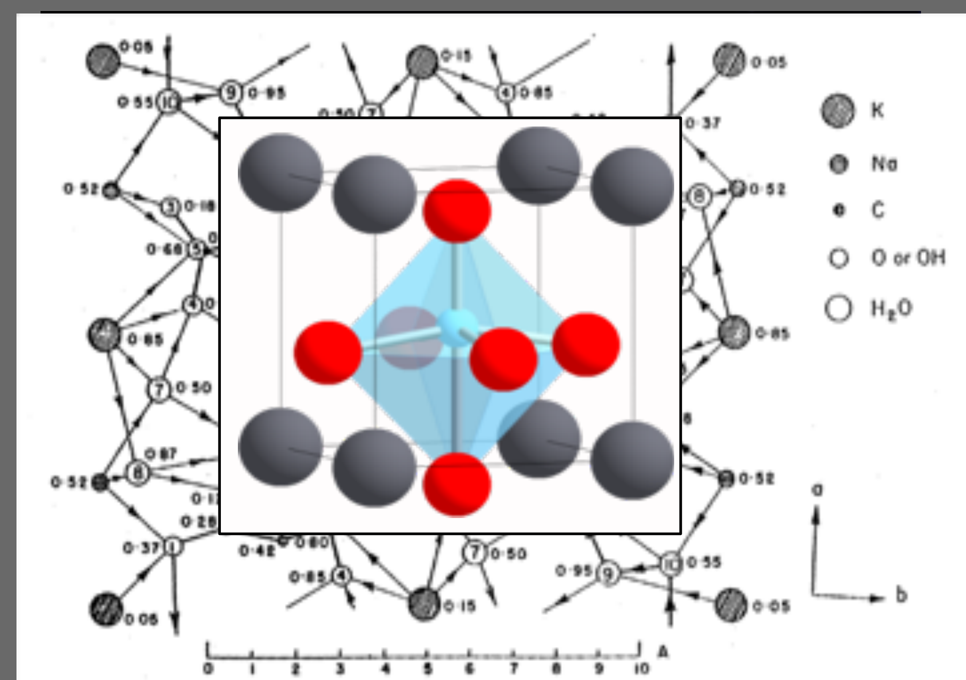

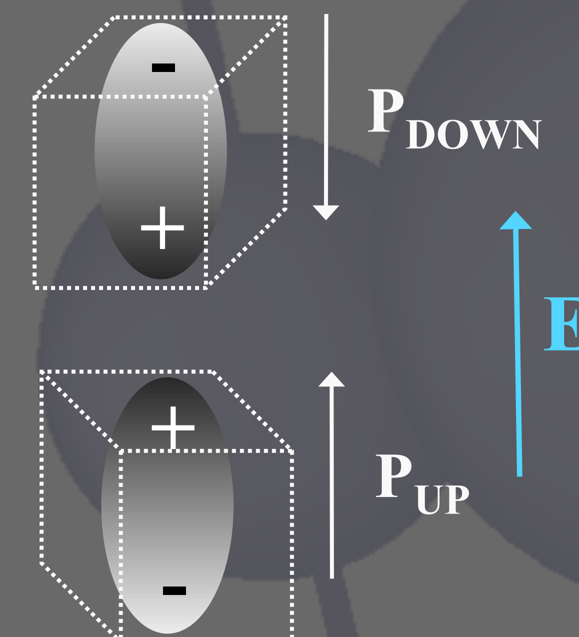

Ferroelectricity

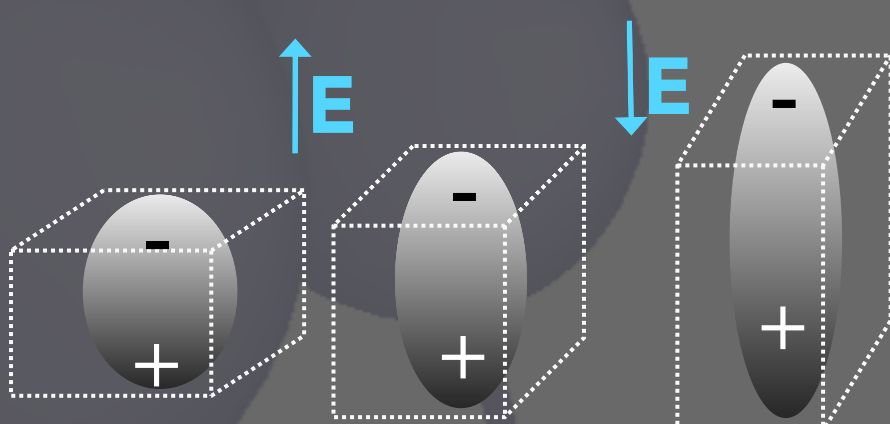

$\Delta X_j = d^t_{ij} E_i$

Piezoelectricity

strain - electricity

compression

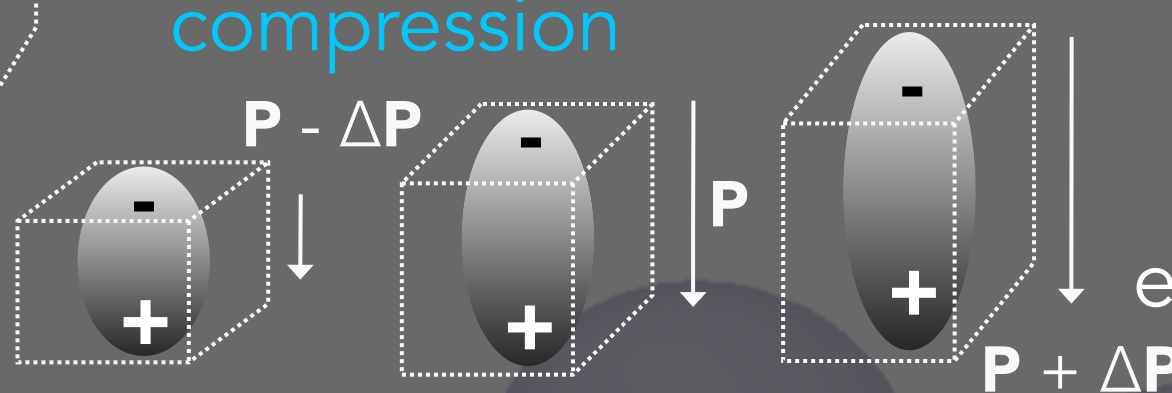

tension

$\Delta P_j = d_{ij} T_i$

spontaneous

switchable

electric polarization

Instabilities in ABO_3 perovskites

$$R_A + R_O = \sqrt{2}(R_B + R_O)$$

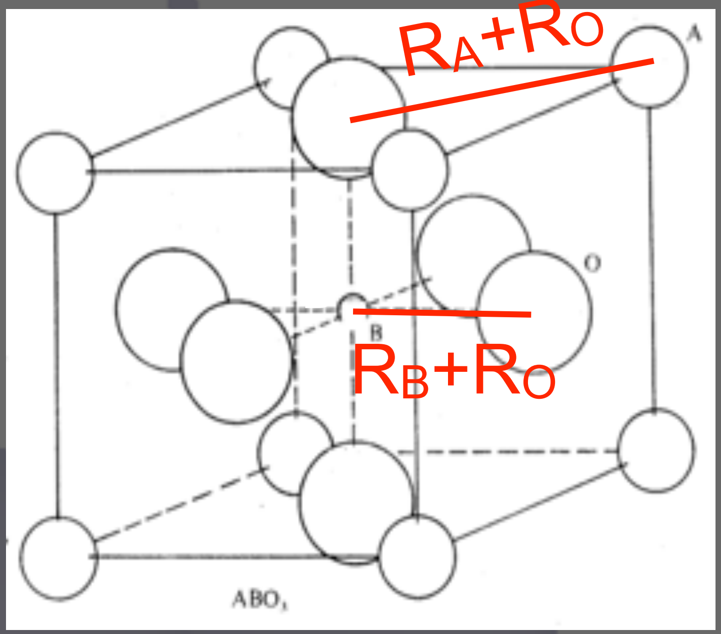

ideal perovskite structure
t = 1

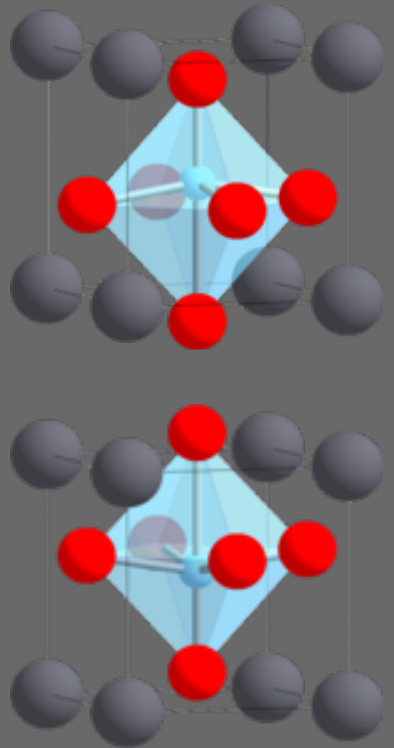

t > 1

$BaTiO_3$

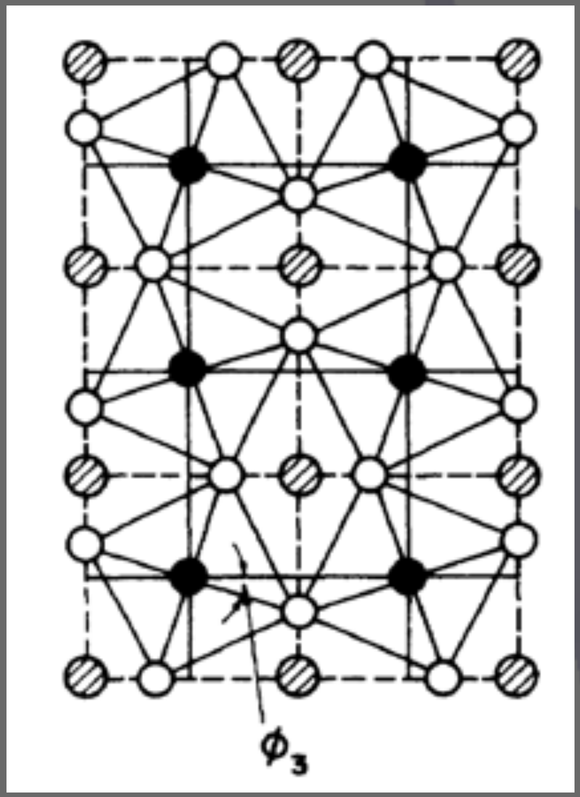

t < 1

$CaTiO_3$

Goldsmith's criterium

tolerance factor $$t = \frac{R_A + R_O}{\sqrt{2}(R_B + R_O)}$$

Origin of the ferroelectric instability

<u>Cochran's model:</u>

Competition between SR and LR forces

$$\langle\eta|\, \mathbf{D}\, |\eta\rangle = \langle\eta|\, \mathbf{D}^{SR}\, |\eta\rangle + \langle\eta|\, \mathbf{D}^{LR}\, |\eta\rangle$$

$$\omega^2 \qquad \omega_{SR}^2 \qquad \omega_{LR}^2$$

$$<0 \qquad >>0 \qquad <<<0$$

SR interactions
Function of the
Chemical bond
Pauli repulsion
. . .

LR Coulomb forces
Dipole-dipole
interaction

positive curvature $\omega^2 > 0$

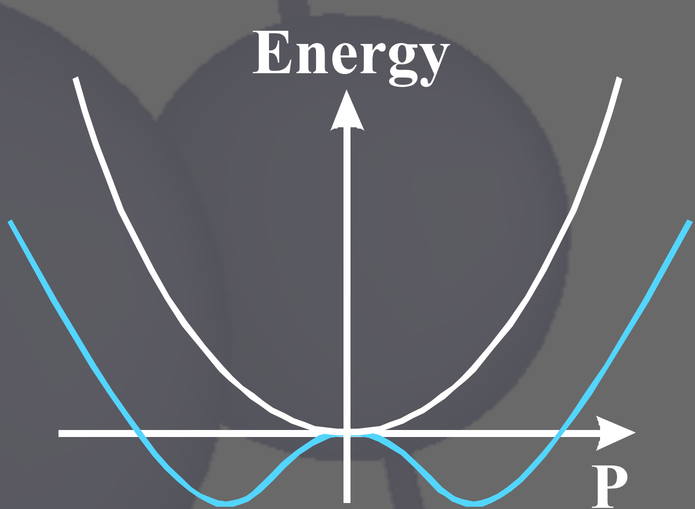

negative curvature $\omega^2 < 0$

DFT calculations of $BaTiO_3$ phonon modes

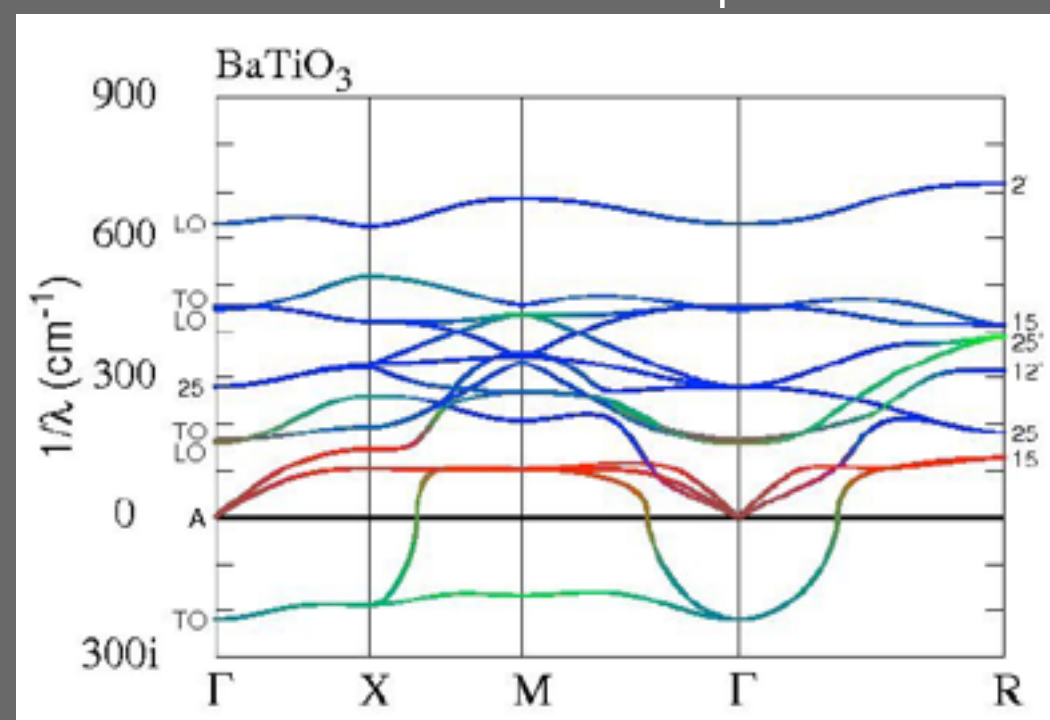

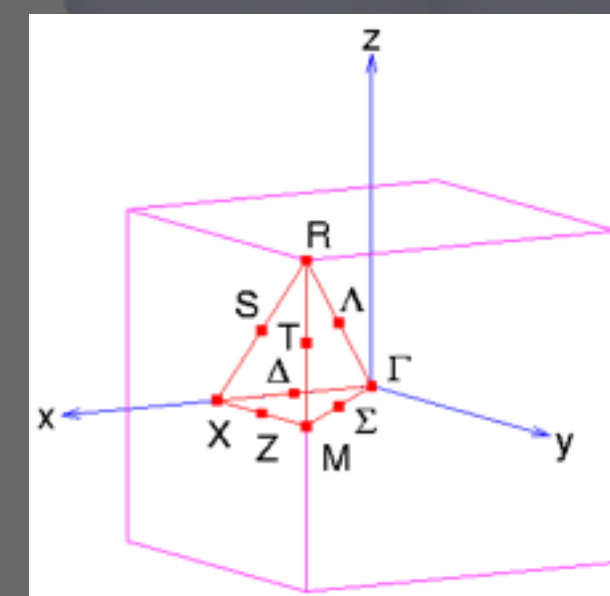

Ghosez et al, PRB **60** 836 (1999)

Pattern of lattice distortion associated with instability (soft phonon mode) freezes in at T_C

Slide after Ph. Ghosez

Landau-Ginzburg-Devonshire

$$U = \frac{\alpha}{2}P^2 + \frac{\gamma}{4}P^4 + \frac{\delta}{6}P^6 - EP$$

$$\alpha = \beta(T - T_c)$$

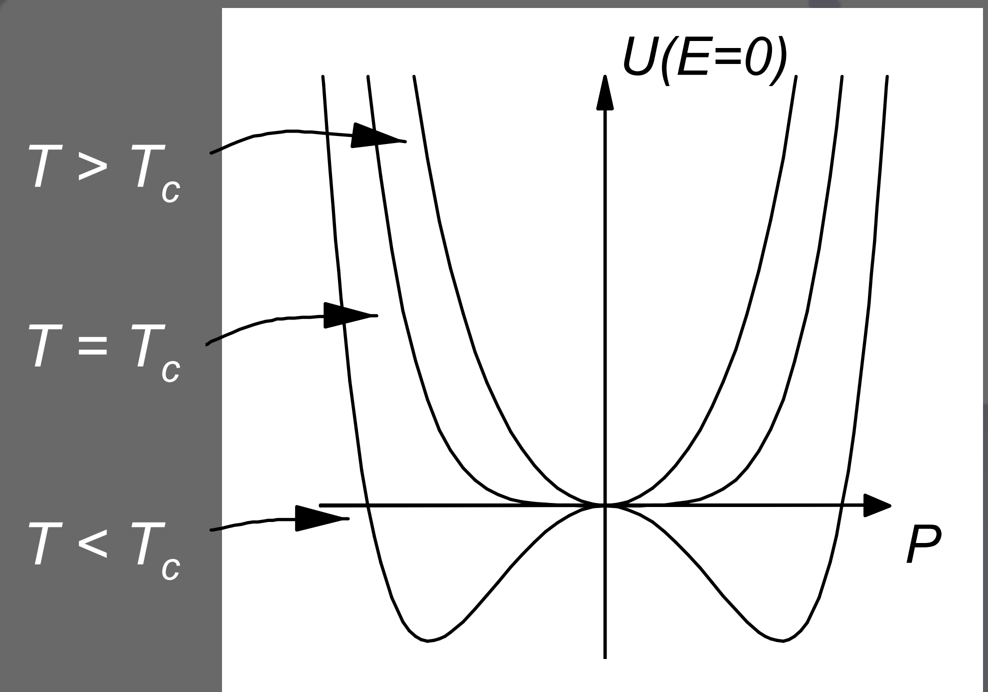

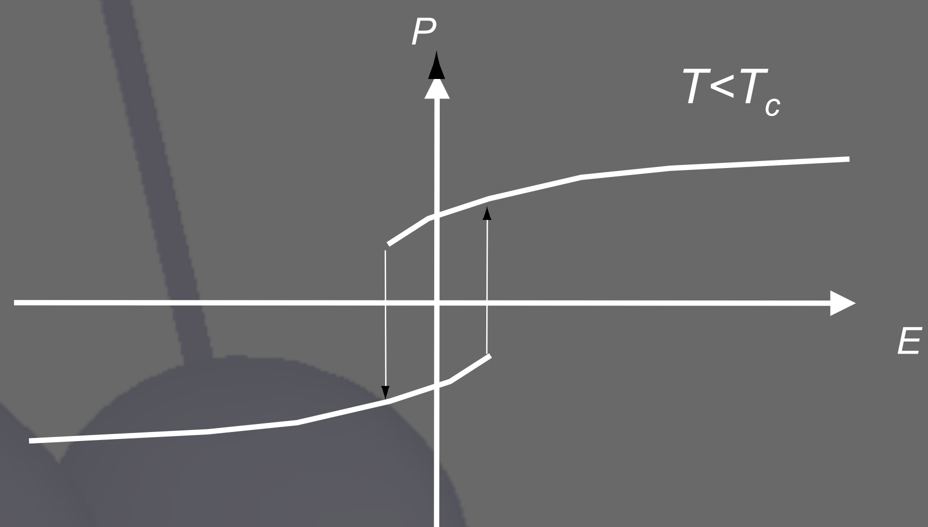

$$\kappa^{X,T} = \beta(T - T_c), T > T_c$$
$$\kappa^{X,T} = 2\beta(T_c - T), T < T_c$$

$$P_S^2 = \frac{\beta}{\gamma}(T_c - T)$$

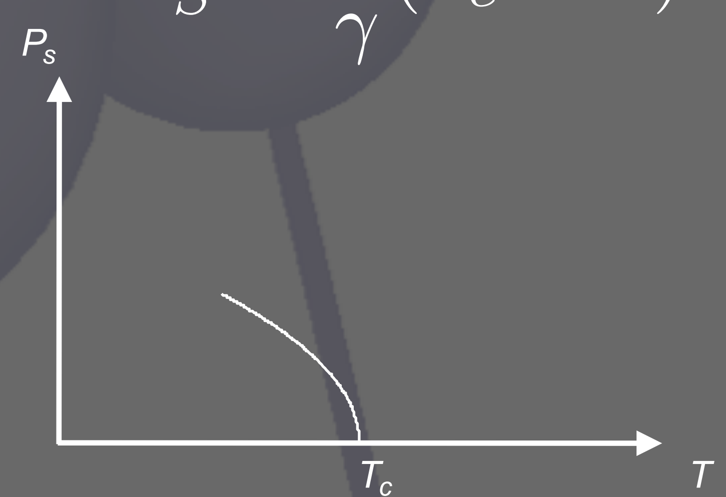

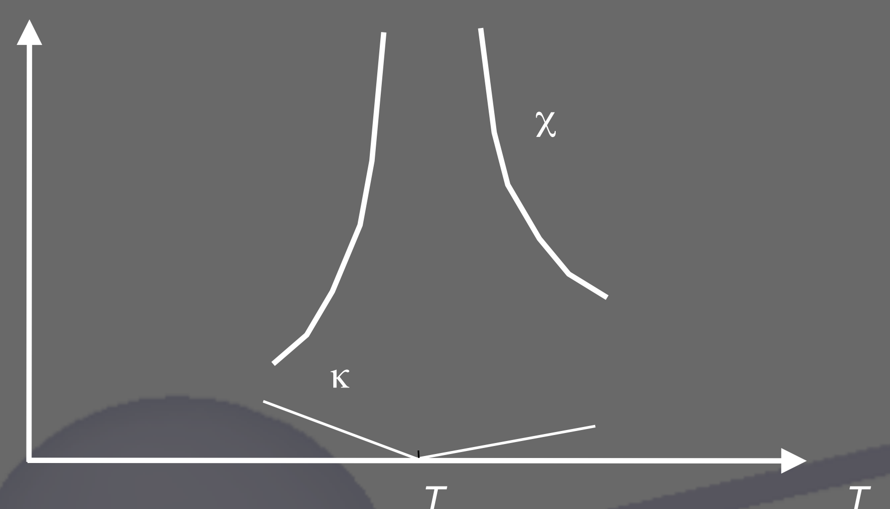

Phenomenological theory of ferroelectricity

Ferroelectricity vs Ferromagnetism

Similarities

- Order parameter decreases with T until transition to para- state
- Coupling between strain and order parameter → piezo- effects
- Large susceptibilities to applied fields (electric/magnetic)
- Order parameter - Field hysteresis useful for storage applications

Differences

FE: off-center ionic displacements caused by long rage interactions → space inversion symmetry breaking

FM: net electronic angular momentum due to spin-spin exchange energy → time inversion symmetry breaking

electric monopoles : screening / electric boundary conditions

collective phenomenon : size, lattice, strain effects

Energy considerations in domain formation

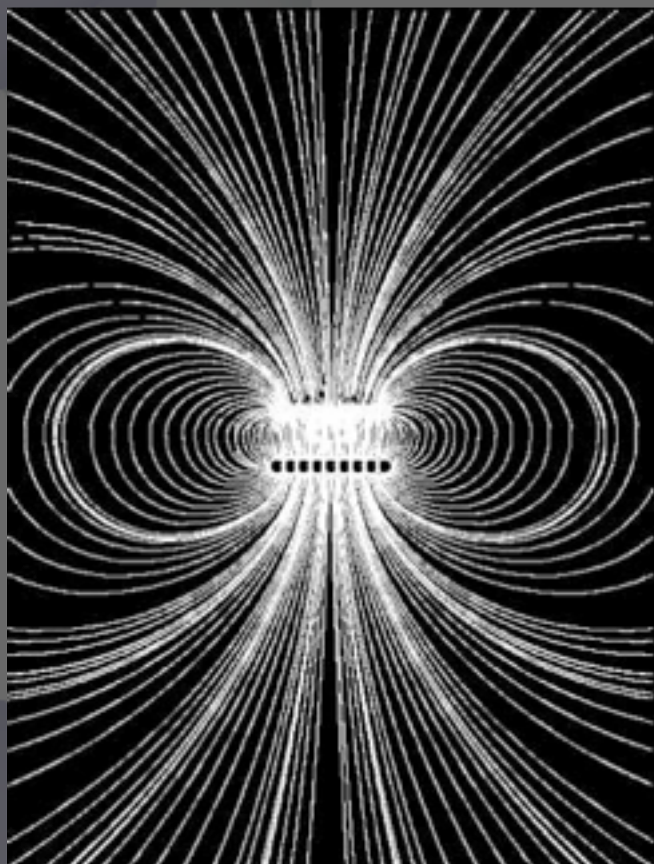

Boundary conditions: screening, dead layers, symmetry

⇒ depolarising field $E = -P/\varepsilon$

⇒ domains

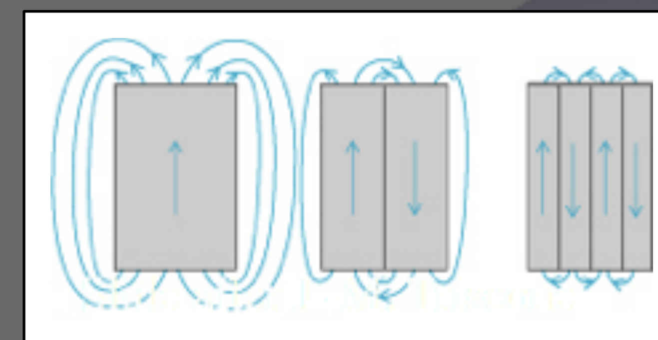

Energy densities per unit area of film $U_{domain} \sim \sigma_{DP} w$

$$U_{DW} \sim \sigma_{DW} N d \sim \sigma_{DW} d/w$$

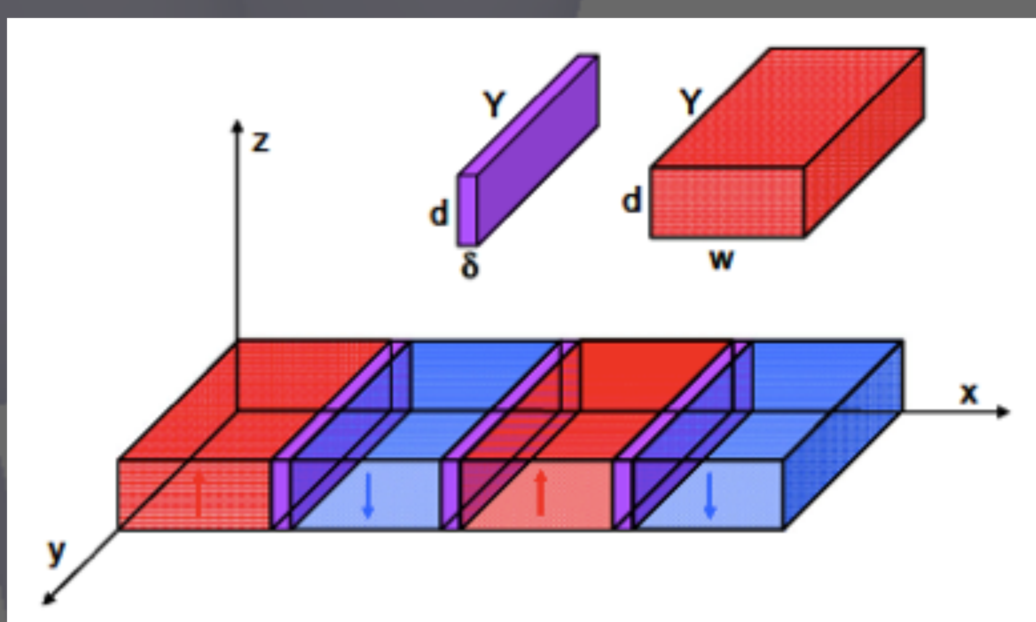

Catalan, Rev. Mod. Phys., **84**, 119 (2012)

Minimising total energy

$$w = \left(\frac{\sigma_{DW}}{\sigma_{DP}} d \right)^{1/2}$$

Landau-Lifshitz-Kittel scaling

Landau and Lifshitz, Phys. Zeits. Sowjetunion **8**, 153 (1935)
Kittel, Phys. Rev., 70, 965 (1946)

Domain walls in ferroic materials

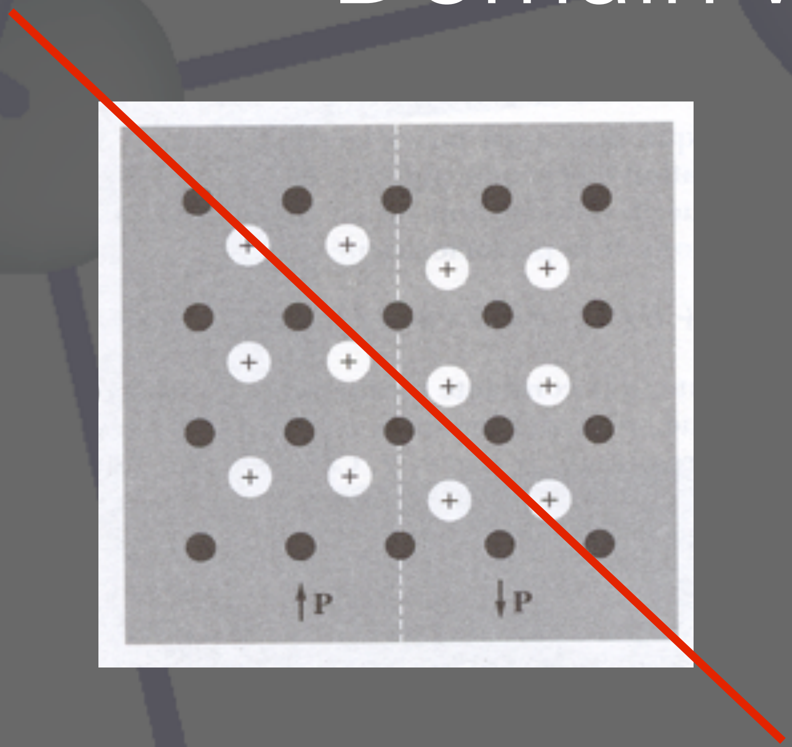

Actual physical objects with a finite (very small) width

FE DWs

atomic displacements in lattice

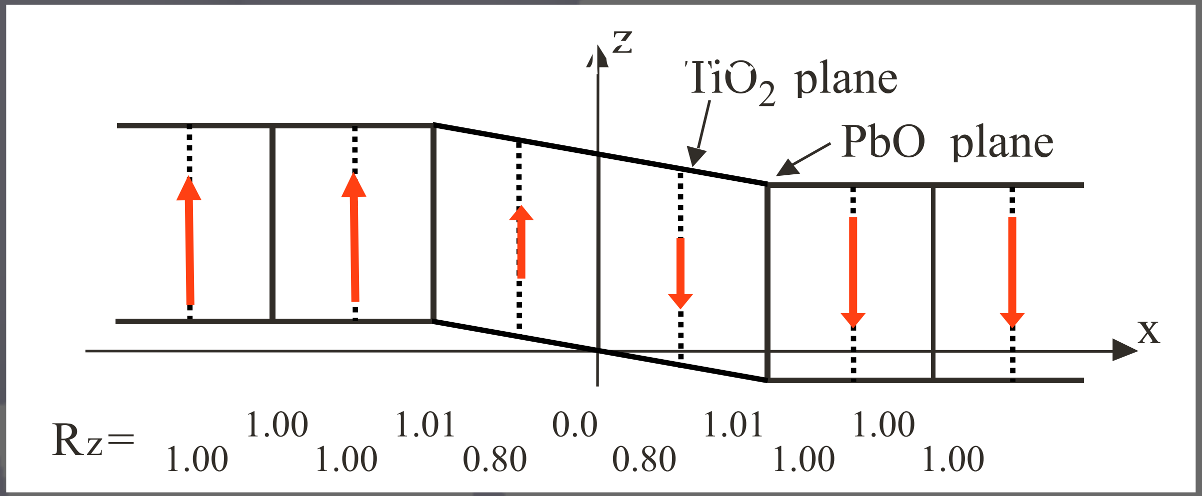

Meyer and Vanderbilt PRB **65**, 104111 (2002)

(O) 1 nm

FM DWs

Bloch or Néel walls

magnetization rotation

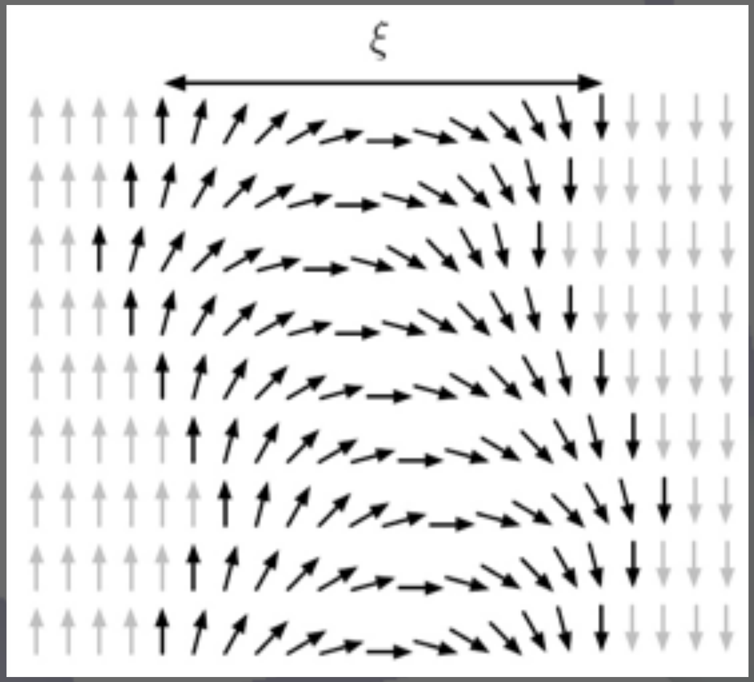

(O) 10-100 nm

Domain walls in ferroelectric materials

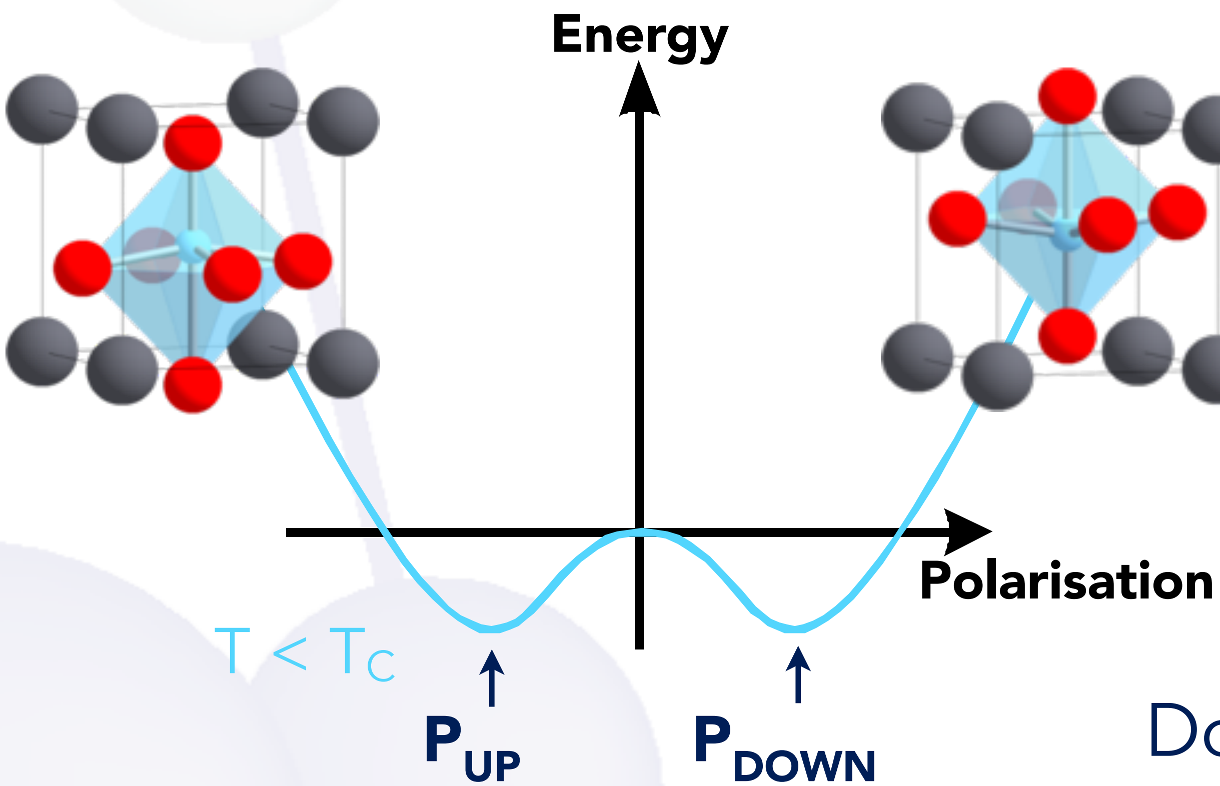

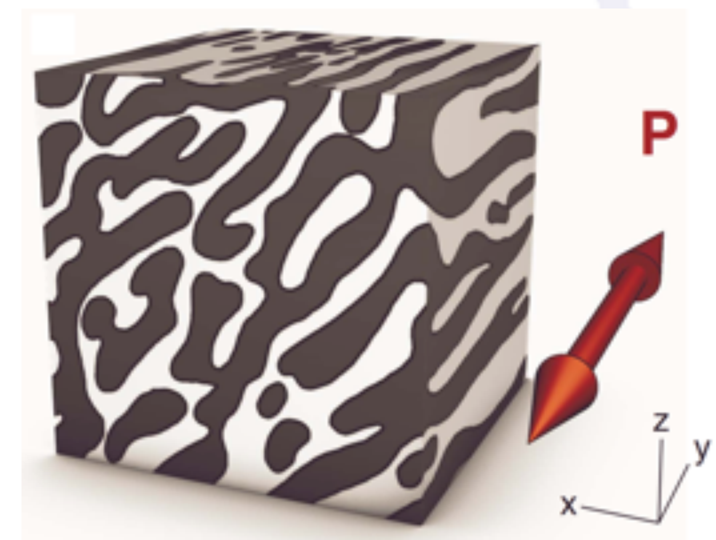

Domain walls separate regions with different polarisation orientation
- and can alter or enhance material properties

Catalan et al. Rev. Mod. Phys., 84, 119 (2012)
D. Damjanovic: Ferroelectric Domain Walls

As samples get thinner, more domain walls can be expected

Landau, Lifshitz, Phys. Zeits. Sowjetunion 8, 153 (1935)
Kittel, Phys. Rev., 70, 965 (1946)

$$w = \left(\frac{\sigma_{DW}}{\sigma_{DP}} d \right)^{1/2}$$

Complex polarisation textures at domain walls

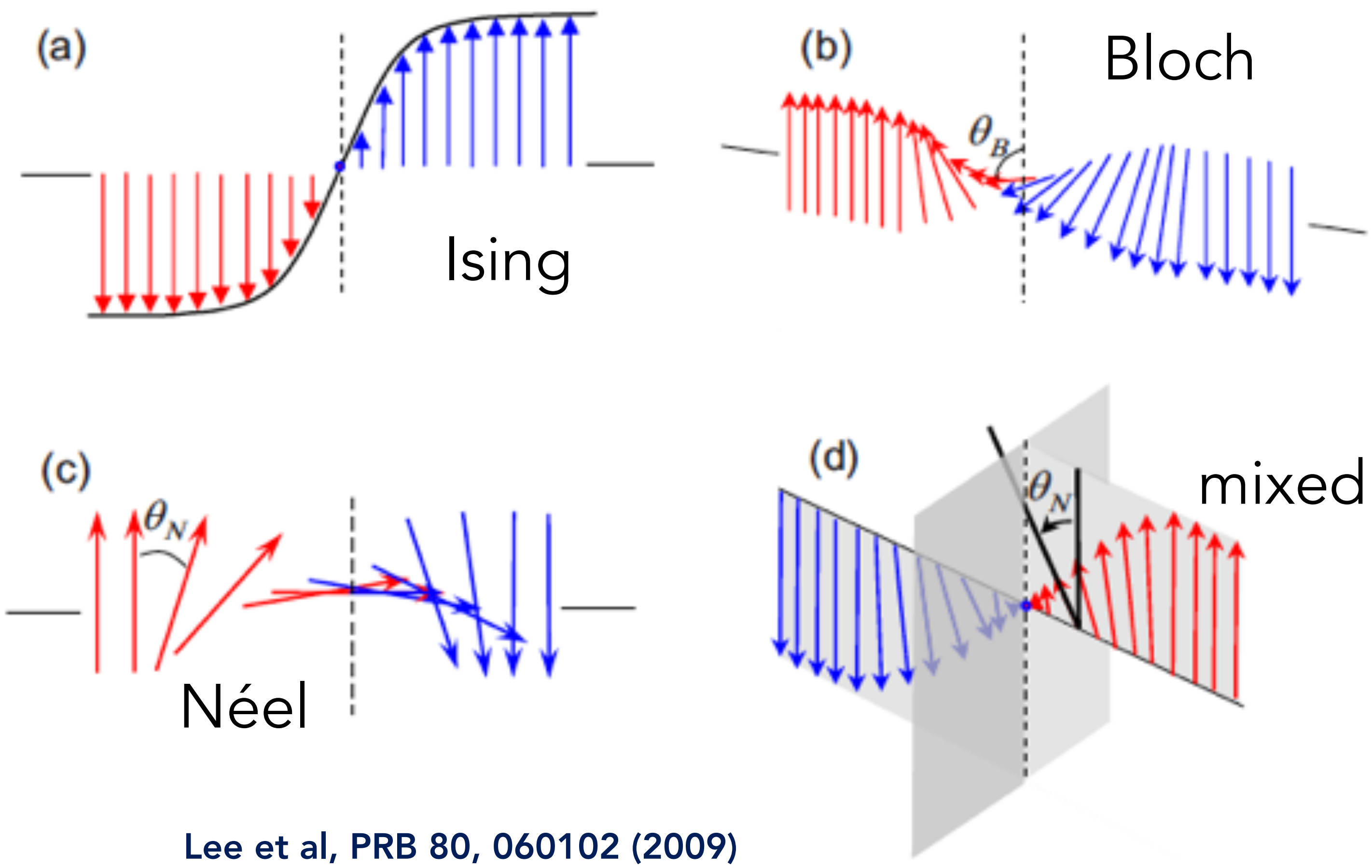

Lee et al, PRB 80, 060102 (2009)

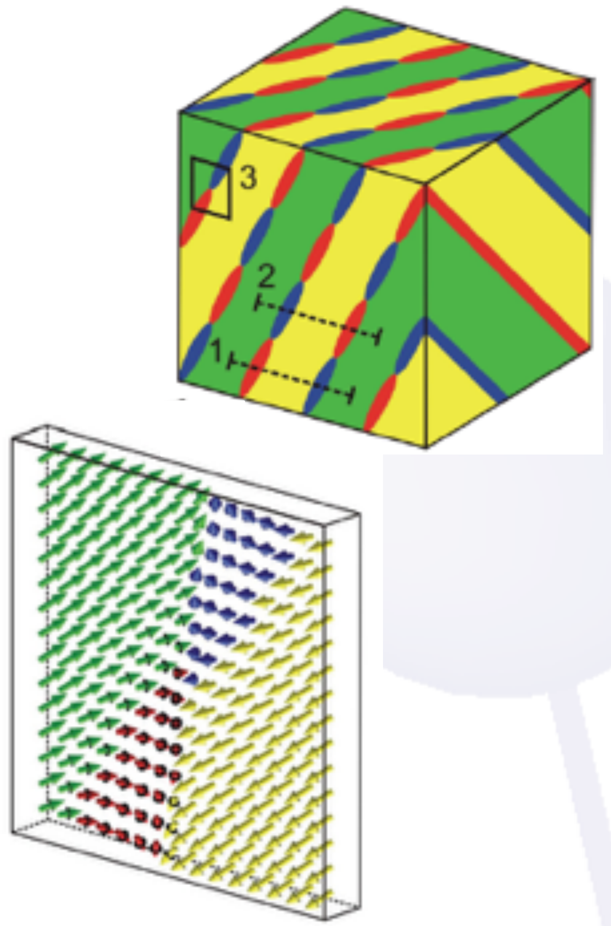

Stepkova et al, PRB 92, 094106 (2015)

Predictions of Néel, Bloch and mixed structures in different ferroelectrics

Lajzerowicz and Niez, J. Phys. Lett. 40, 165 (1979)
Stepkova et al, JPCM 24, 212201 (2012)
Eliseev et al, PRB 85, 045312 (2012)
Morozovska, Ferro 438, 3 (2012)
Wojdel et al, PRL 112, 247603 (2014)

Complex polarisation textures at domain walls

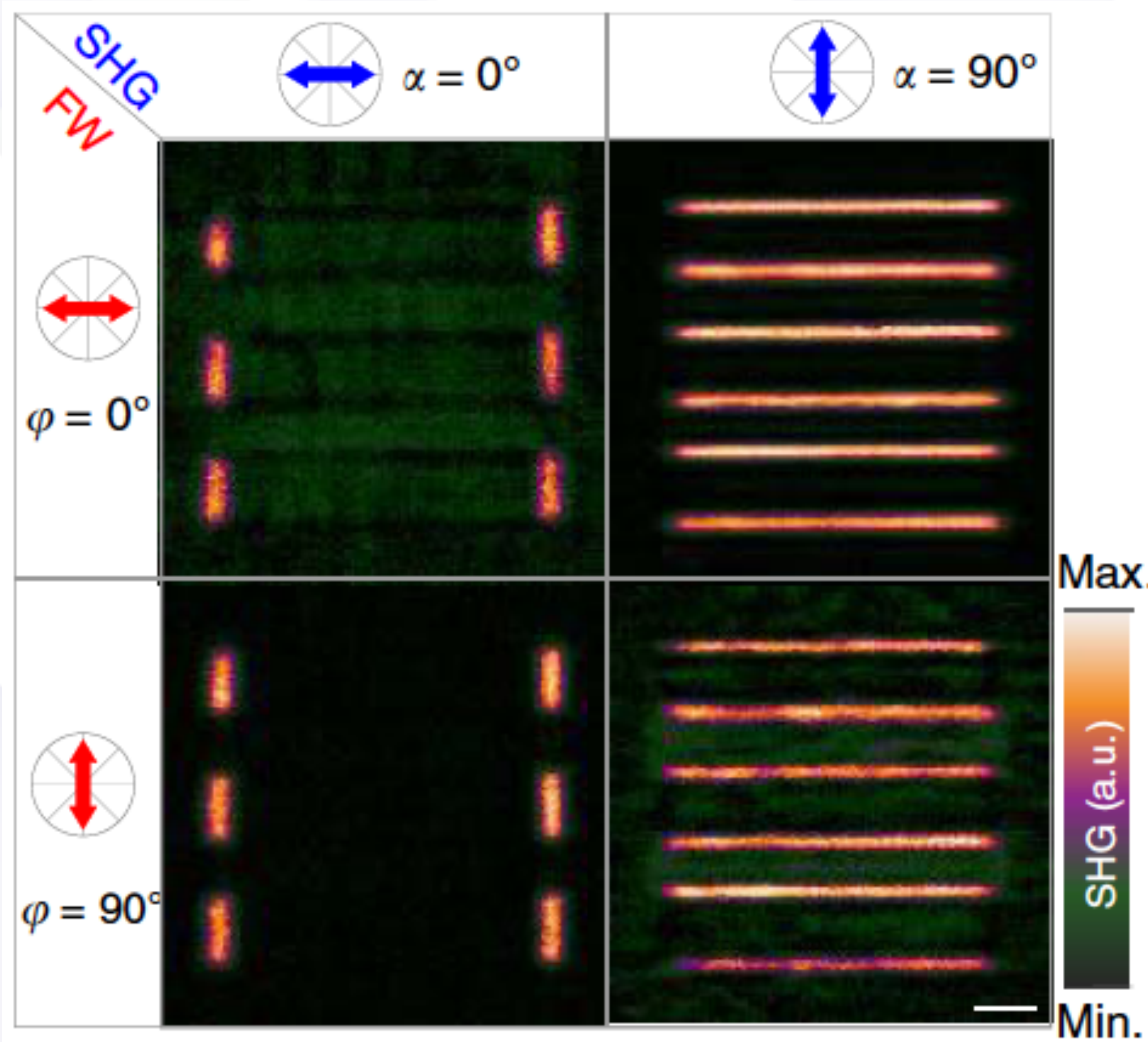

Néel polarisation at 180° domain walls in PZT

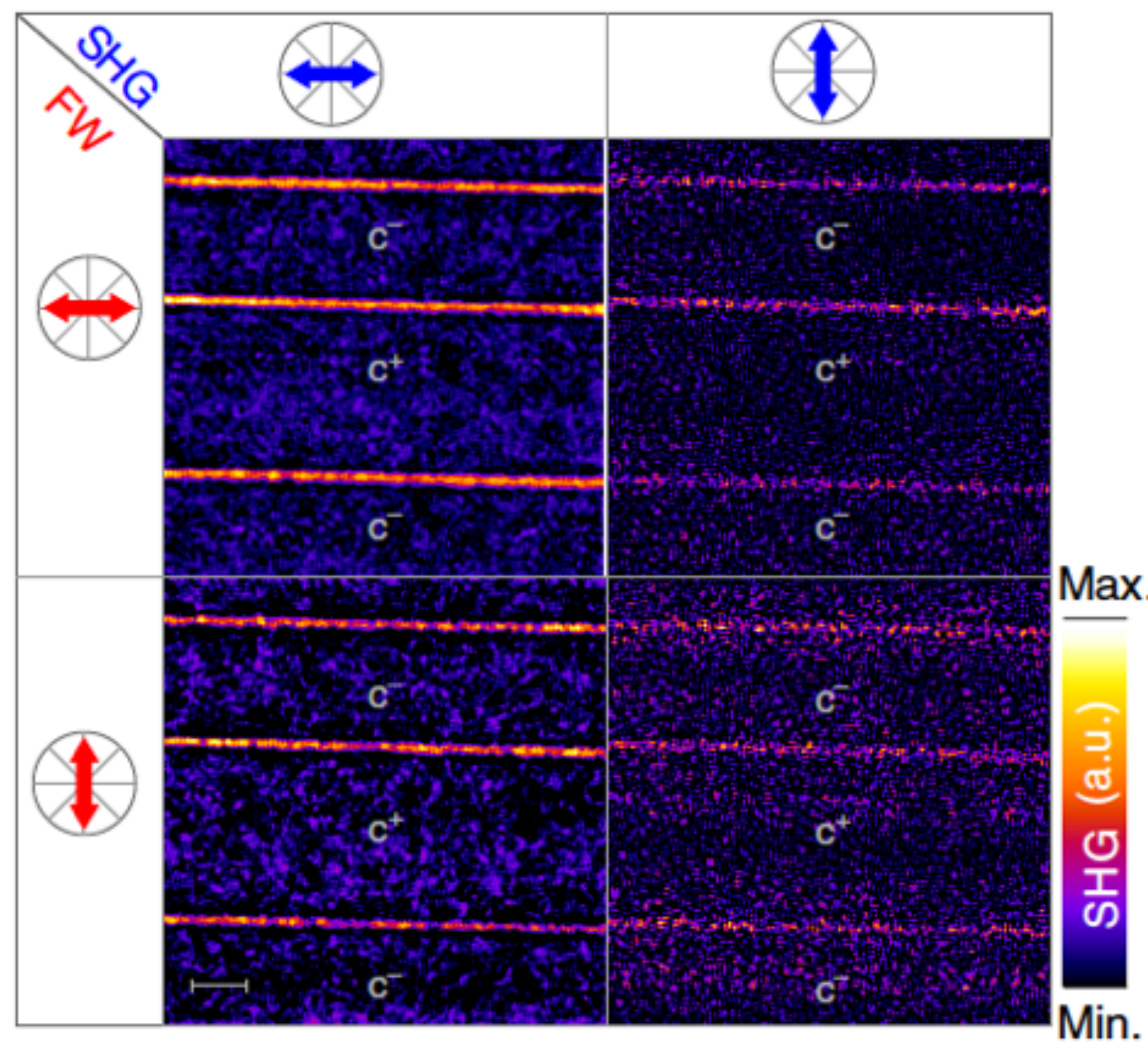

mixed Bloch-Néel polarisation with chirality reversal possible at 180° domain walls in $LiTaO_3$

Cherifi et al. Nat. Comm. 8, 15768 (2017)

Wei et al, Nat. Comm. 7, 12385 (2016)
De Luca et al, Adv. Mat. 29, 1605145 (2017)

Domain walls present novel, highly localised functional properties

Domain walls can show quite different physics from the parent phase

Ferrielectric domain walls in $CaTiO_3$

Goncalves-Ferreira et al. PRL (2008)

Conducting domain walls in $BiFeO_3$

Seidel, et al. Nat. Mat. 8, 229 (2009)

Photovoltaic domain walls in $BiFeO_3$

Yang et al. Nat. Nanotech. (2010)

Magnetism at domain walls (?)

Bartels. et. al J. P. Cond. Mat 15, 957-962 (2003)
Přívratská, Janovec, Ferroelectrics 222, 23 (1999)
Daraktchiev et al. PRB 81, 224118 (2010)

Different polar/structural order

Aguado-Puente and Junquera. PRL 100, 177601 (2008)

Polar domain walls in $SrTiO_3$

Zubko. et al. PRL 99, 167601 (2007)

Domain walls are extremely small

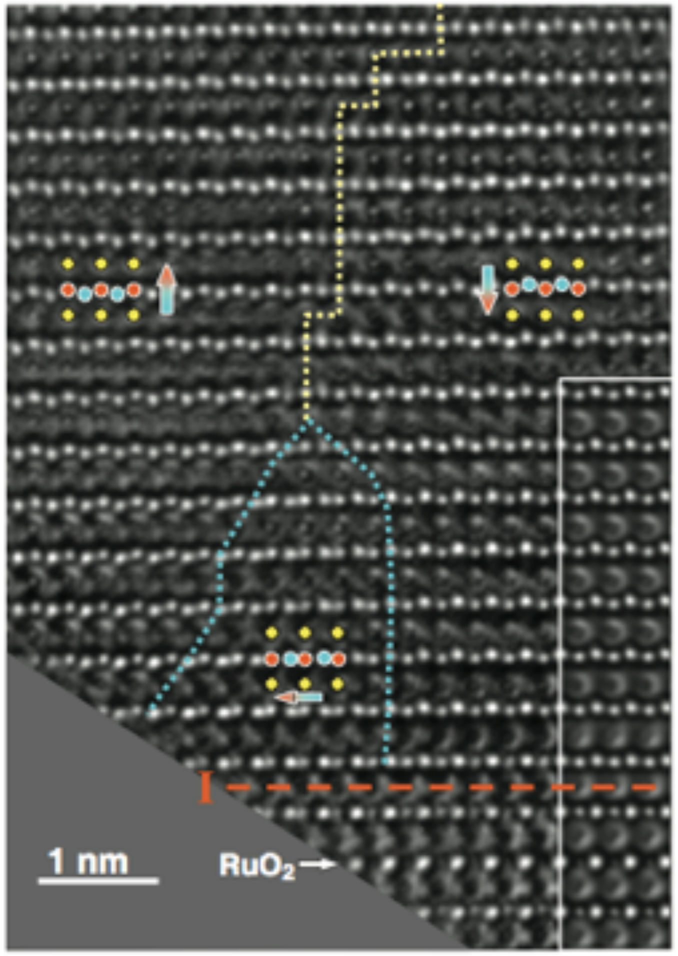

Jia et al. Science 331, 1420 (2011)
Lee et al. PRB 80, 060102 (2009)

Towards domain wall nanoelectronics

Domain walls can show quite different physics from the parent phase

Domain walls are extremely small

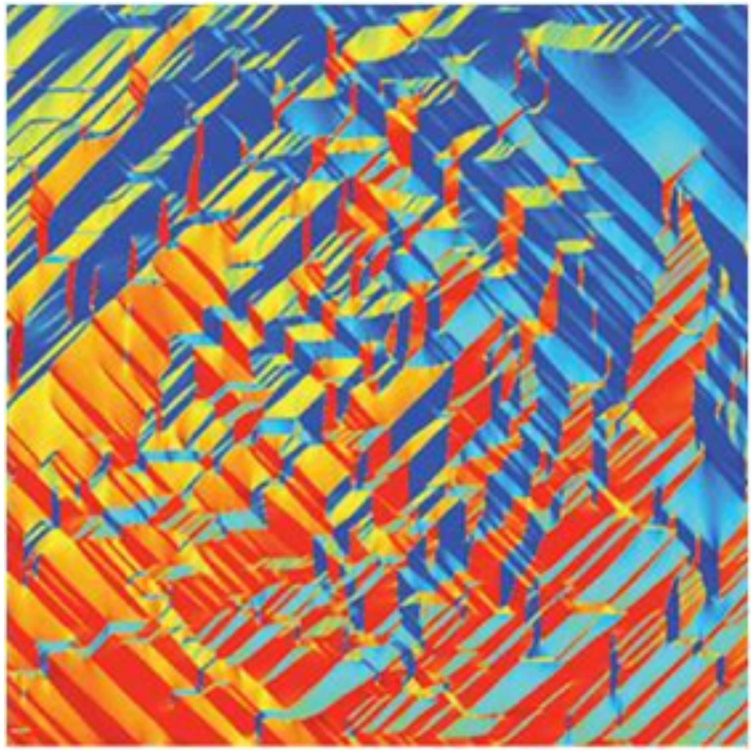

thanks to J. M. Gregg

Parkin et al. Science 320, 190 (2008)
Béa, Paruch. Nat. Mat. 8, 168 (2009)
Salje, ChemPhysChem 11, 940 (2010)
Yang et al. Nat. Nanotech. (2010)
Catalan et al., Rev. Mod. Phys. 84, 119 (2012)
Whyte and Gregg, Nat. Comm. 6, 7361 (2015)
Meier and Selbach, Nat. Rev. Mater 7, 157 (2021)

Can we use ferroelectric domain walls as active device components?

Need nanoscale access to probe/control their properties
Need to understand their fundamental behaviour

Mapping polarisation and functional properties with scanning probe microscopy

piezoresponse force microscopy
PFM

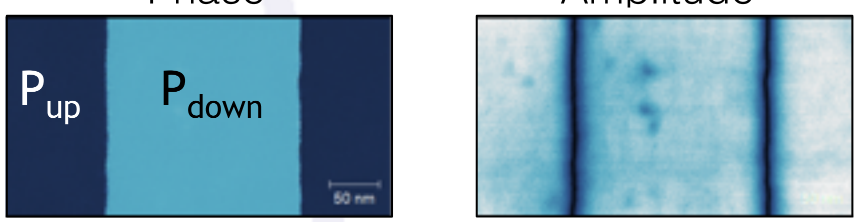

Tuckmantel et al, PRL 126, 117601 (2021)
Guyonnet et al. APL 95, 132902 (2009)
Guyonnet et al. PRL 109, 147601 (2012)
Ziegler et al. PRL 111, 247604 (2013)
Paruch, Guyonnet, C.R.A.S. Physique 14, 667 (2013)

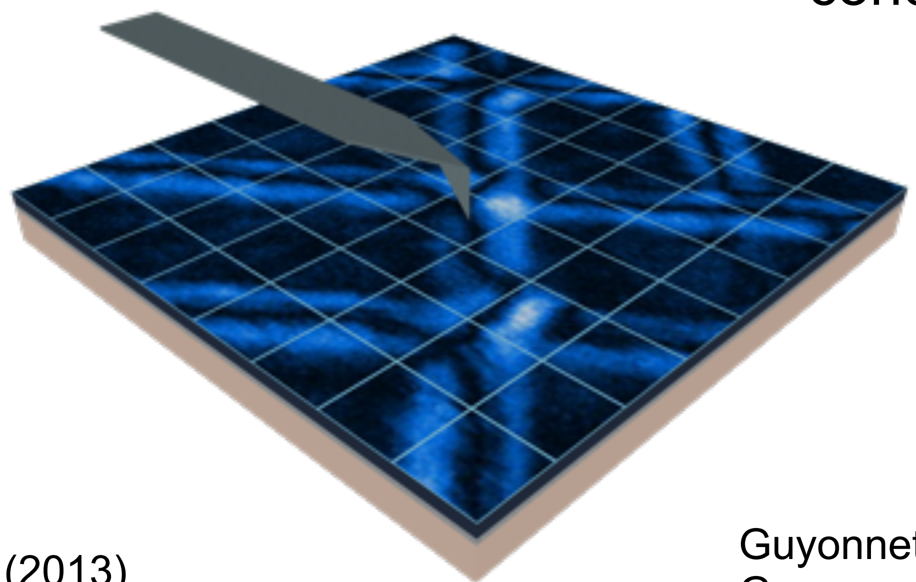

conductive atomic force microscopy
CAFM

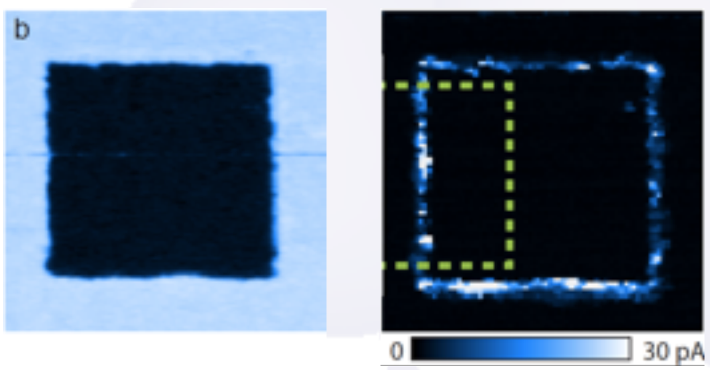

Guyonnet, Gaponenko et al, Adv. Mat. 23, 5377 (2011)
Gaponenko et al. APL 106, 162902 (2015)

contact resonance frequency microscopy
CRFM

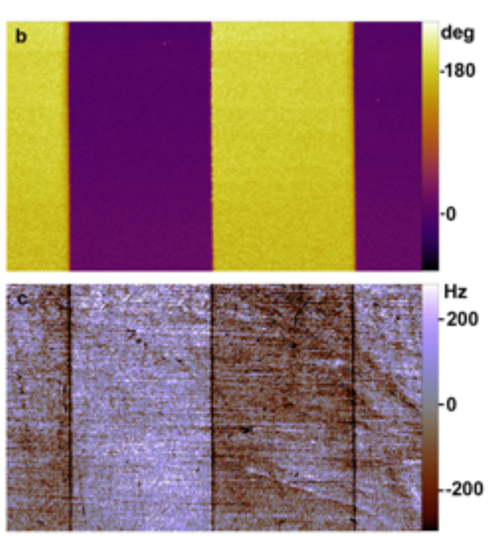

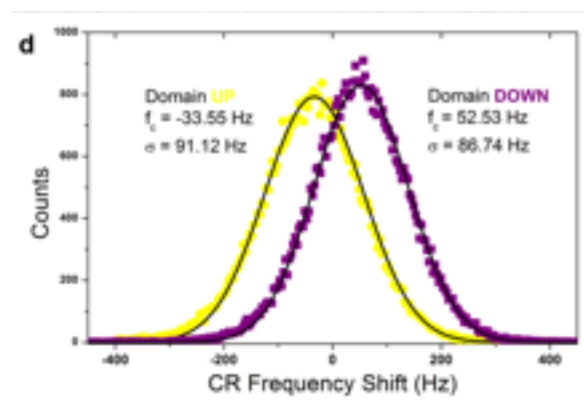

Cordero-Edwards et *al*. Adv. Mat. 29, 1702210 (2017)
Stefani et al. PRX 10, 041001 (2020)

Imaging domains and domain walls : PFM

Piezoresponse Force Microscopy

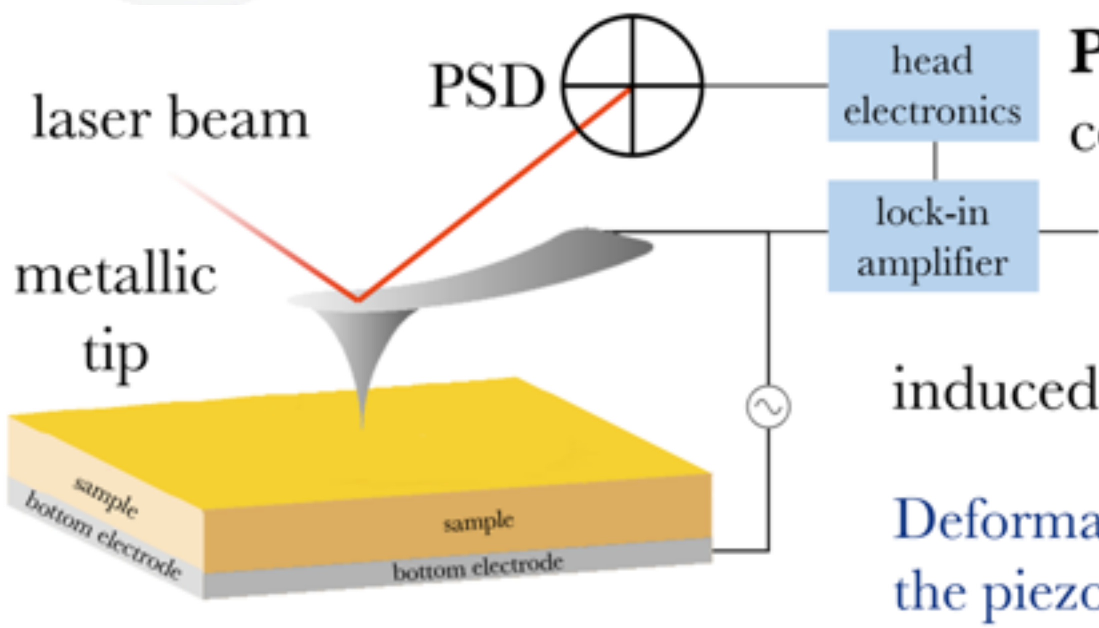

Piezoresponse : first harmonic component of tip deflection

$$A = A_0 + A_{1\omega}\cos(\omega t + \varphi)$$

induced by $V_{tip} = V_{dc} + V_{ac}\cos(\omega t)$

Deformation is given by the piezoelectric tensor : $X_j = d_{ij}E_i$

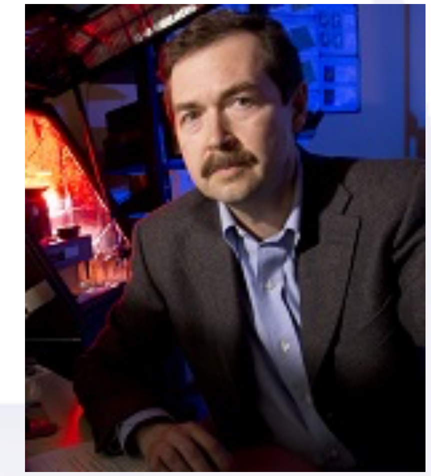

Alexei Gruverman

ruverman et al. APL 69, 3191 (1996)
Eng et al. APL 74, 233 (1999)
Tybell et al. APL 75, 856 (1999)
Eng et al. APL 74, 233 (1999)
Hong et al. JAP 89, 1377 (2001)
Kalinin et al. PRB 63, 125411 (2001)
Harnagea et al. APL 83, 338 (2003)
Jesse et al. RSI 77, 073702 (2006)
Jesse et al. Nanotech. 18, 435503 (2007)
Morozovska et al. PRB 80, 214110 (2009)
Johann et al. PRB 81, 094109 (2010)
Balke et al. ACS Nano 8, 10229 (2014)

PFM phase

PFM amplitude

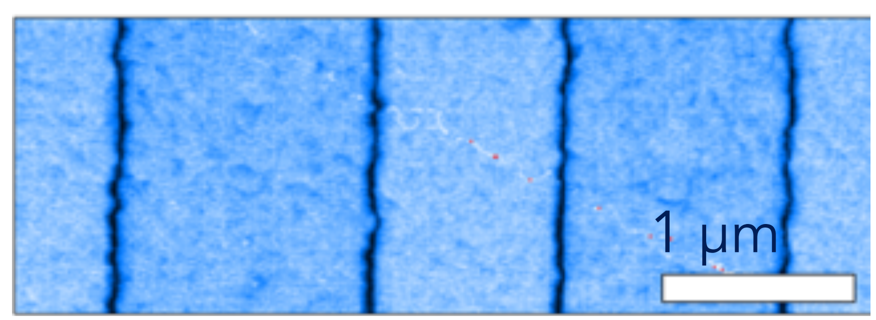

PFM has become a key tool for nanoscale studies of ferroelectrics

Outline

Ferroelectric domain walls as a disordered elastic system

untangling the effects of defects and surface adsorbates

(Roughness and dynamics of epithelial cell fronts)

different regimes to identify characteristic lengthscales

Every wall is a door

Emerson

Characteristic self-affine roughening of interface

$$B(r) = \overline{\langle |\Delta u(r)|^2 \rangle}$$

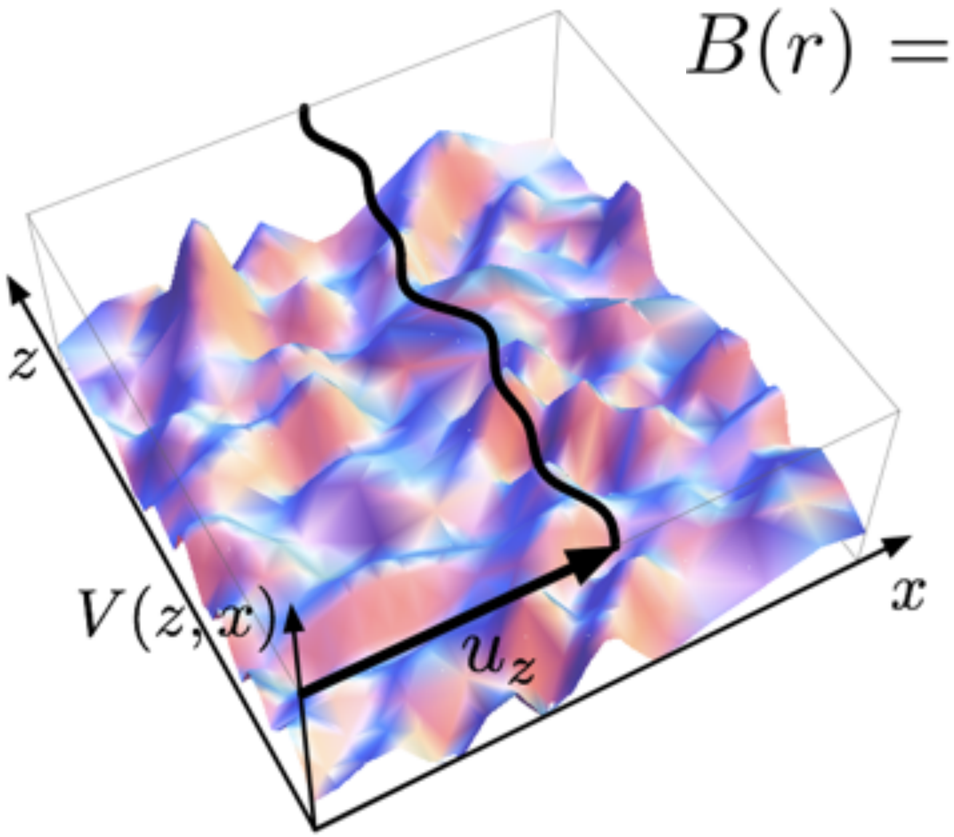

Agoritsas, Phys. B 407, 1725 (2012)

Paruch, Guyonnet, C.R.A.S. Physique 14, 667 (2013)

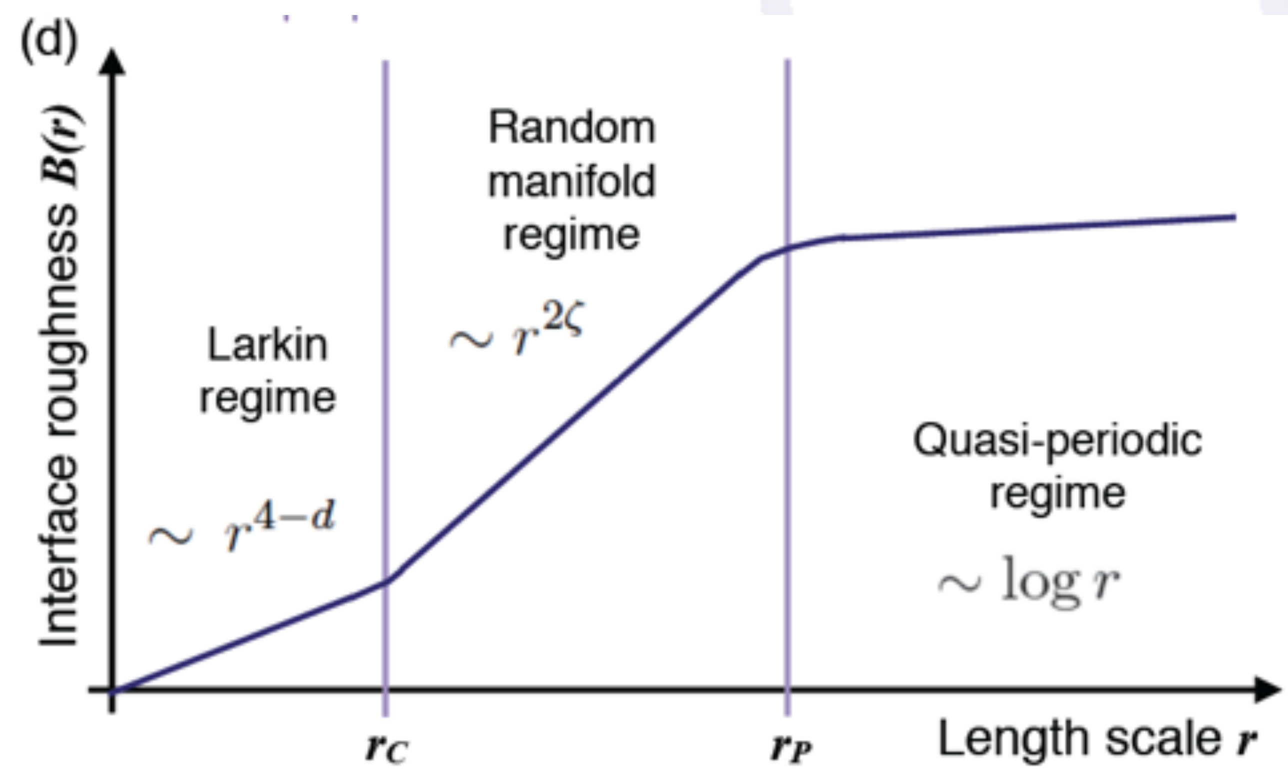

random bond random field

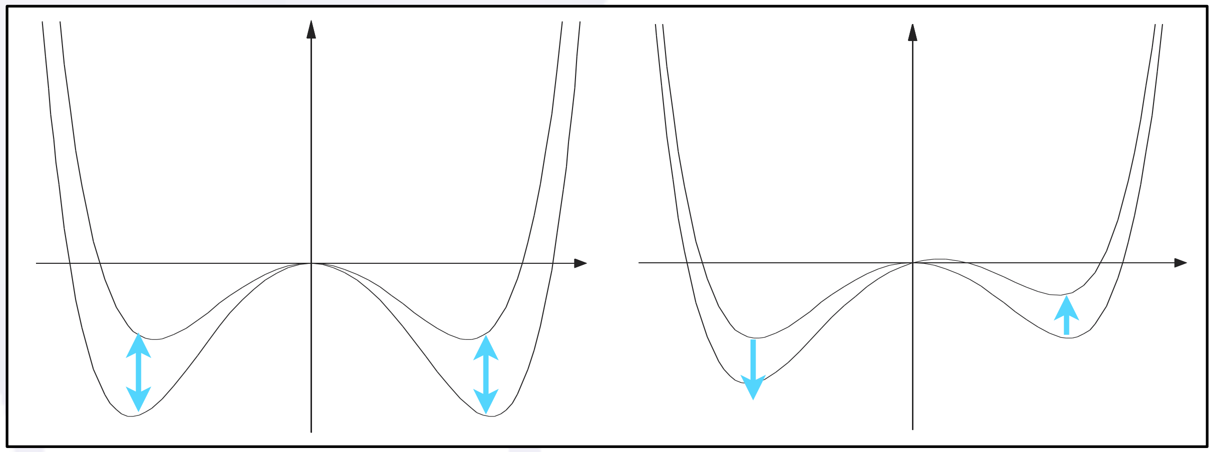

ζ_{TH} = 1/2 (d = 1)

ζ_{RB} = 2/3 (d = 1)

ζ_{RB} ~ 0.2084 (4 - d_{eff})

ζ_{RF} = (4 - d_{eff}) / 3

Dimensionality and disorder determine roughness scaling

Complex dynamic response of interface

Paruch, Guyonnet, C.R.A.S. Physique 14, 667 (2013)

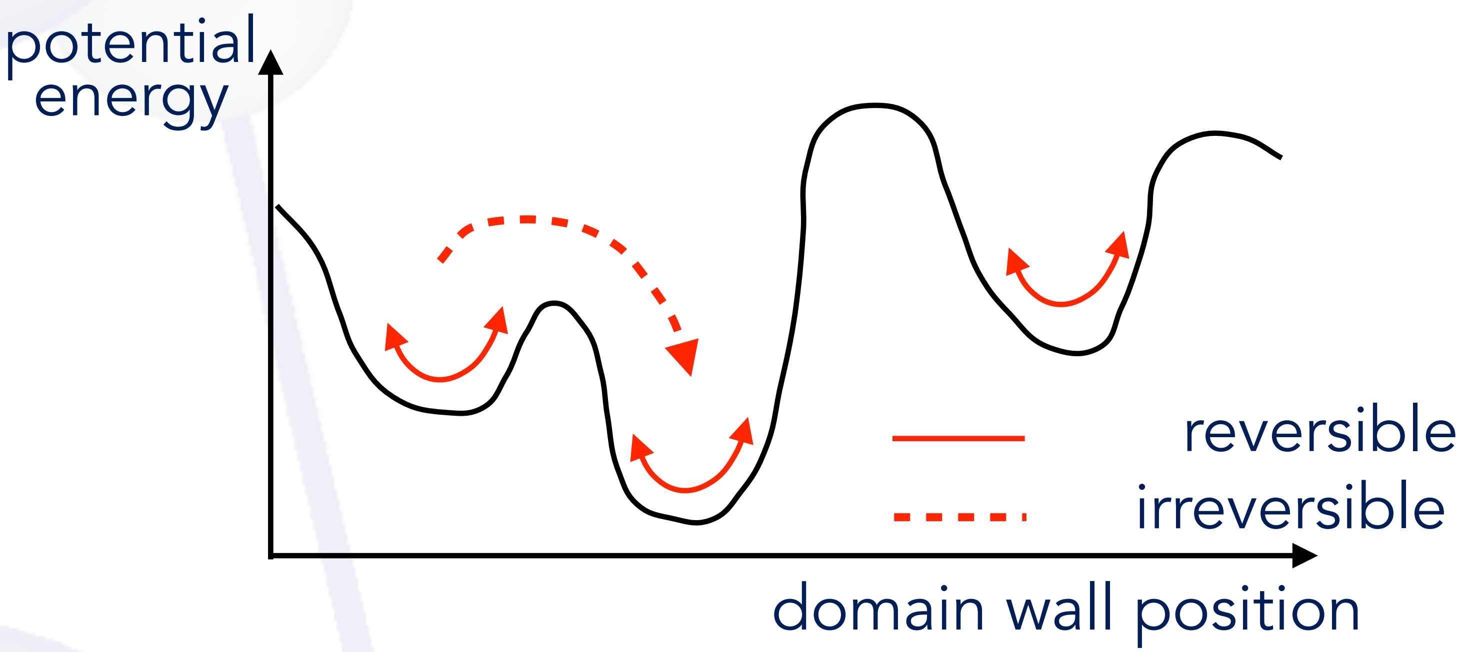

Damjanovic, Rep. Prog. Phys. 61, 1267 (1998)

Interface has to move through fluctuations in potential energy landscape

Dimensionality and disorder determine creep response

$$\mu = \frac{d_{eff} - 2 + 2\zeta}{2 - \zeta}$$

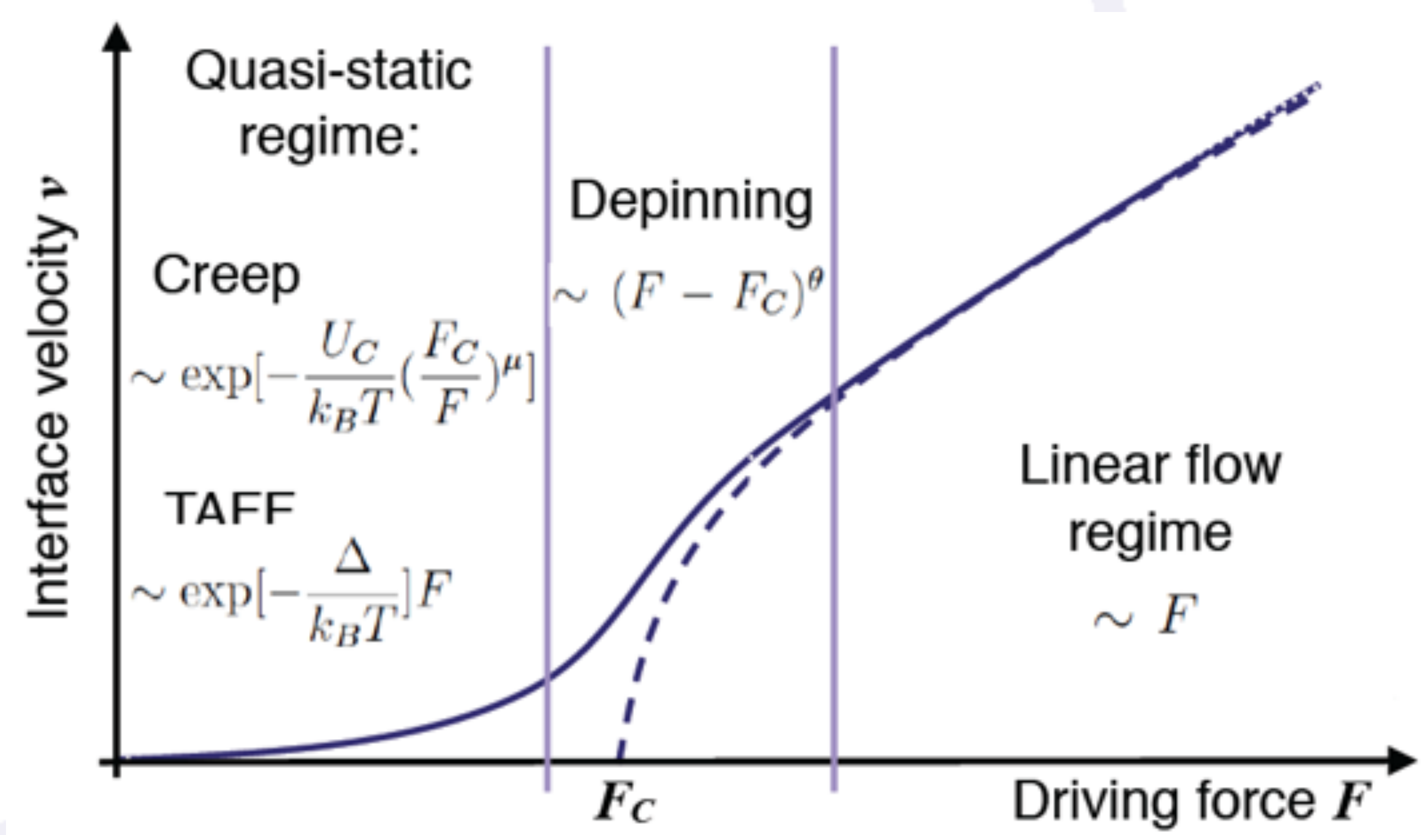

Measuring domain wall roughness and dynamics

mapping DW position

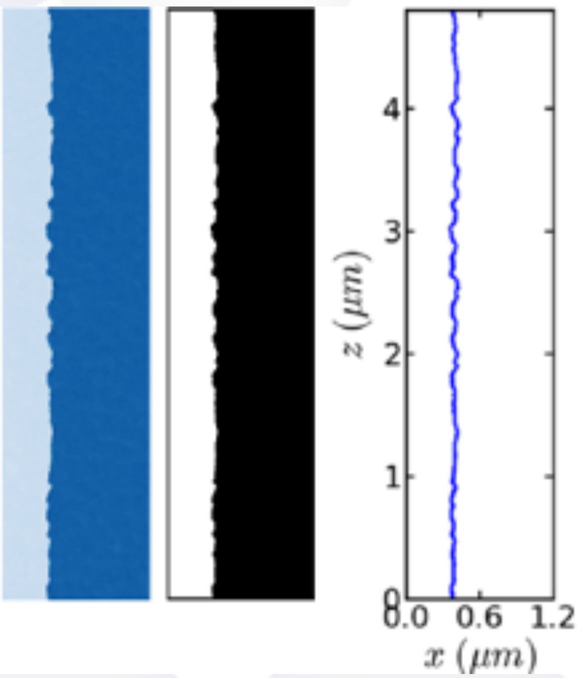

Paruch, Guyonnet, C.R. Physique 14, 667 (2013)

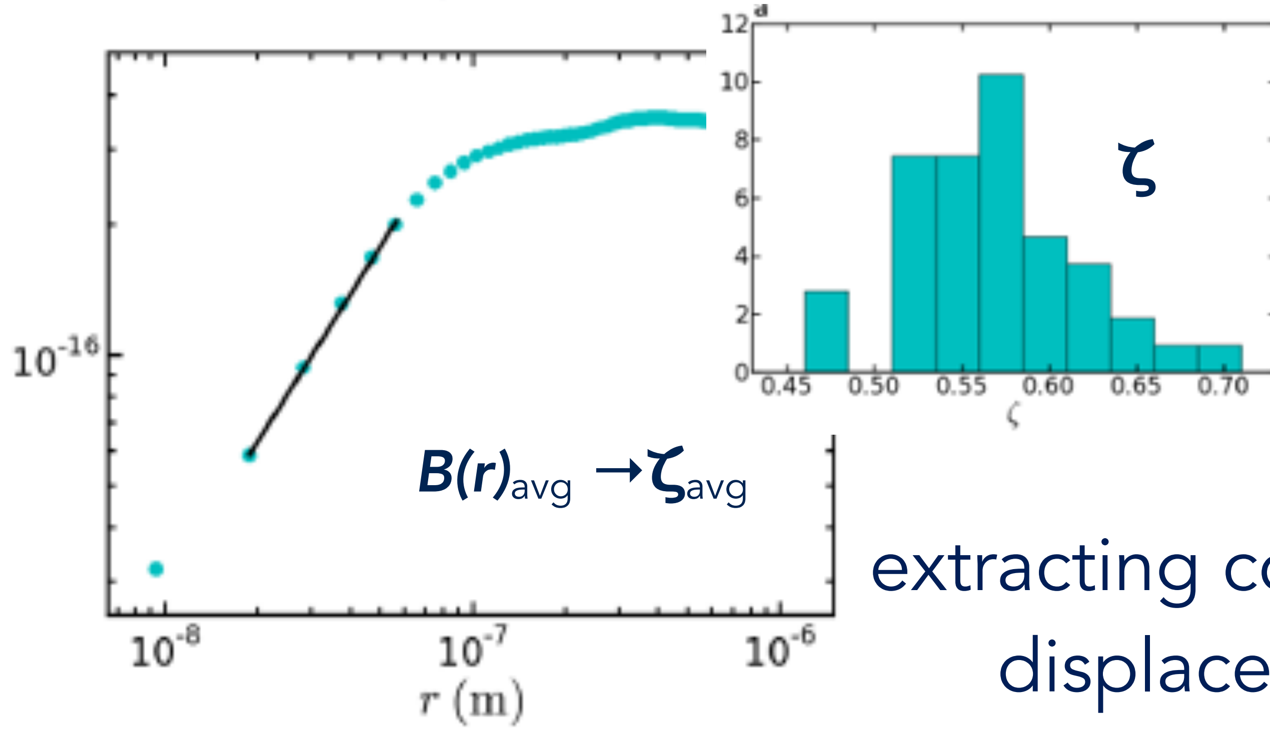

Jill Guyonnet

Benedikt Ziegler

extracting correlations of relative displacements along DW

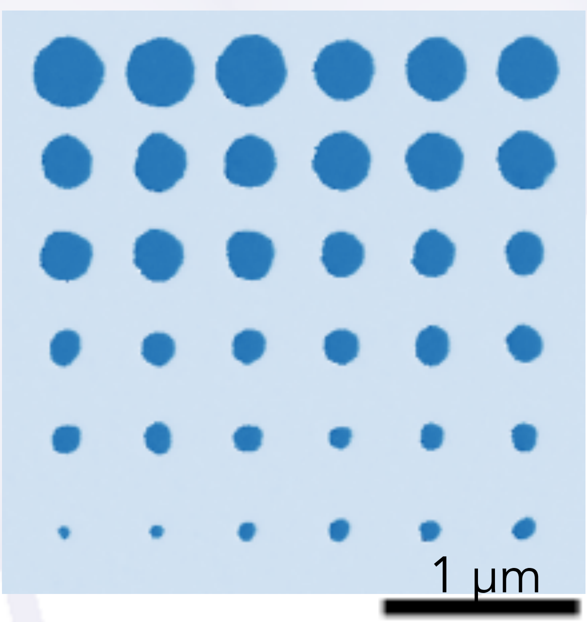

$$v(r) = \frac{r_{n+1} - r_n}{t_{n+1} - t_n} \quad \text{vs.} \quad E_z(r)$$

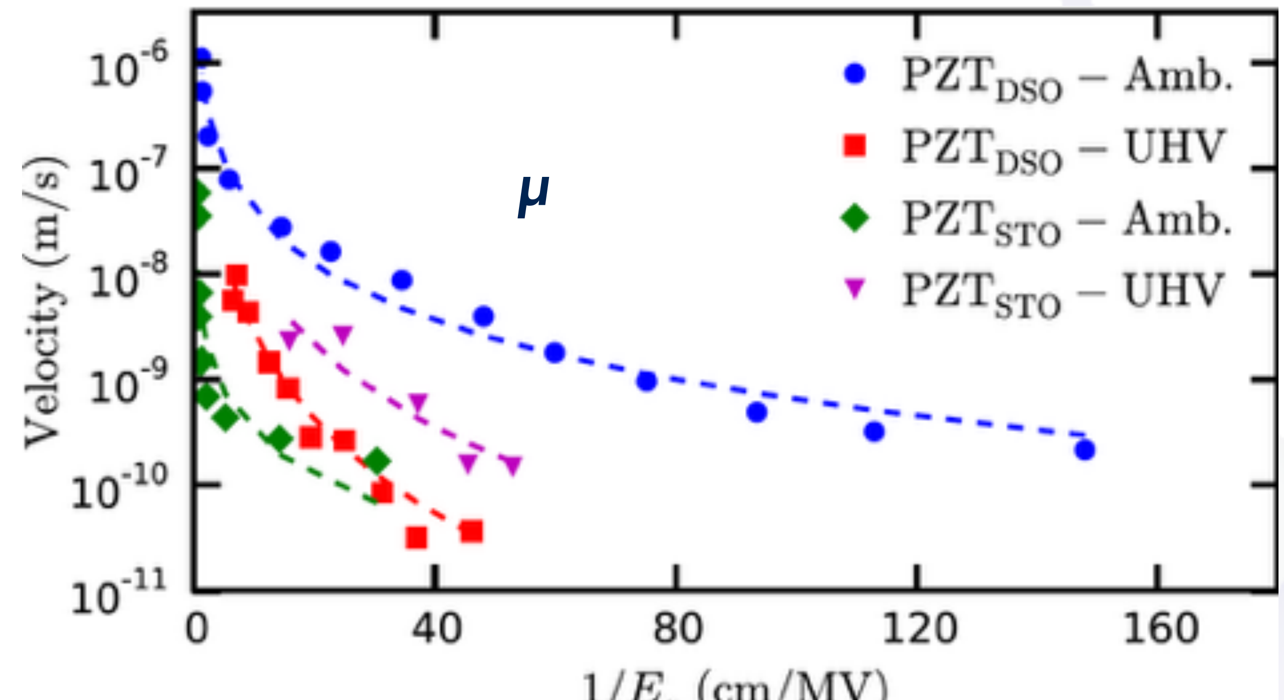

extracting electric field driven DW dynamics

A universal behaviour in ferroelectrics

written domain walls

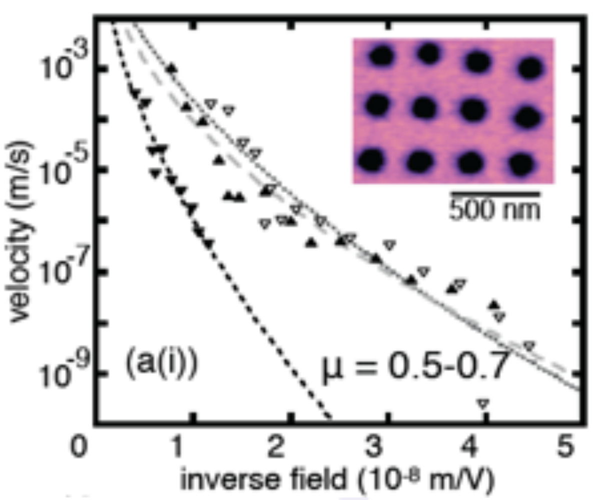

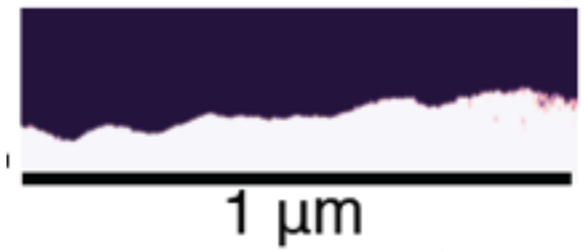

ζ ~ 0.25

Tybell et al. PRL 89, 097601 (2002)
Paruch et al. PRL 94, 197601 (2005)
Paruch et al. JAP 100, 051608 (2006)
Guyonnet et al. PRL 109, 147601 (2012)

intrinsic domain walls

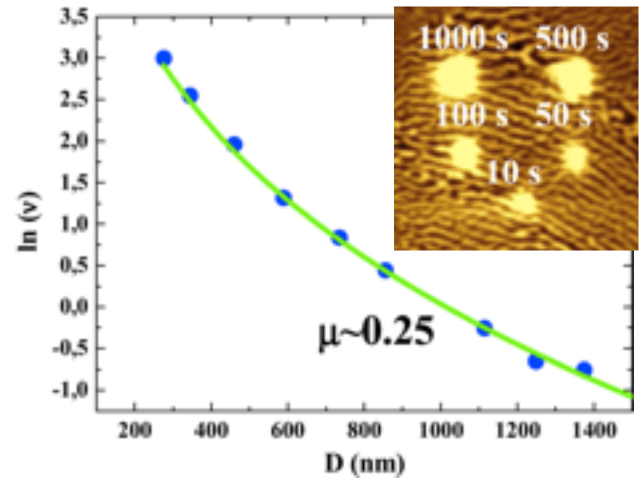

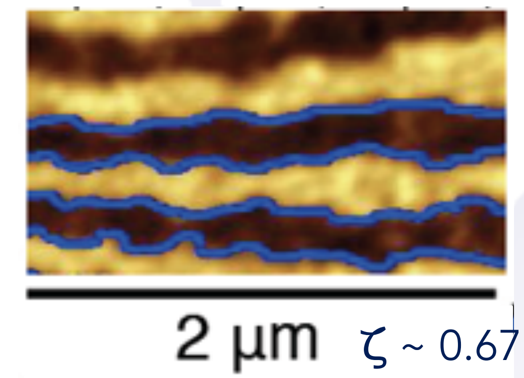

ζ ~ 0.67

Pertsev et al. JAP 110, 052001 (2011)

domain walls in single crystals

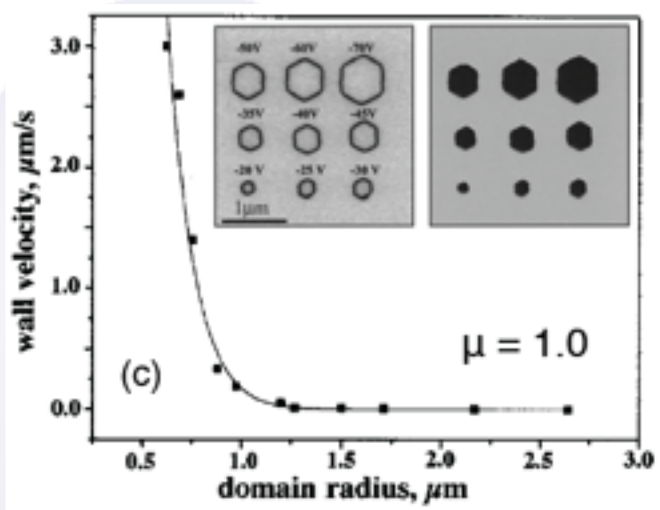

Rodriguez et al. APL 86, 012906 (2005)

multiferroic domain walls

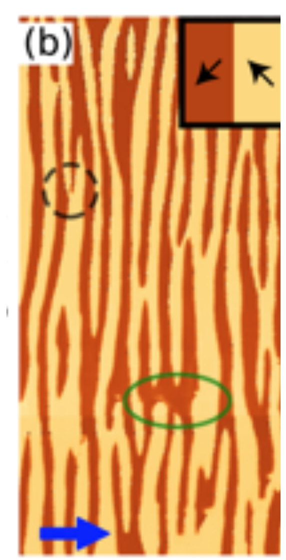

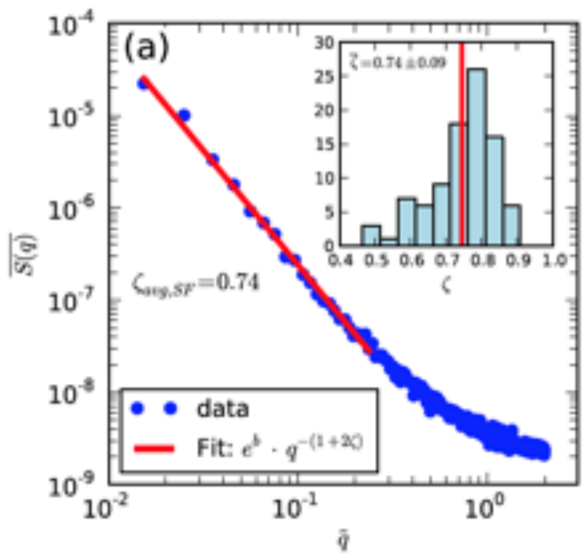

ζ ~ 0.74

Catalan et al. PRL 100, 027602 (2008)
Ziegler et al. PRL 111, 247604 (2013)

Scaling behaviour with characteristic roughness exponent ζ

Highly nonlinear dynamic response with creep exponent μ

Artificial pinning sites and engineering motion

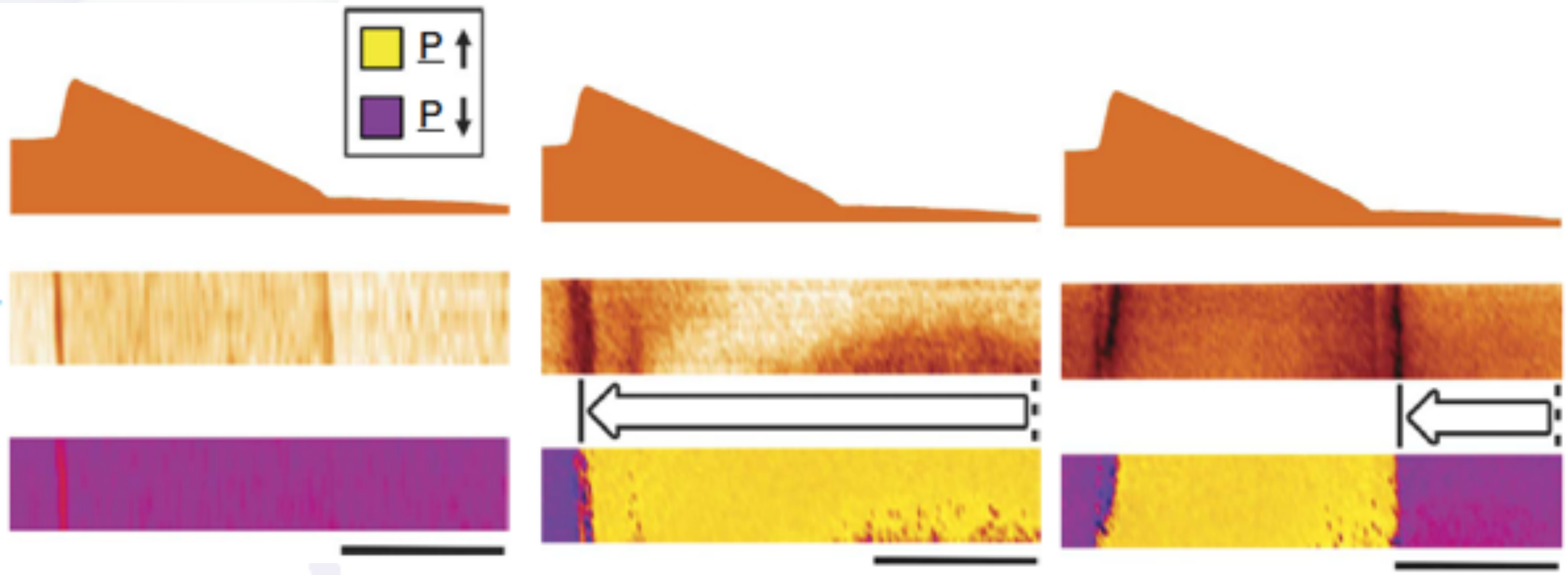

Whyte and Gregg. Nat. Comm. 6, 7361 (2015)

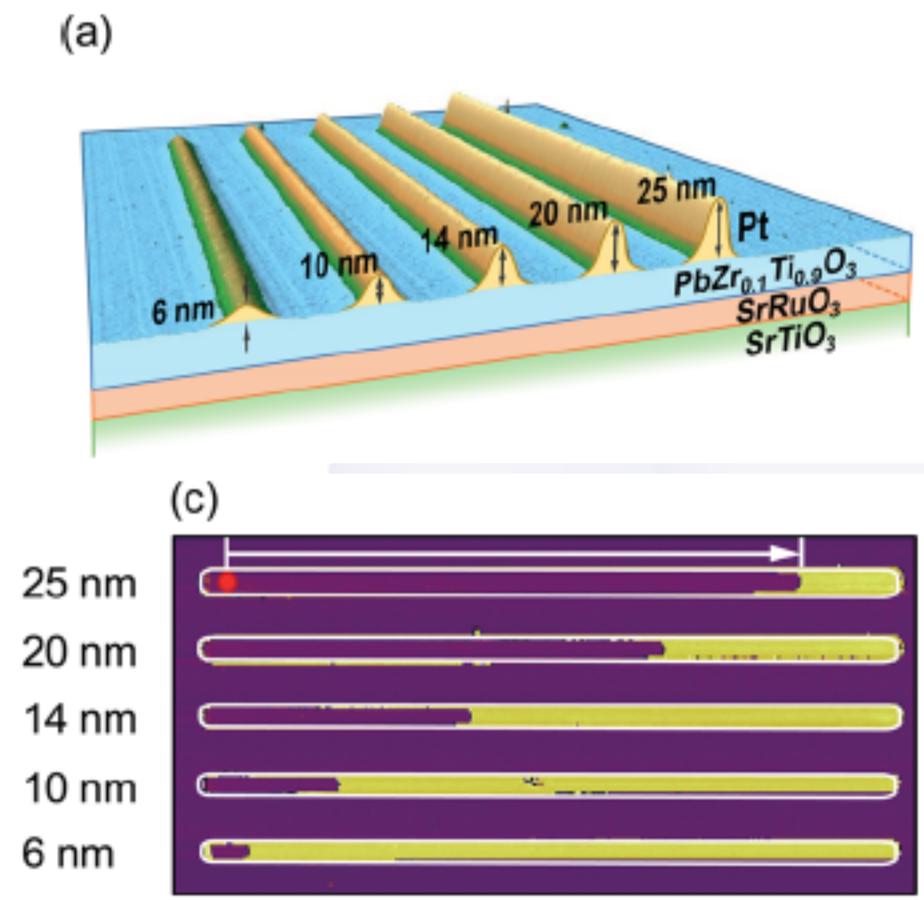

McGilly et al, Nano Lett 16, 68 (2016)
McGilly et al, Nat. Nanotech 10, 145 (2015)

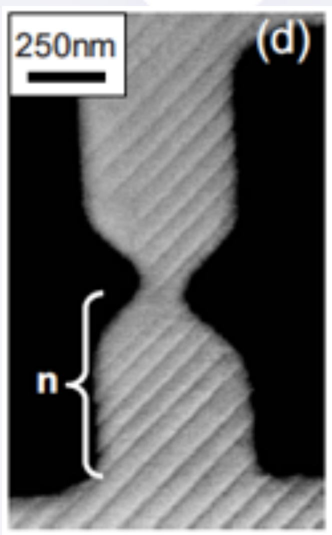

(anti)notches and sawtooth diodes to control DW pinning in nanofabricated BaTiO3 lamellae

McMillan et al. APL 96, 042904 (2010)
McQuaid et al. NL 10, 3566 (2010)

mobility control via electrode conductance

Towards domain wall nanoelectronics

Béa and Paruch Nat. Mat. 8, 168 (2009)
Salje ChemPhysChem 11, 940 (2010)
Yang et al. Nat. Nanotech. (2010)
Catalan et al. Rev. Mod. Phys. 84, 119 (2012)

Moving away from equilibrium

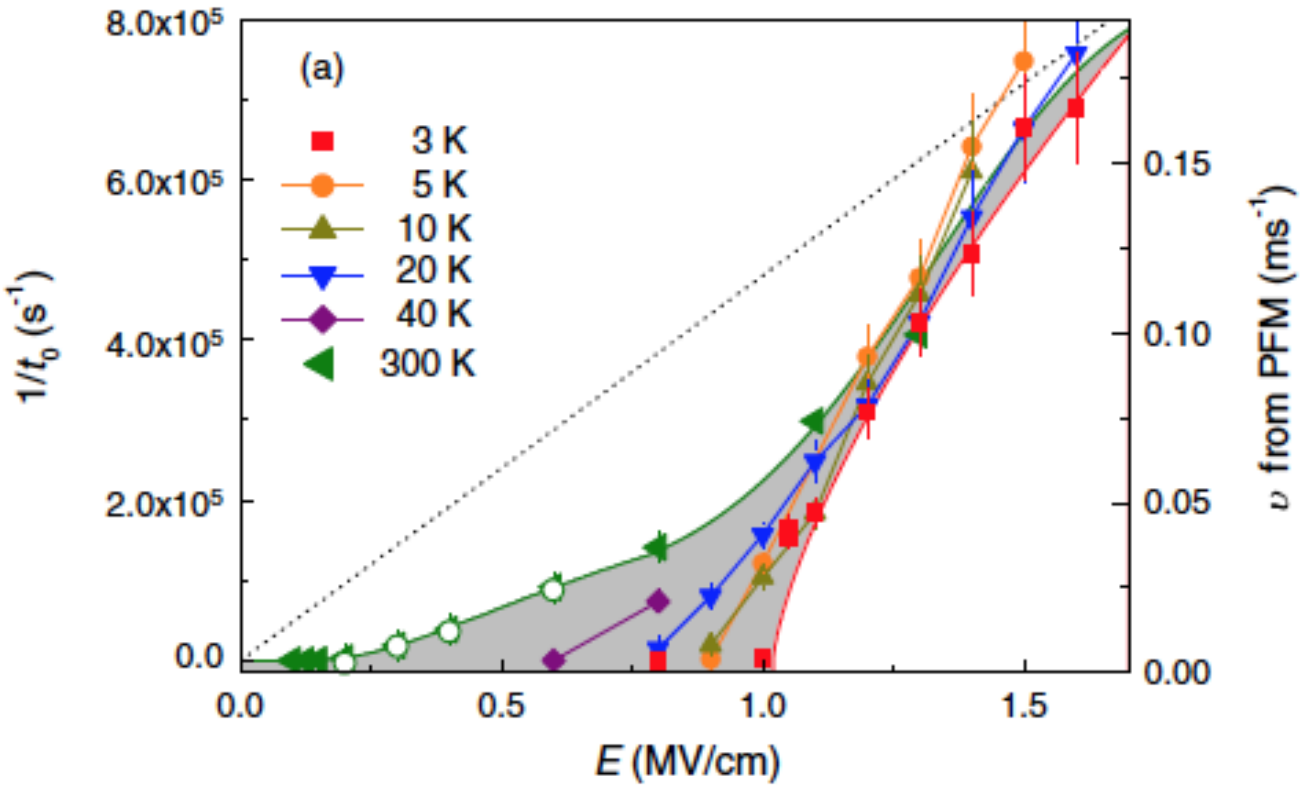

Jo, et al. PRL 102, 045701 (2009)

exploring depinning

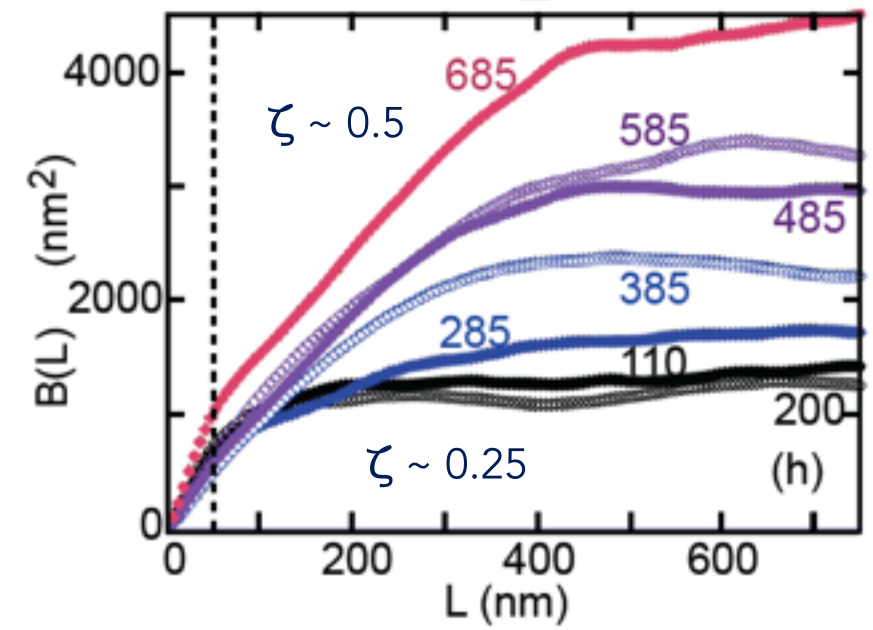

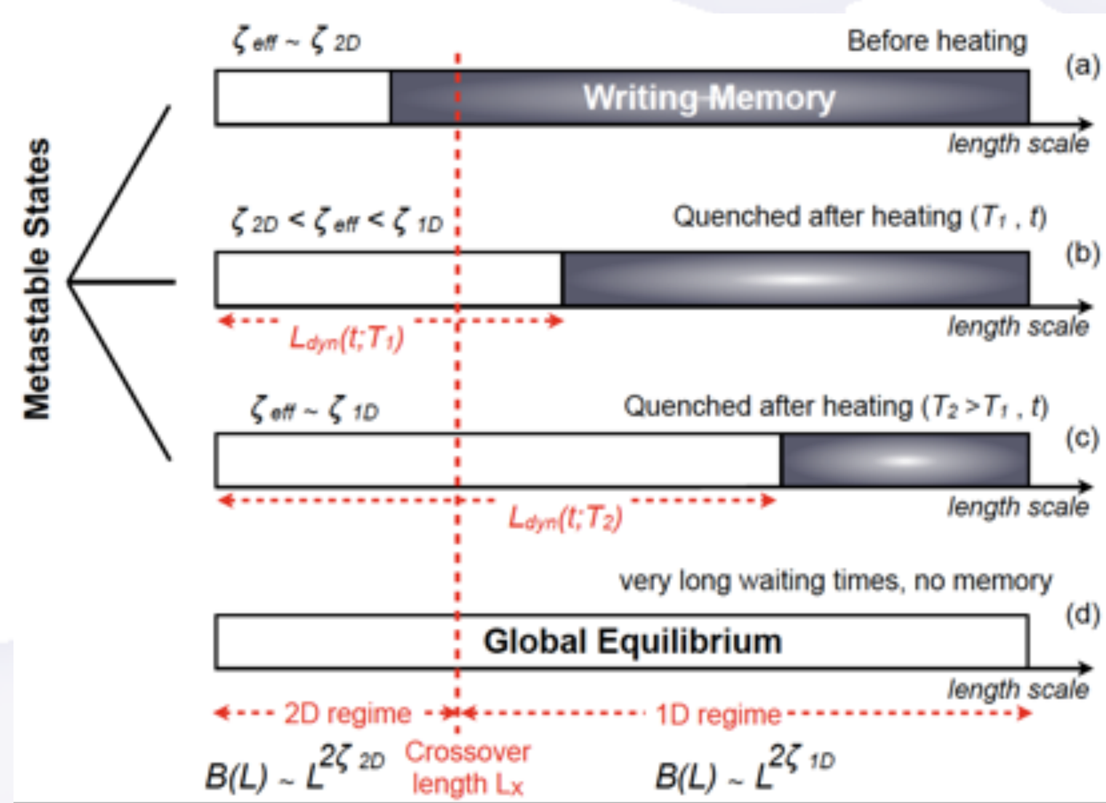

ageing and memory effects after thermal quenching

Paruch, et al. PRB 85, 214115 (2012)

Nanoscale studies of individual domain walls, switching events, and their global contribution

Want to correlate DW structure and defect interactions (specific, local) with dynamics/roughness (statistical, global) and properties (functional)

high-resolution mapping of DW evolution over long duration

Tukmantel et al. PRL. 126, 117601 (2021)
Gaponenko, Tückmantel et al, Sci. Rep 7, 669 (2017)

correlate structural and functional measurements at multiple length scales

Croes et al., Adv. Phys. Res. 2, 2200037 (2023)
Weymann et al. PRB 106, L241404 (2022)
Gaponenko et al., Sci. Rep. 12, 165 (2022)
Musy, Bulanadi et al. Ultramicroscopy 228, 113345 (2021)
Cherifi-Hertel et al. Nat. Comm. 8, 15768 (2017)

identify physically relevant regimes/behaviours

Gaponenko et al. npj Comp. Mat. 7, 163 (2021)
Griffin, Gaponenko et al, Adv. Mat. 32, 2002425 (2020)
Domingo et al., Nanoscale 11, 17920 (2019)
Griffin, Gaponenko et al, npj Comp. Mat. 5, 85 (2019)


Iaroslav Gaponenko


Philippe Tückmantel


Ralph Bulanadi


Loïc Musy


Christian Weymann


Kumara Cordero-Edwards

https://github.com/paruch-group

Bridging approach - linking the local and global switching dynamics in ferroelectrics

Eckhart Salje

Thierry Giamarchi

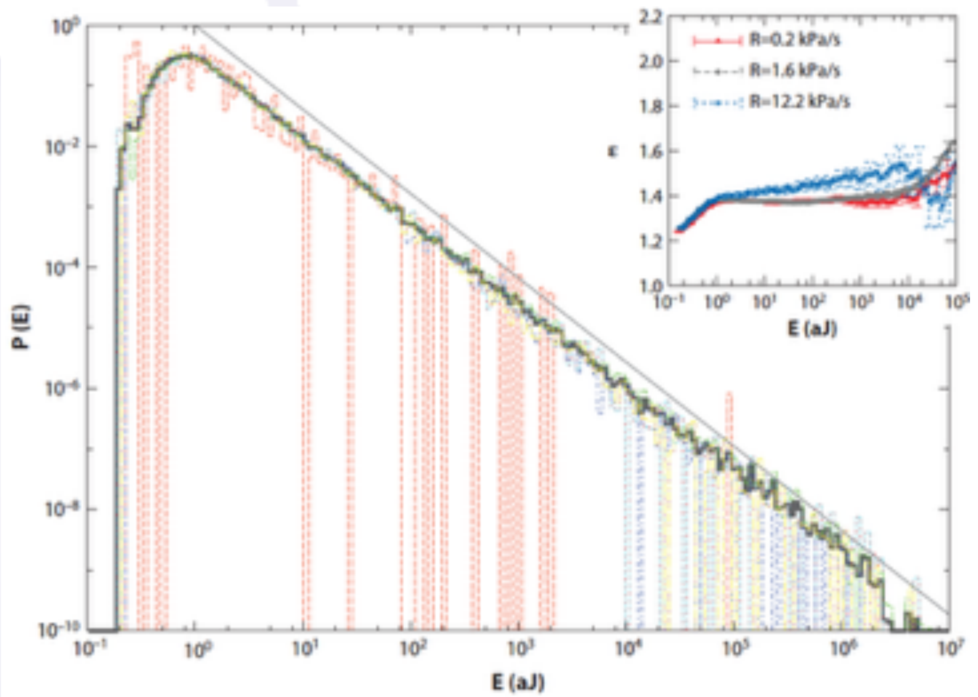

Salje, Dahmen. Ann. Rev. Cond. Mat. Phys. 5, 233 (2014)

Size/Power distribution of slip avalanches in compressed porous media and ferroelastic crystals

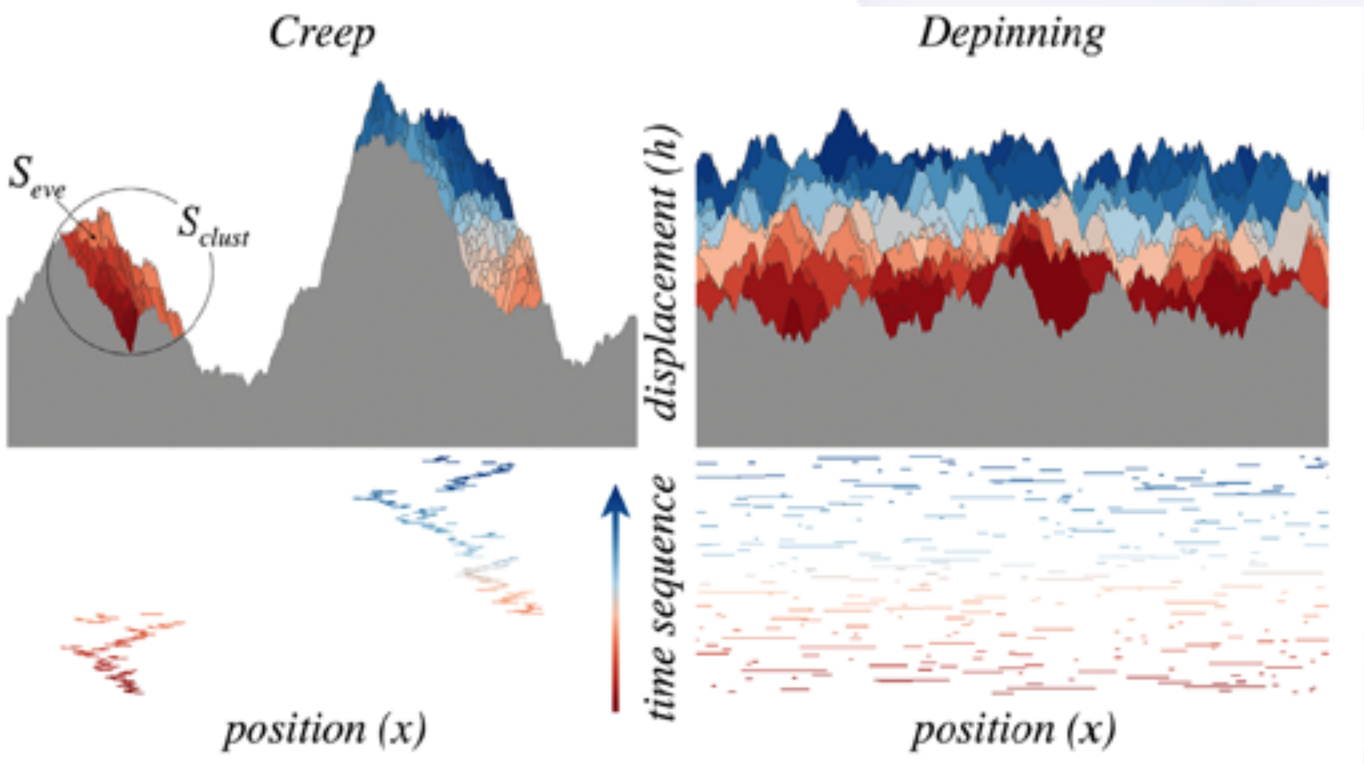

Ferrero et al. PRL 118, 147208 (2017)

Distinguishing creep and depinning from avalanche statistics

PZT thin films with different defect densities

Tuckmantel et al. PRL. 126, 117601 (2021)

Philippe Tückmantel

Control density and type of defects during thin film growth

rough AFM written domain walls, in-plane strain relaxation
-> higher density of stronger pinning sites, extended defects

PZT_{RFS}

PZT_{PLD}

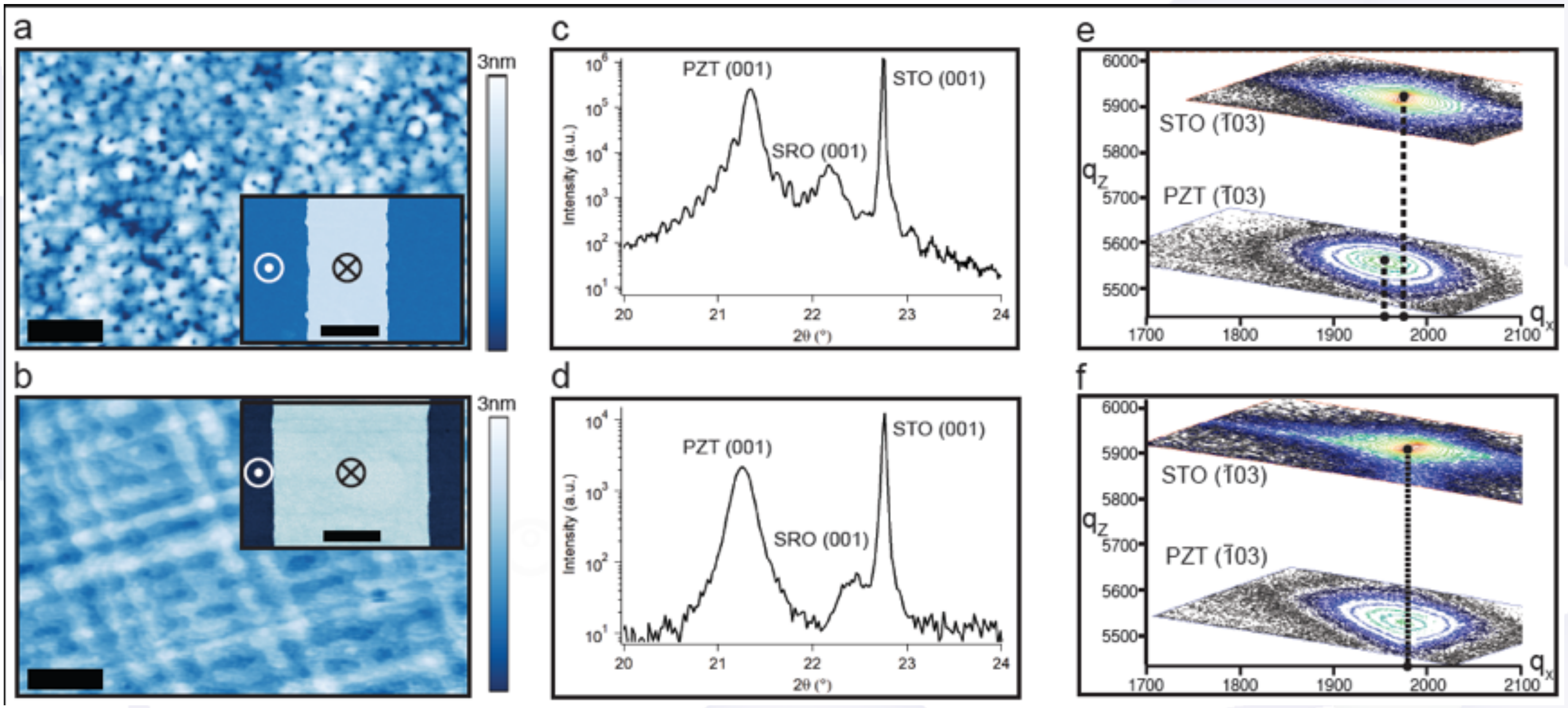

smooth AFM written domain walls, fully strained in-plane
-> higher density of point defects

UHV measurements of polarisation switching

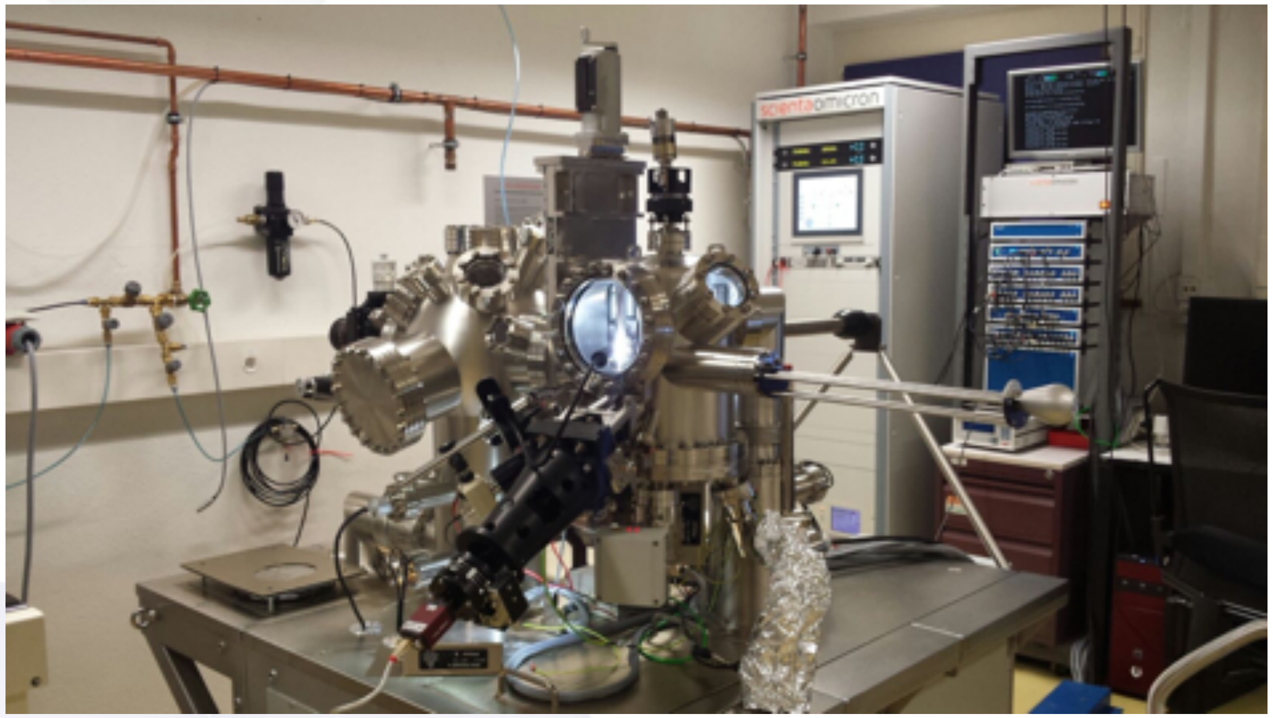

Alternate PFM scans with switching scans at incrementally increasing bias or at constant bias

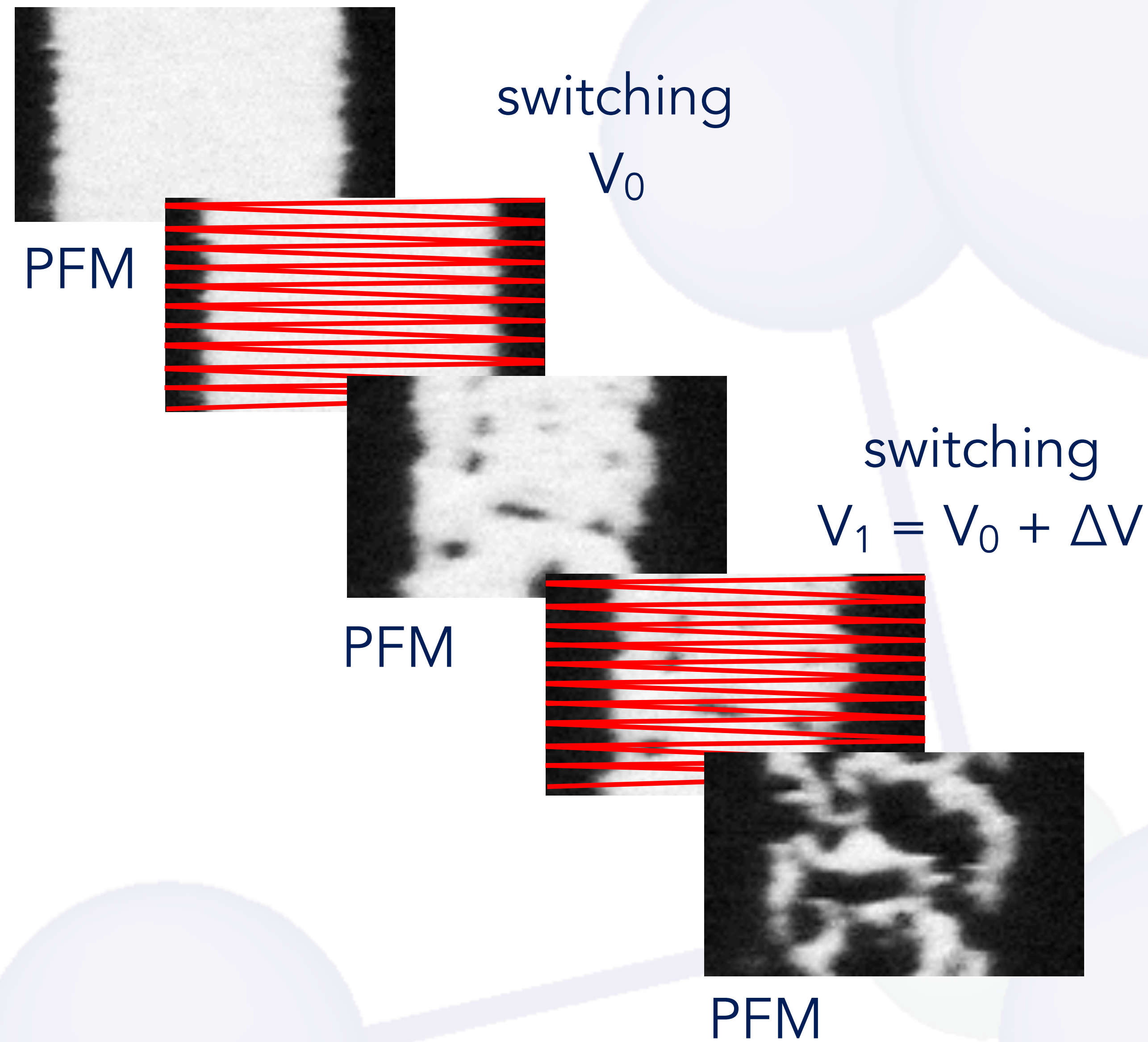

Stripe domain structures written in as-grown monodomain P_{UP} films

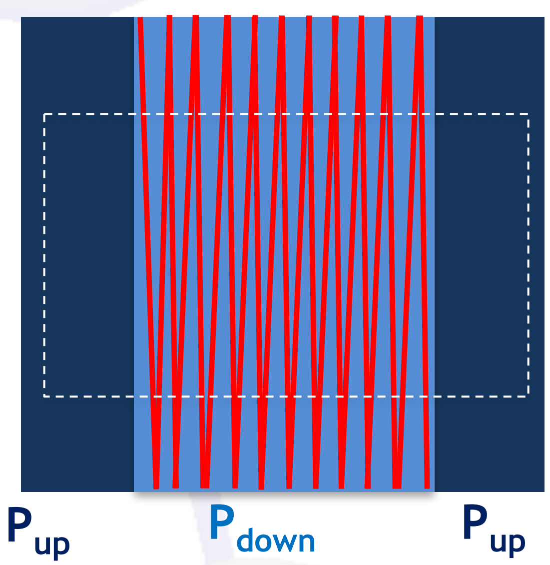

Locally mapping polarisation switching

PZT$_{RFS}$ negative bias

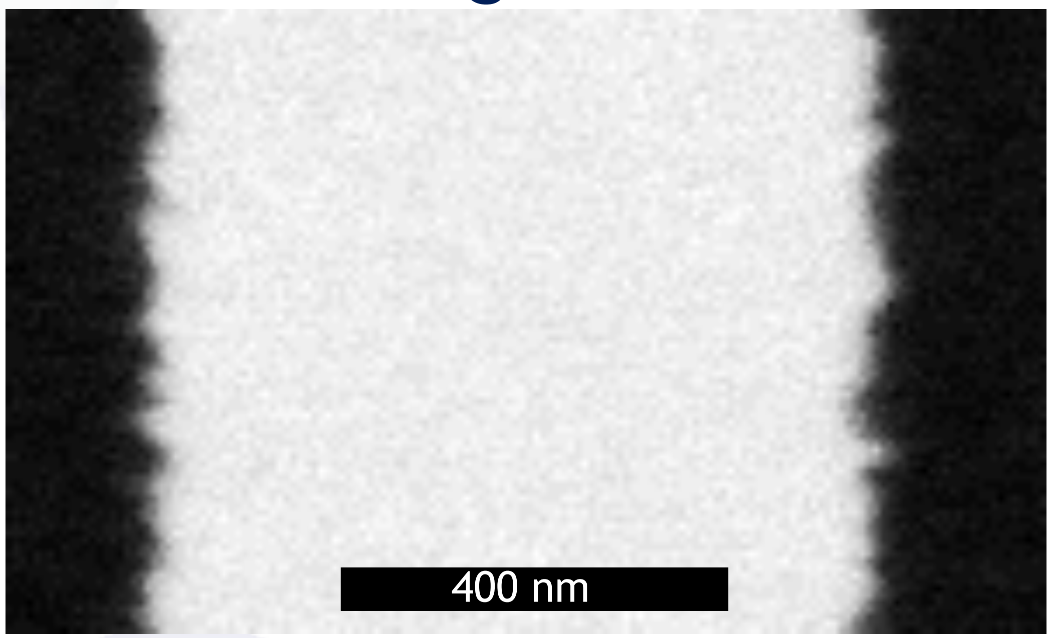

PZT$_{RFS}$ positive bias

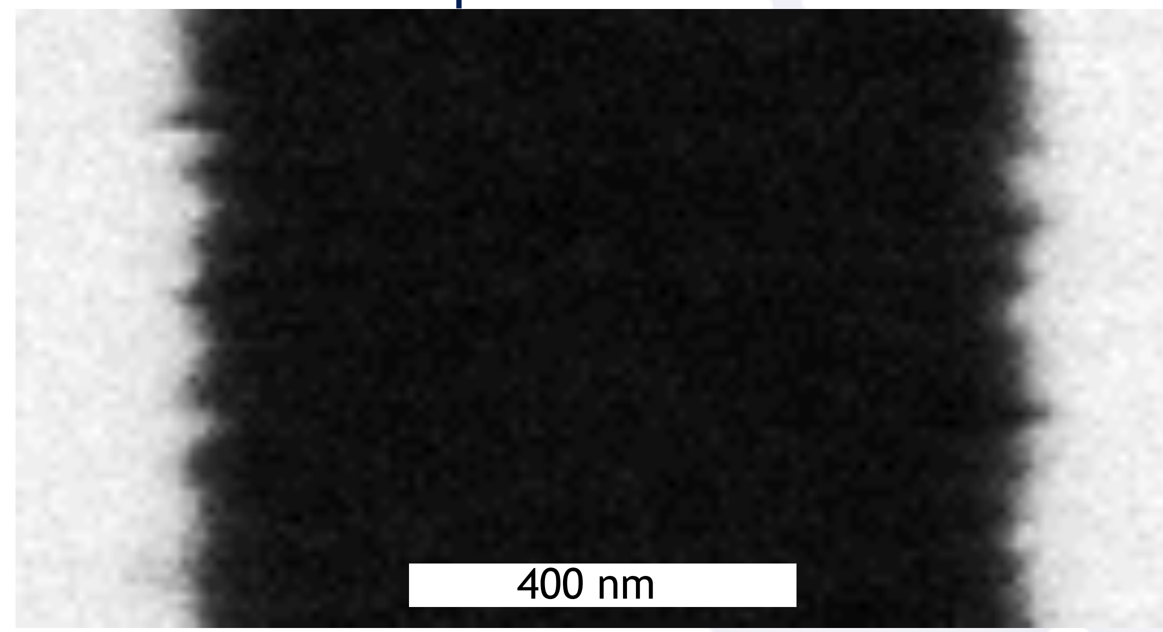

PZT$_{PLD}$ negative bias

PZT$_{PLD}$ positive bias

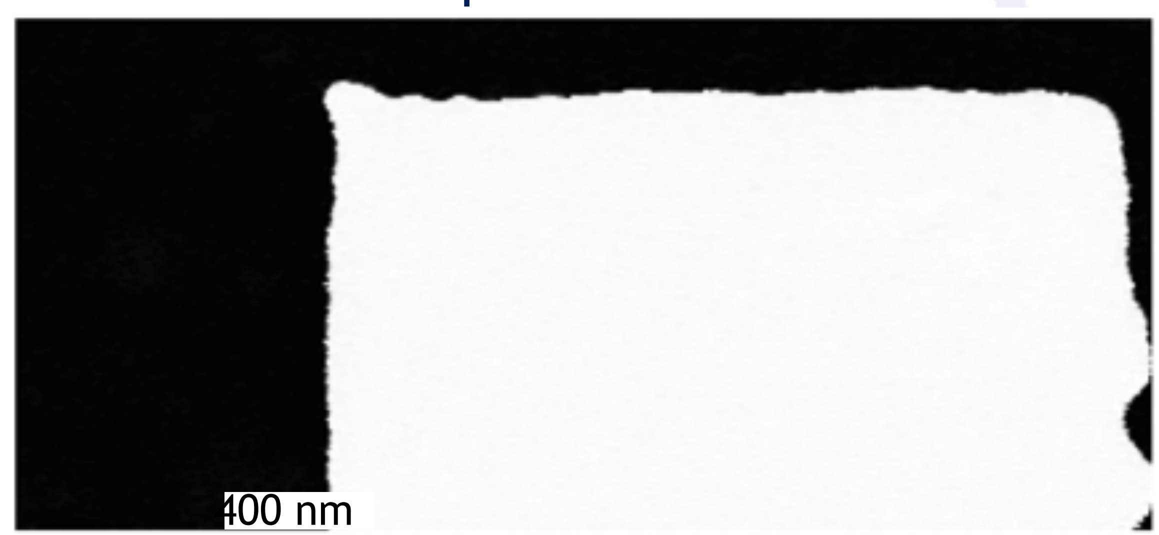

Locally mapping polarisation switching

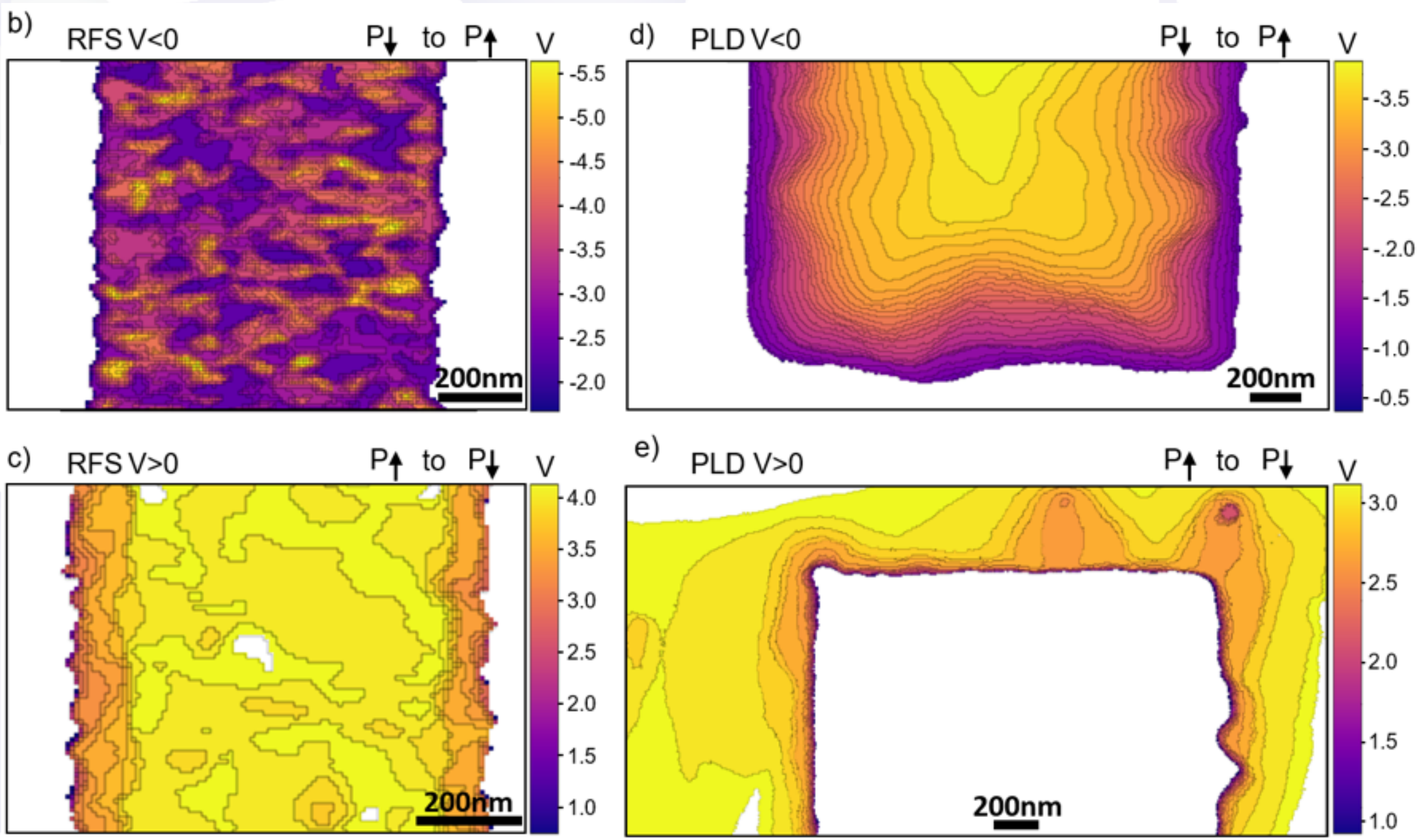

Lower switching threshold in PZT_{PLD}

Lower threshold for negative bias switching (written areas) in both

Switching dynamics - polarity AND history

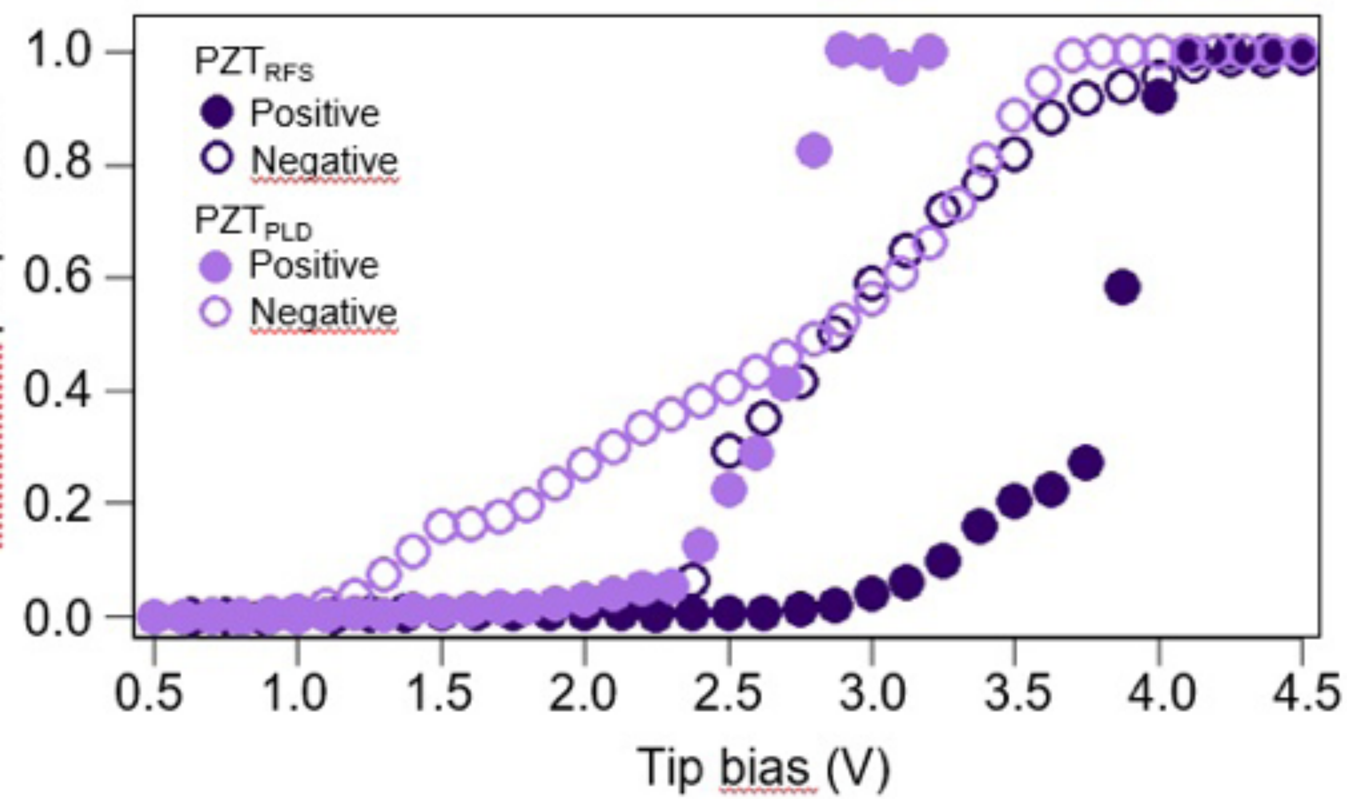

Highly asymmetric switching under positive vs. negative bias

Strong influence of a prior switching cycle which modifies the disorder/defect landscape

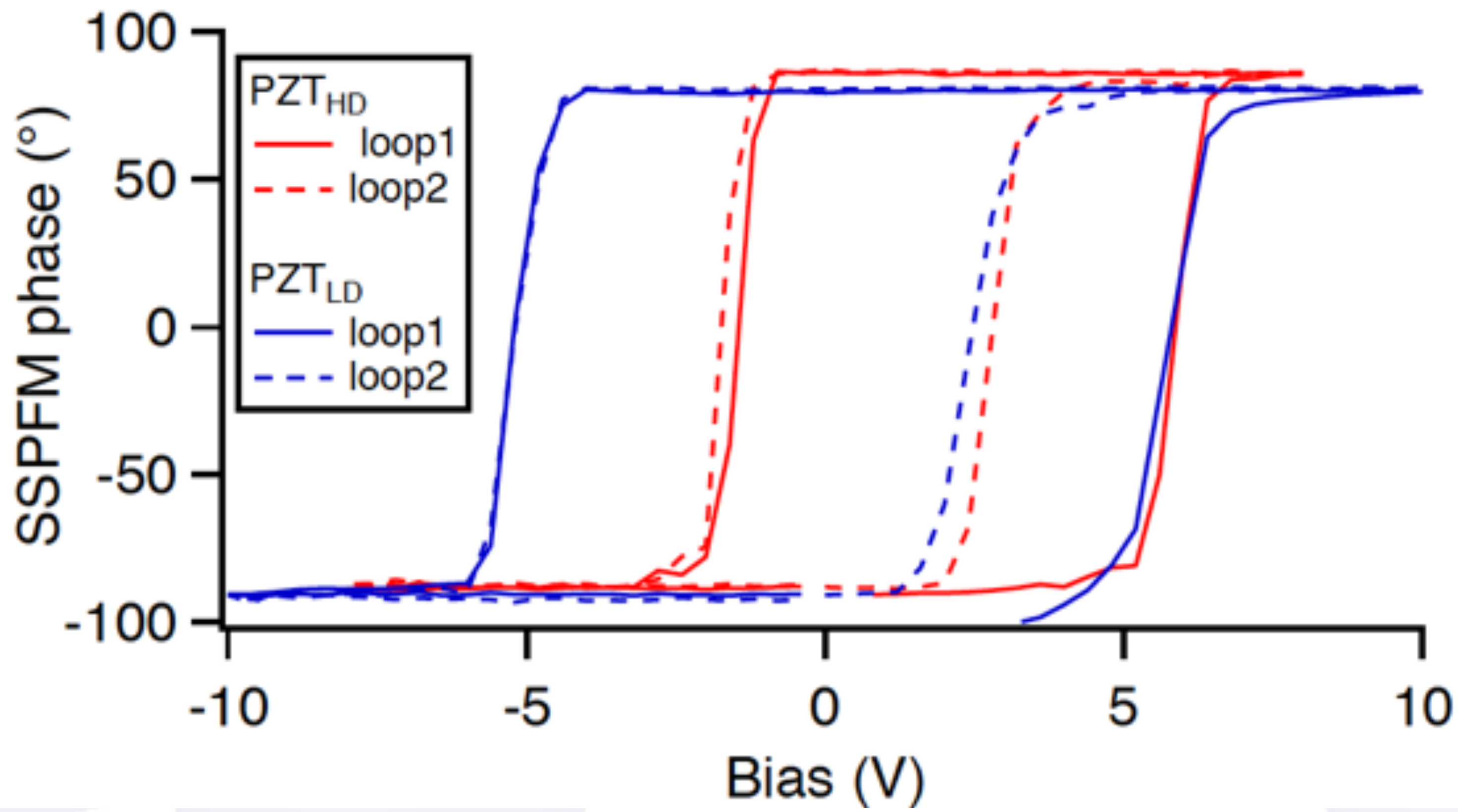

Identify contributions to size spectrum from nucleation, DW motion and domain merging

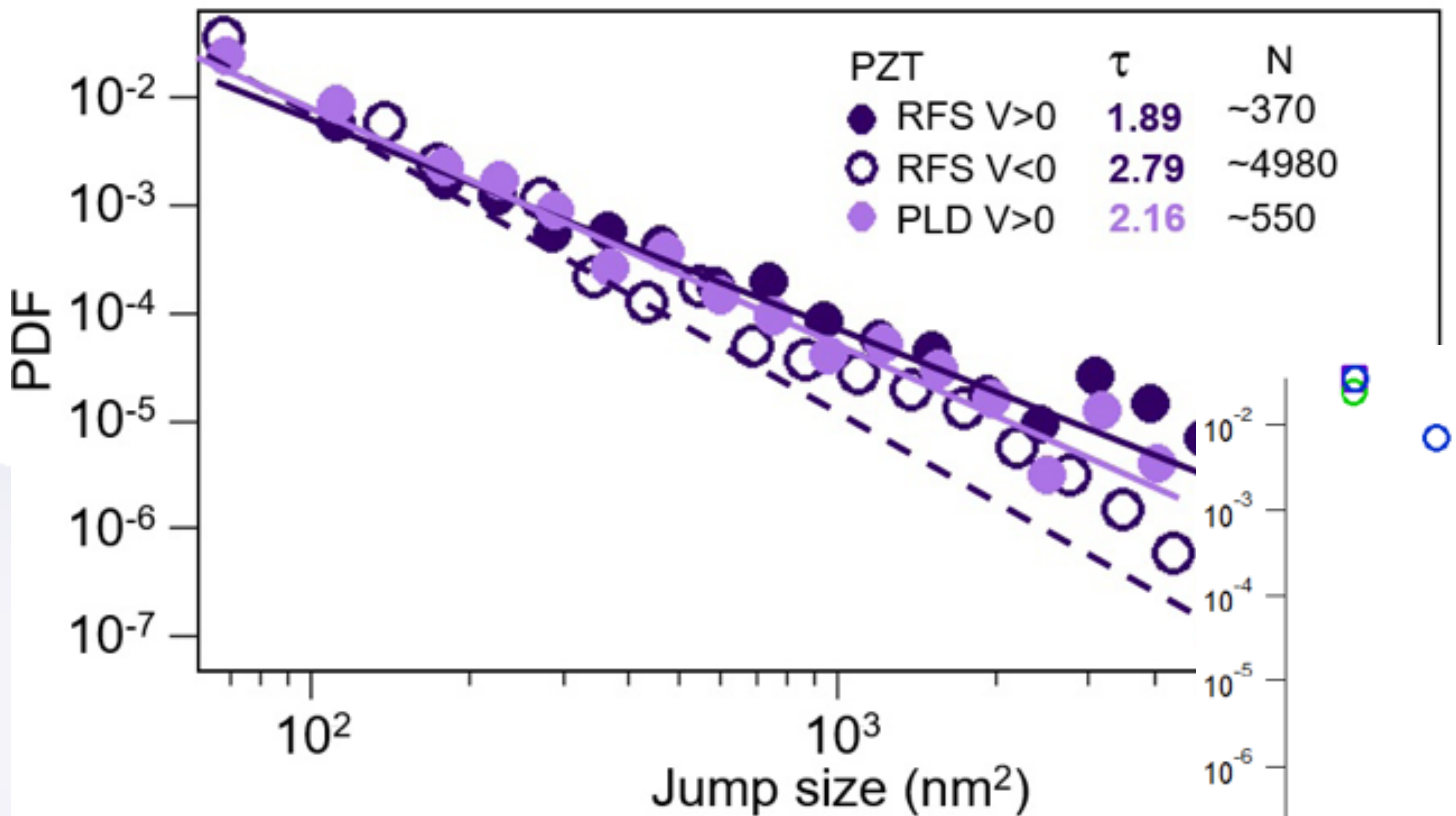

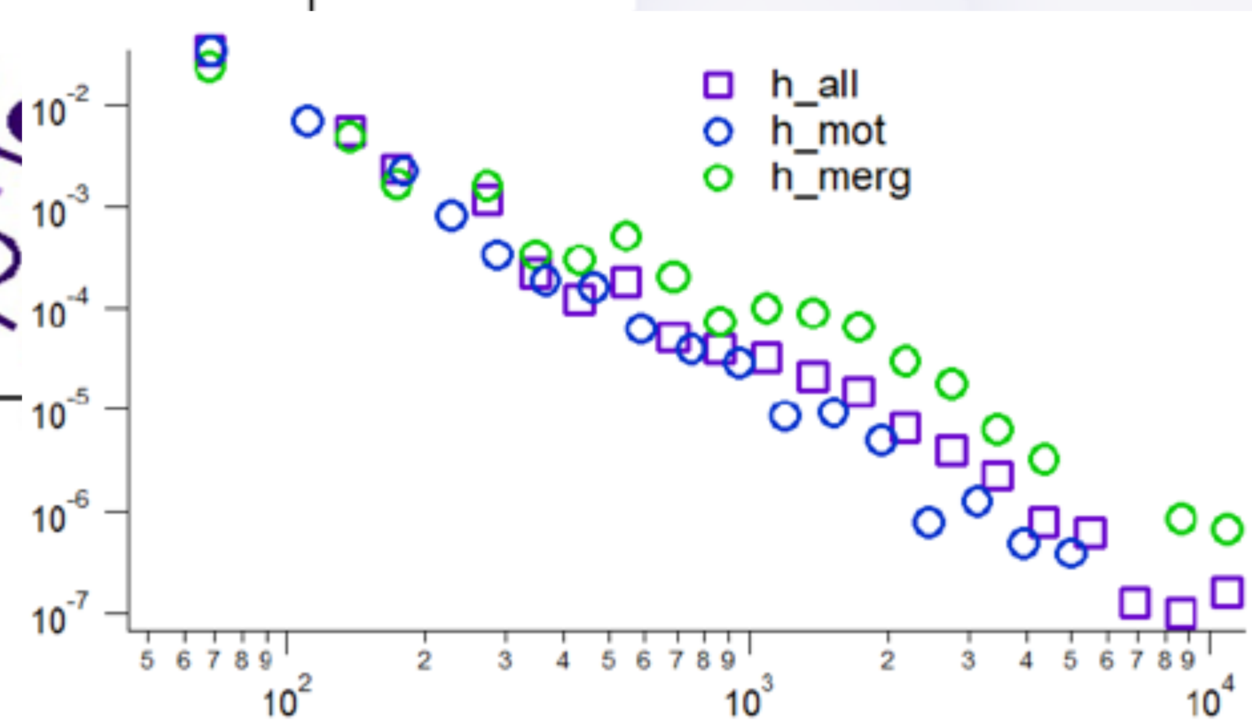

Avalanche size spectrum exponent sensitive to intrinsic defect landscape and defect injection during writing

DW motion events increase τ, merging events decrease τ

Effect of pinning strength on jump size exponent

In as-grown areas, switching events occur further from initial DW position with increasing tip bias

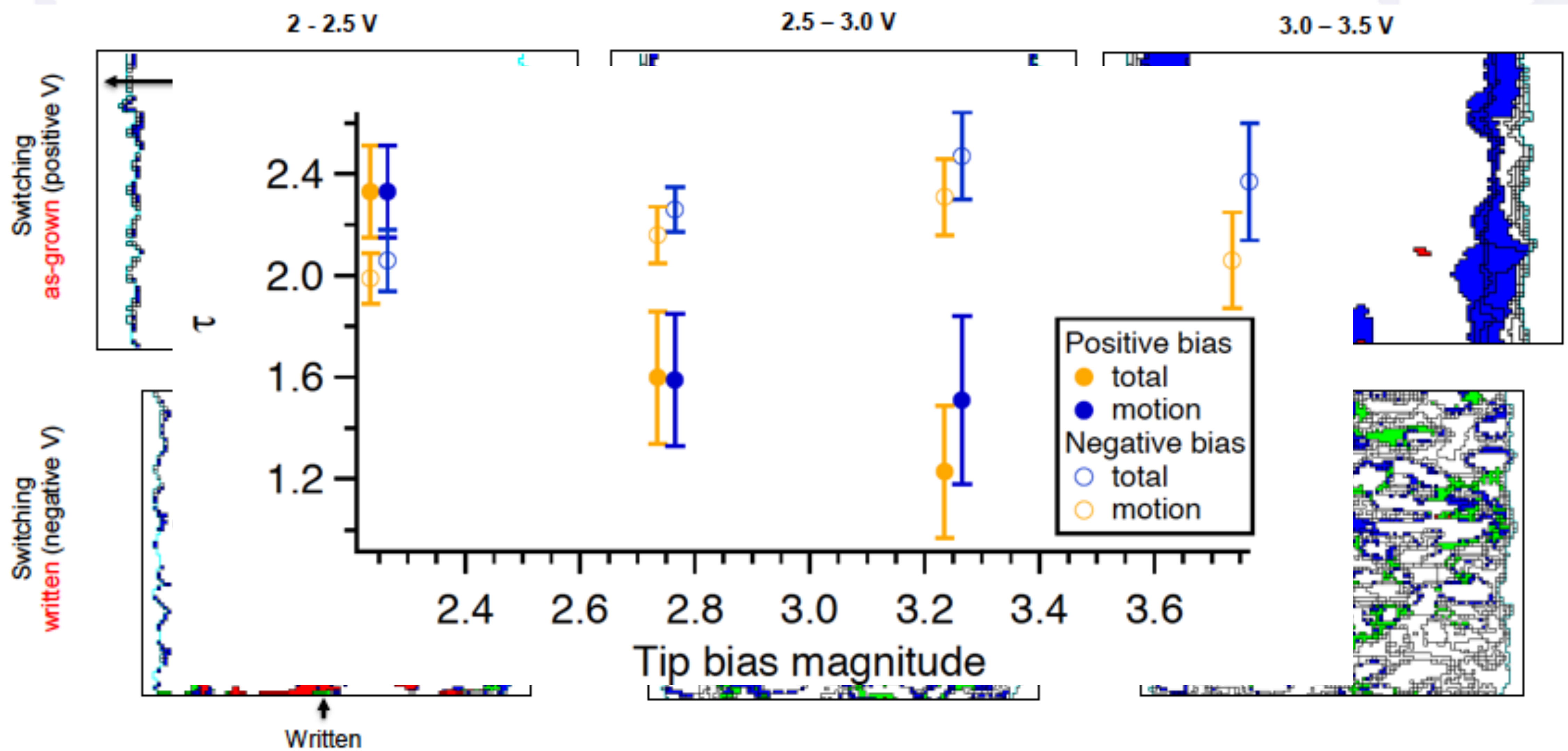

In previously switched areas, switching dominated by nucleation, possibly as a result of defect redistribution/injection during writing

Identifying creep and depinning regimes

PZT$_{RFS}$ | PZT$_{PLD}$

negative bias (switching written areas)

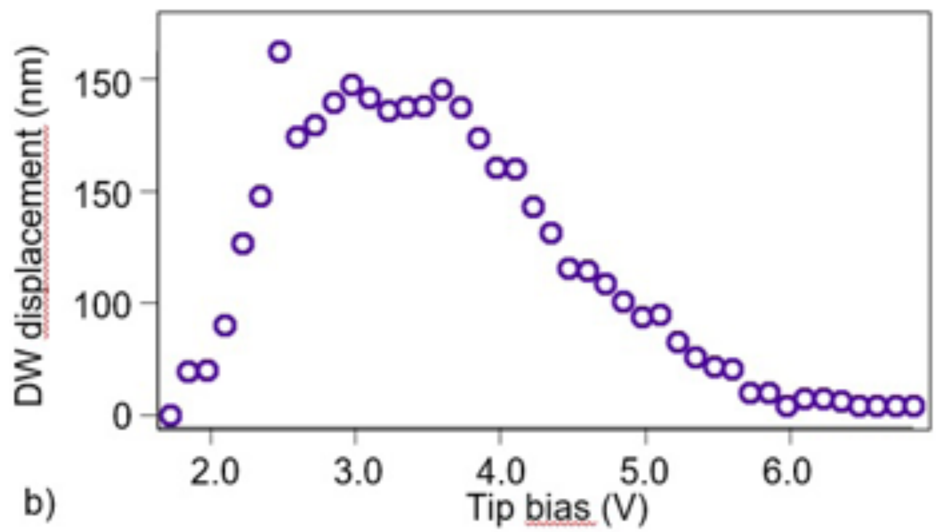

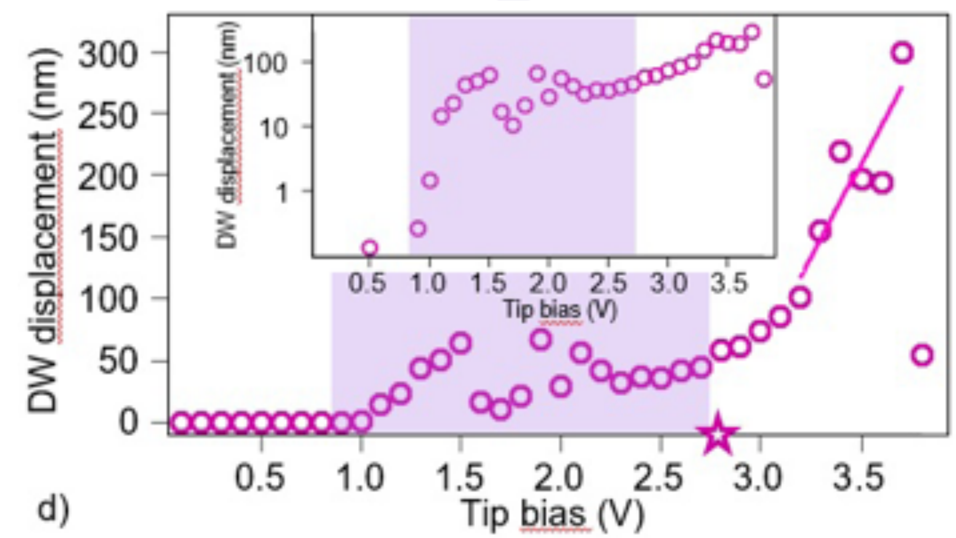

positive bias (switching as grown areas)

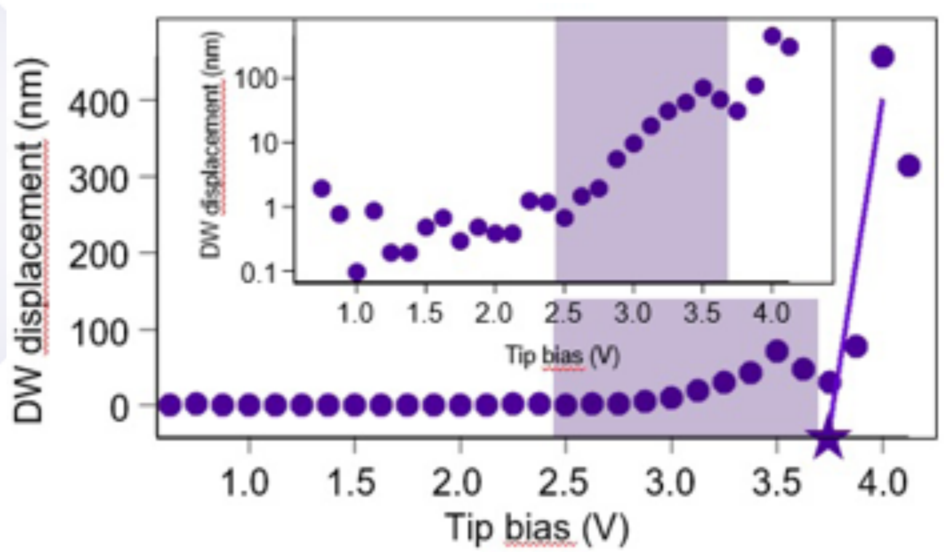

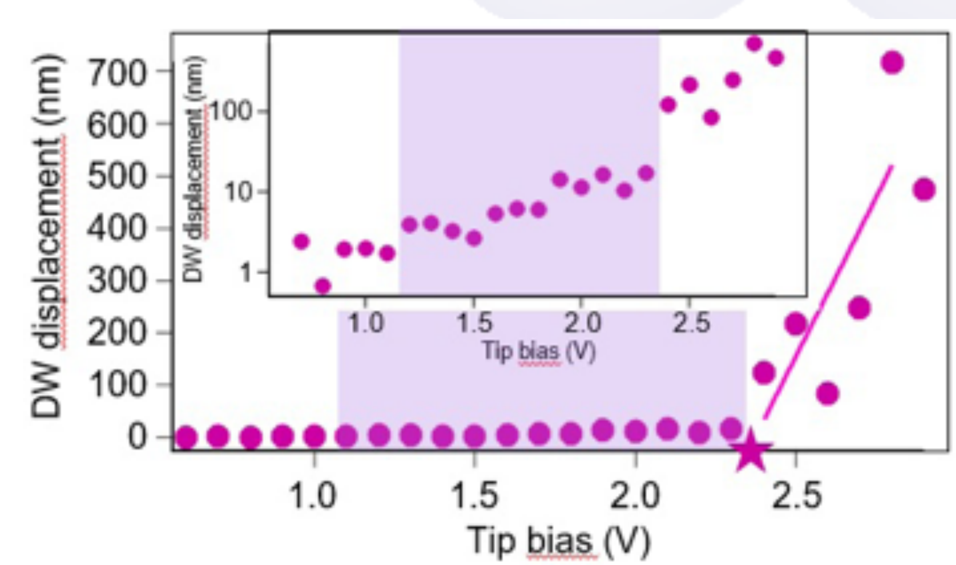

Avalanche size spectrum exponent sensitive to intrinsic defect landscape and defect injection during writing

Polarisation switching at "constant" voltage

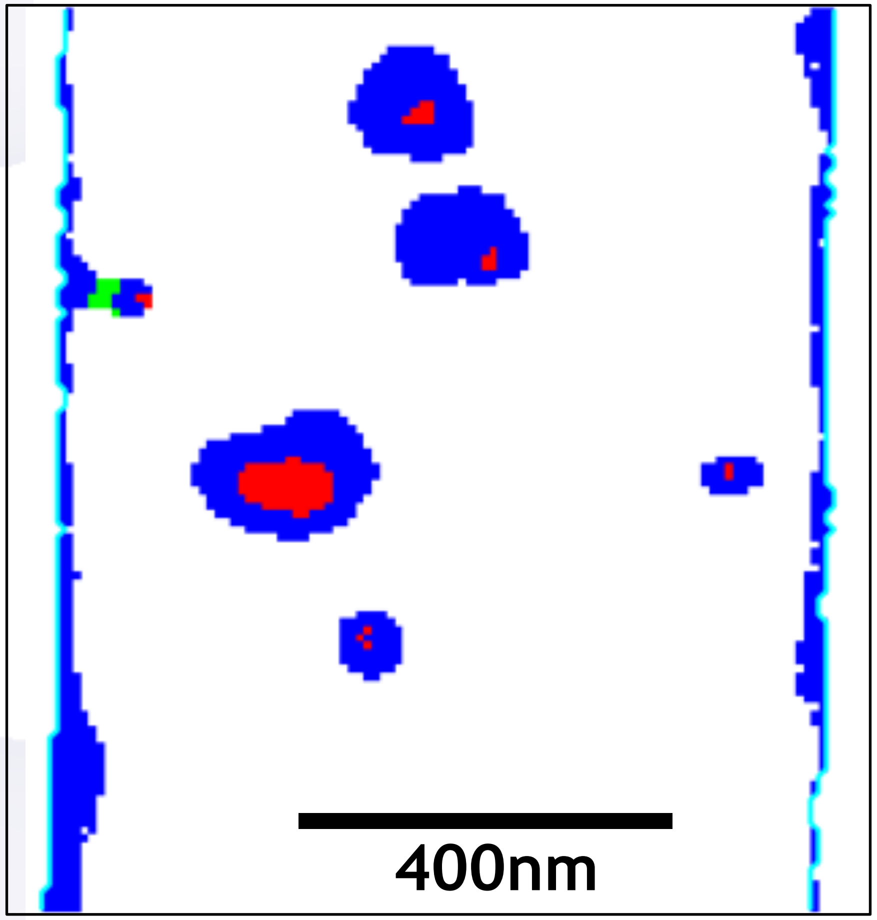

-3.5V

PZT RFS

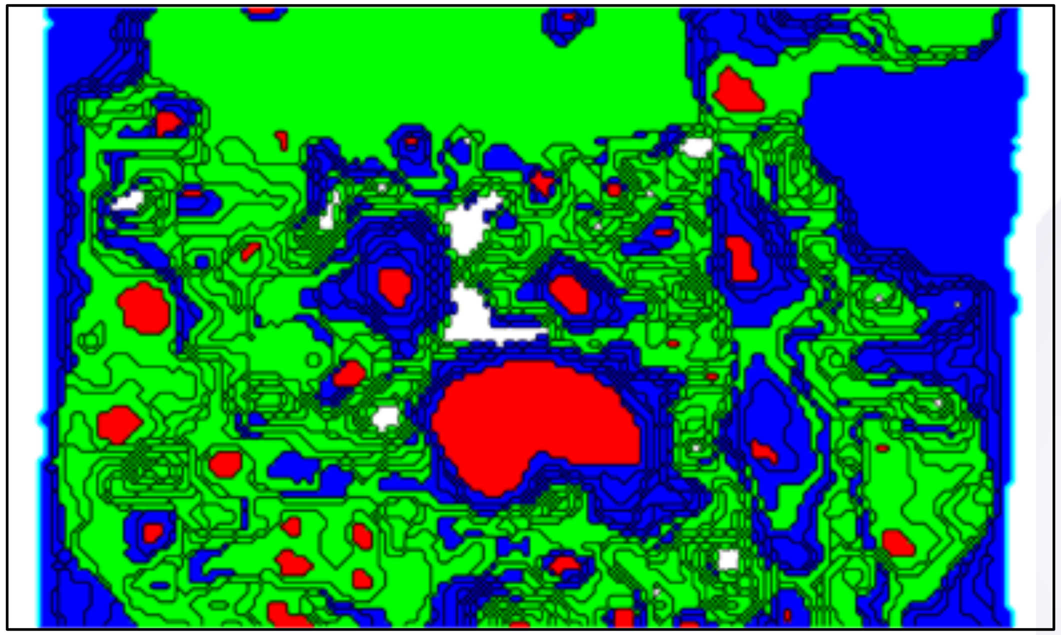

-5.0V

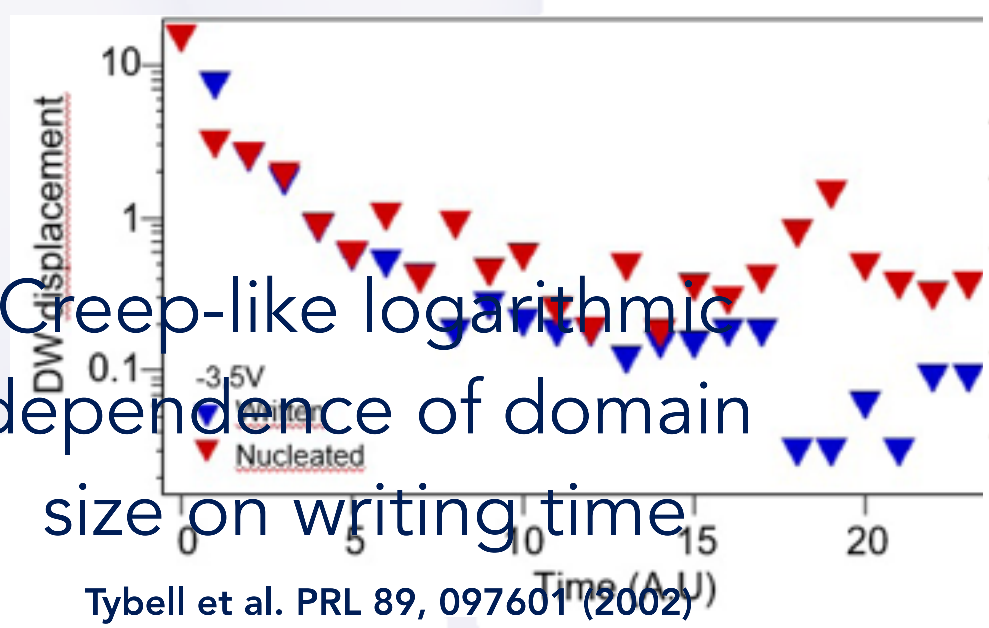

Creep-like logarithmic dependence of domain size on writing time

Tybell et al. PRL 89, 097601 (2002)

Stronger pinning a

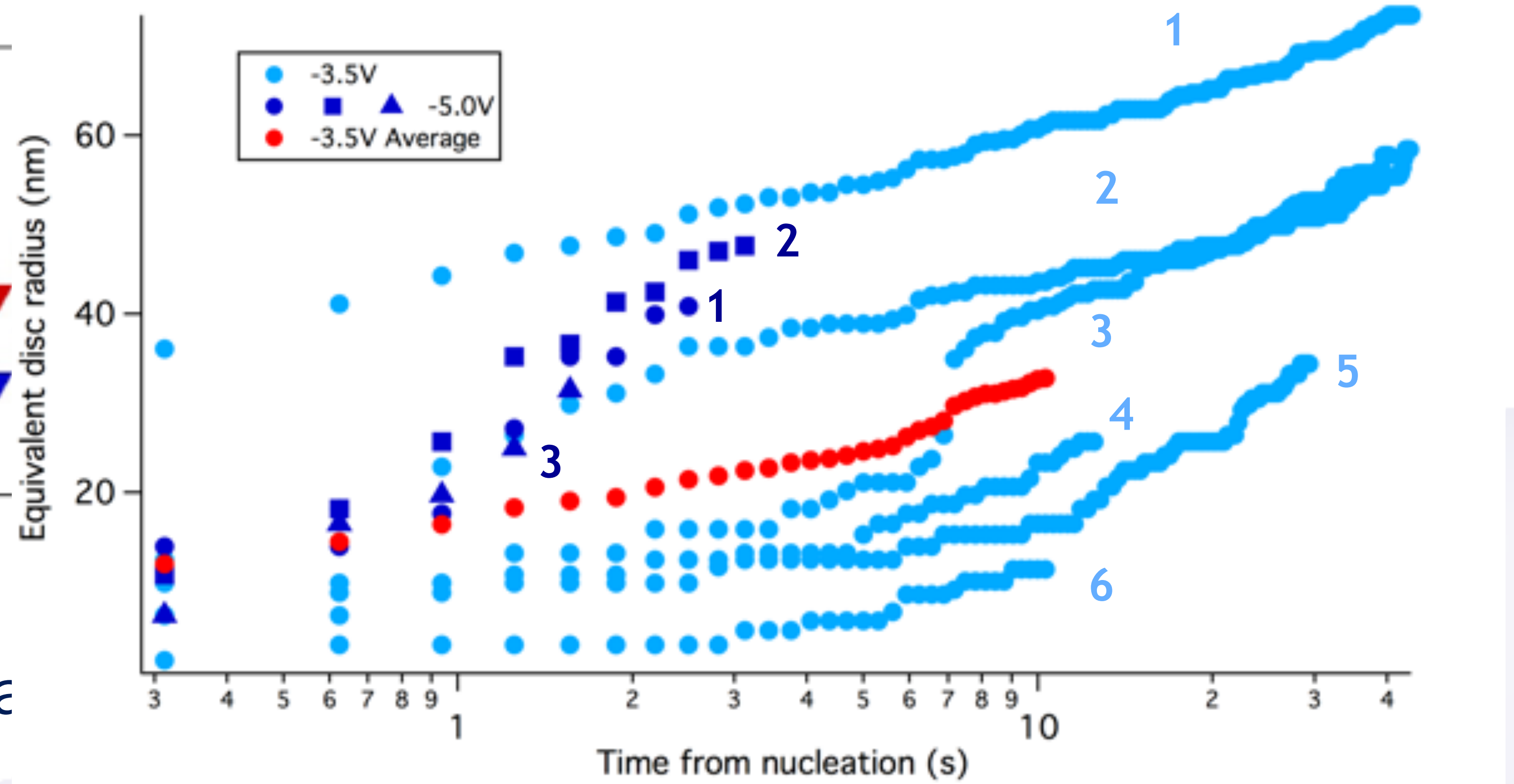

Importance of estimating the pinning force

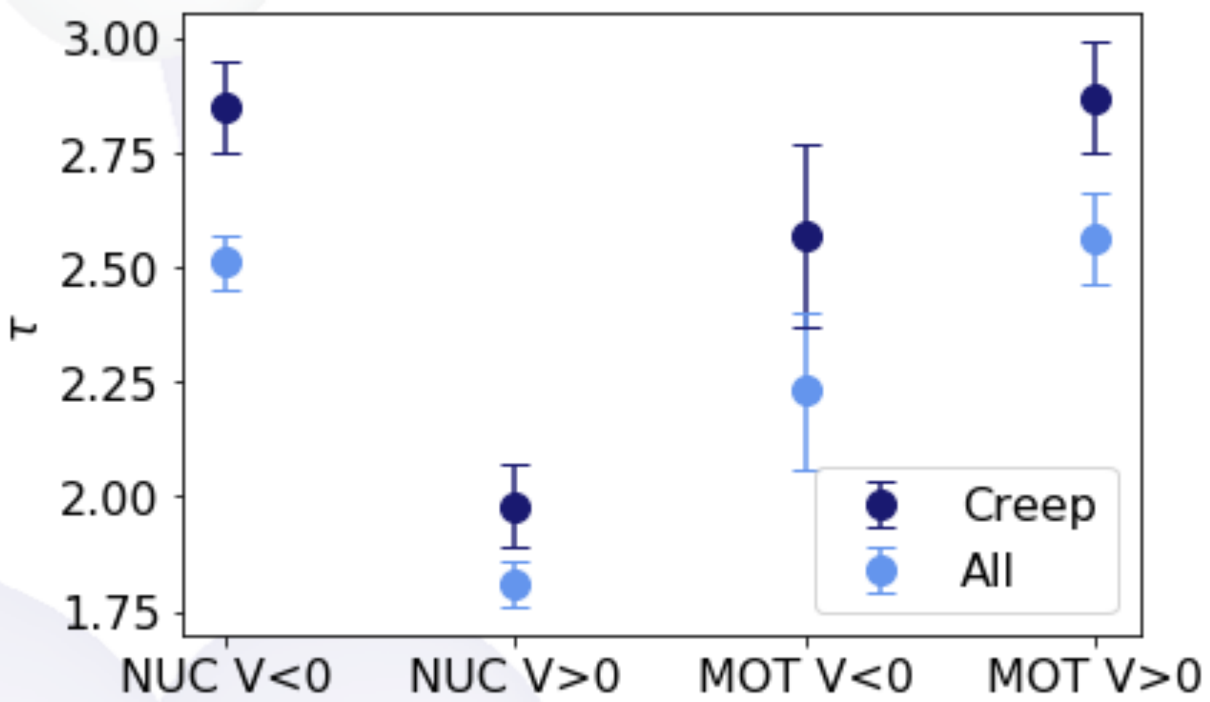

Systematic lowering of exponent values when events above the depinning threshold are included

Tukmantel et al. PRL. 126, 117601 (2021)

Perspectives

- analysis of spatial correlations between switching events in the creep and depinning regimes
- switching dynamics studies in sample families with controlled densities of extrinsic defects
- studies of roughness and dynamics in device-relevant geometries

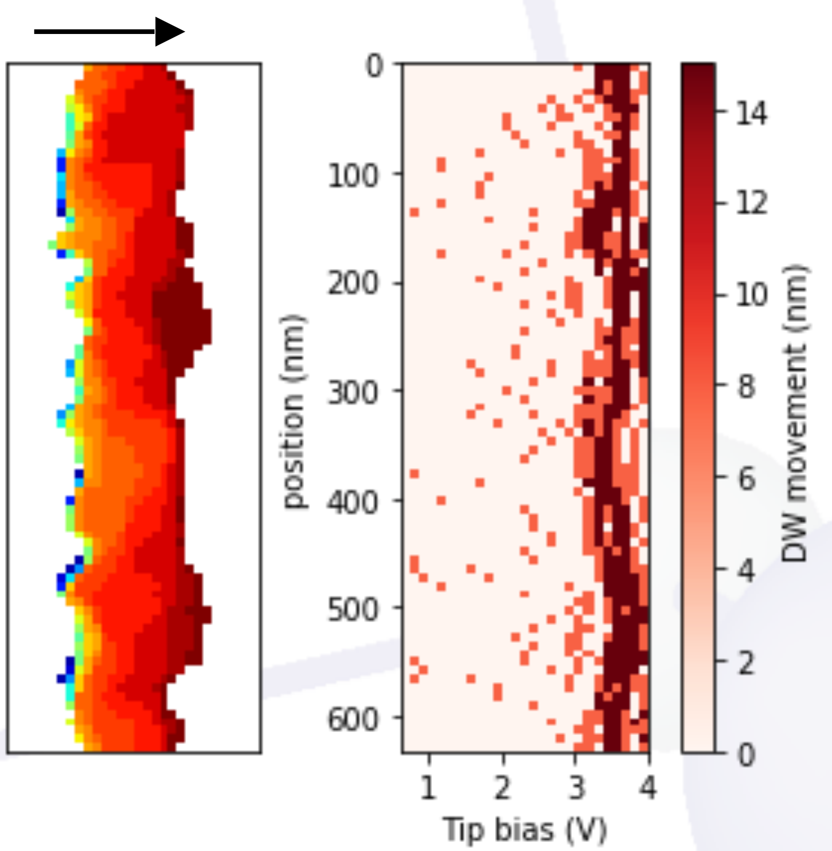

Driving domain walls at planar electrode edges


Guillaume Rapin


Sophia Ehrensperger


Nirvana Caballero

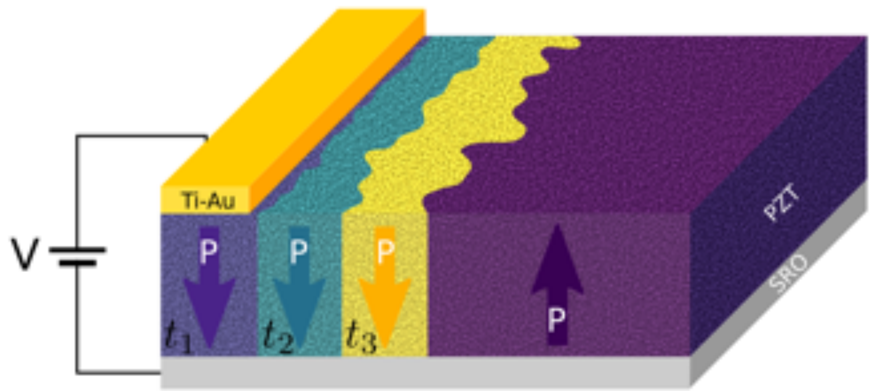

Rapin, Ehrensperger et al., APL. 119, 242903 (2021)

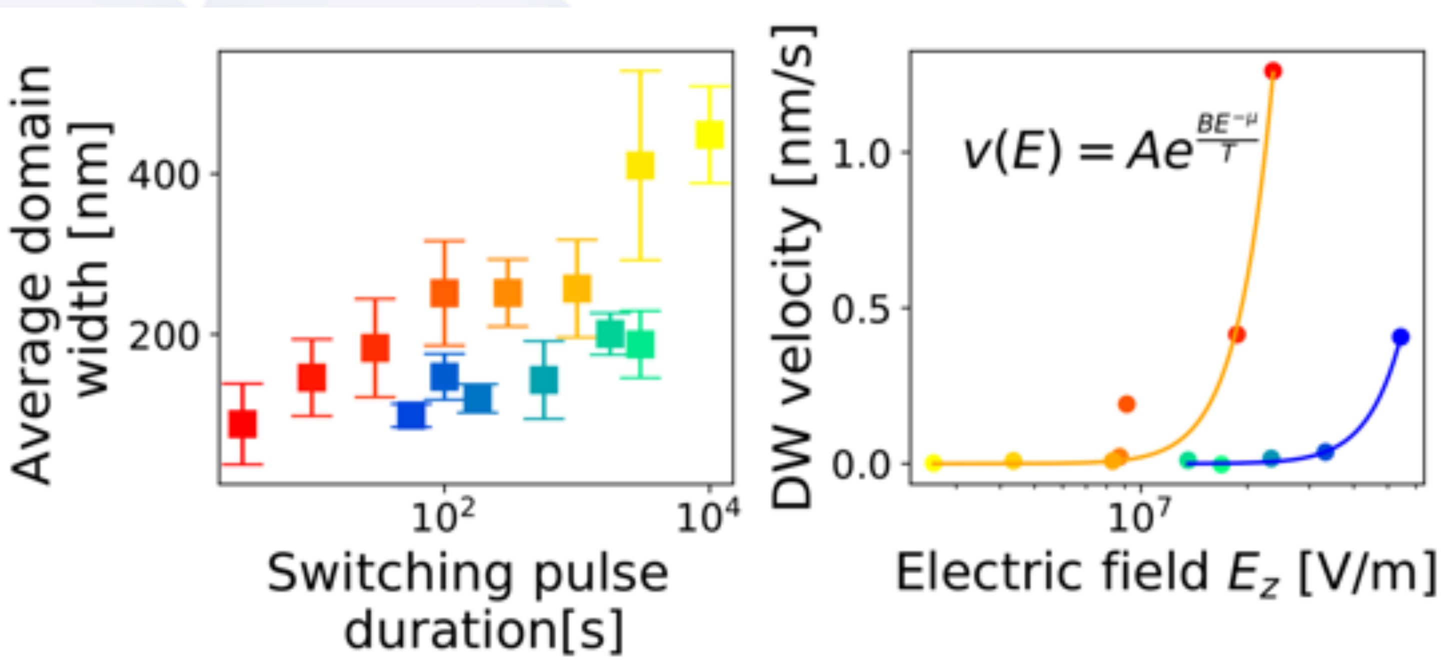

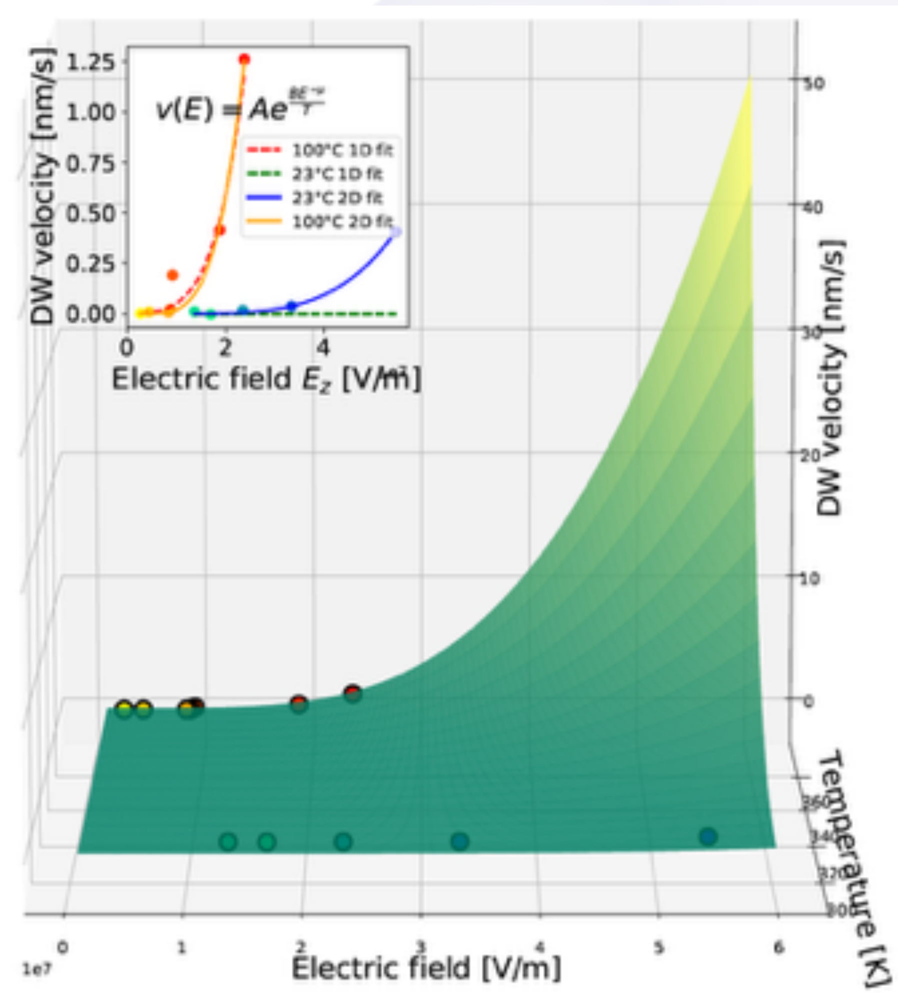

Domain wall dynamics as a function of driving force and temperature show strong effect of thermal activation and visible evolution of geometry

Quantifying evolution of domain wall roughness

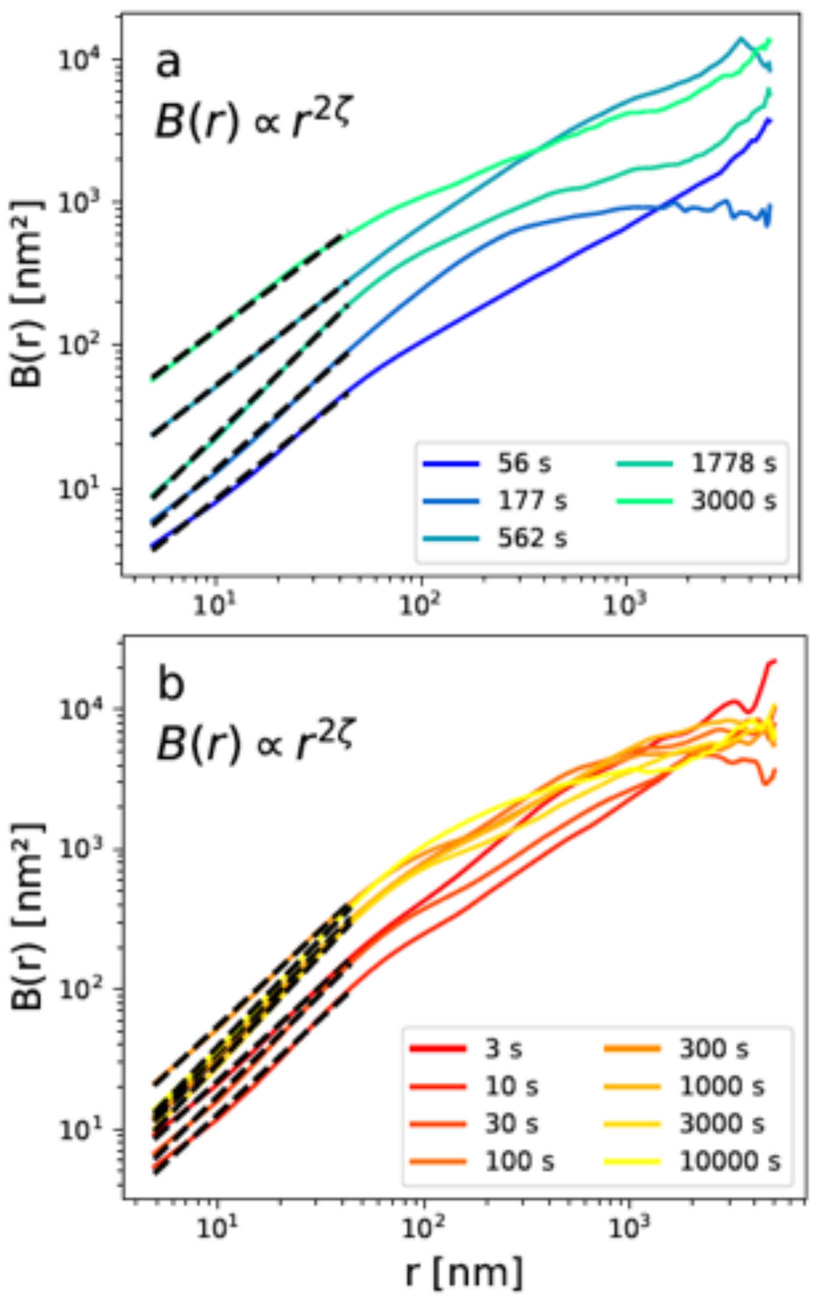

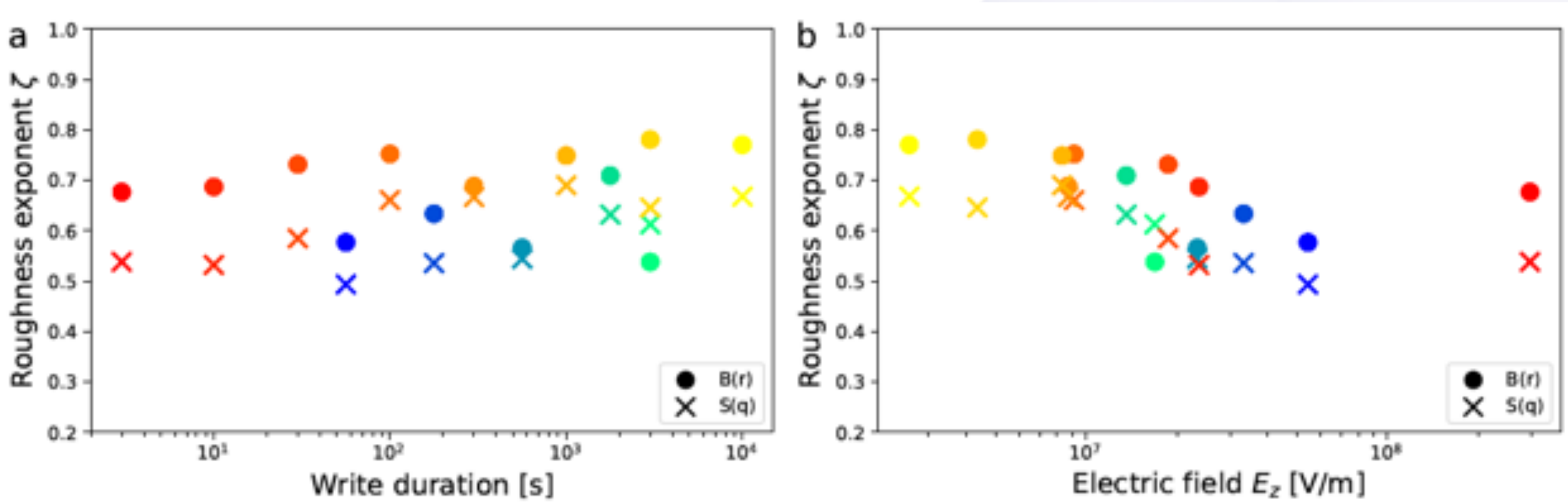

Significant roughening as DWs move into pristine disorder landscape

High roughness exponent values in more "equilibrated" systems

Effects of humidity on the electric field of the SPM tip

Jill Guyonnet

Cédric Blaser

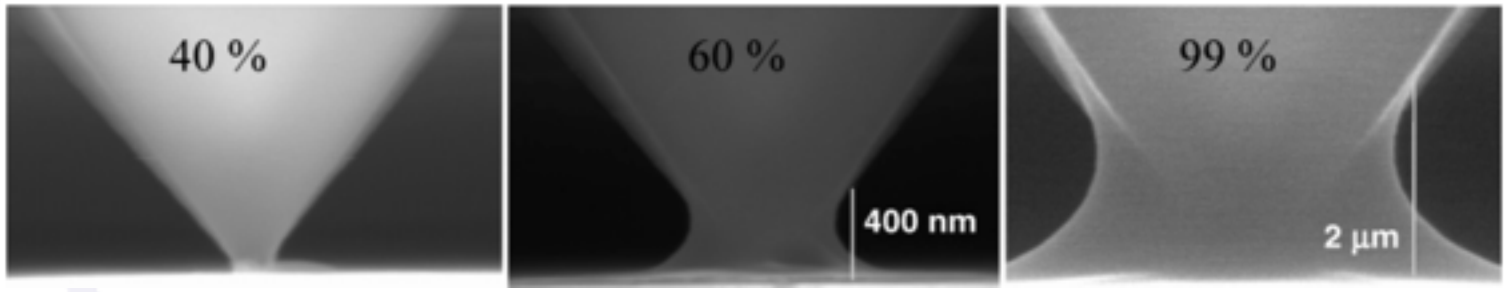

Weeks et al., Langmuir 21, 8096 (2005)

use Kelvin equation to

ork

lel with

ce water

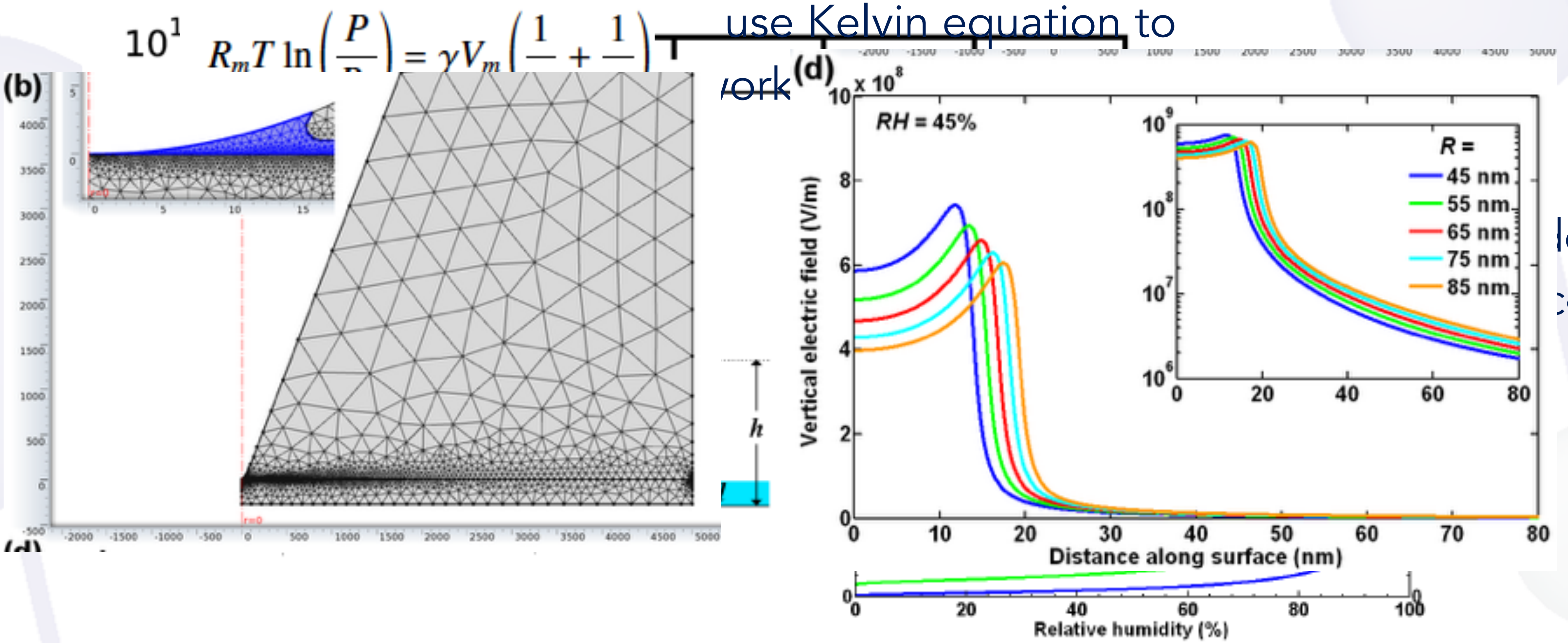

Disorder and environmental effects in UHV and ambient conditions

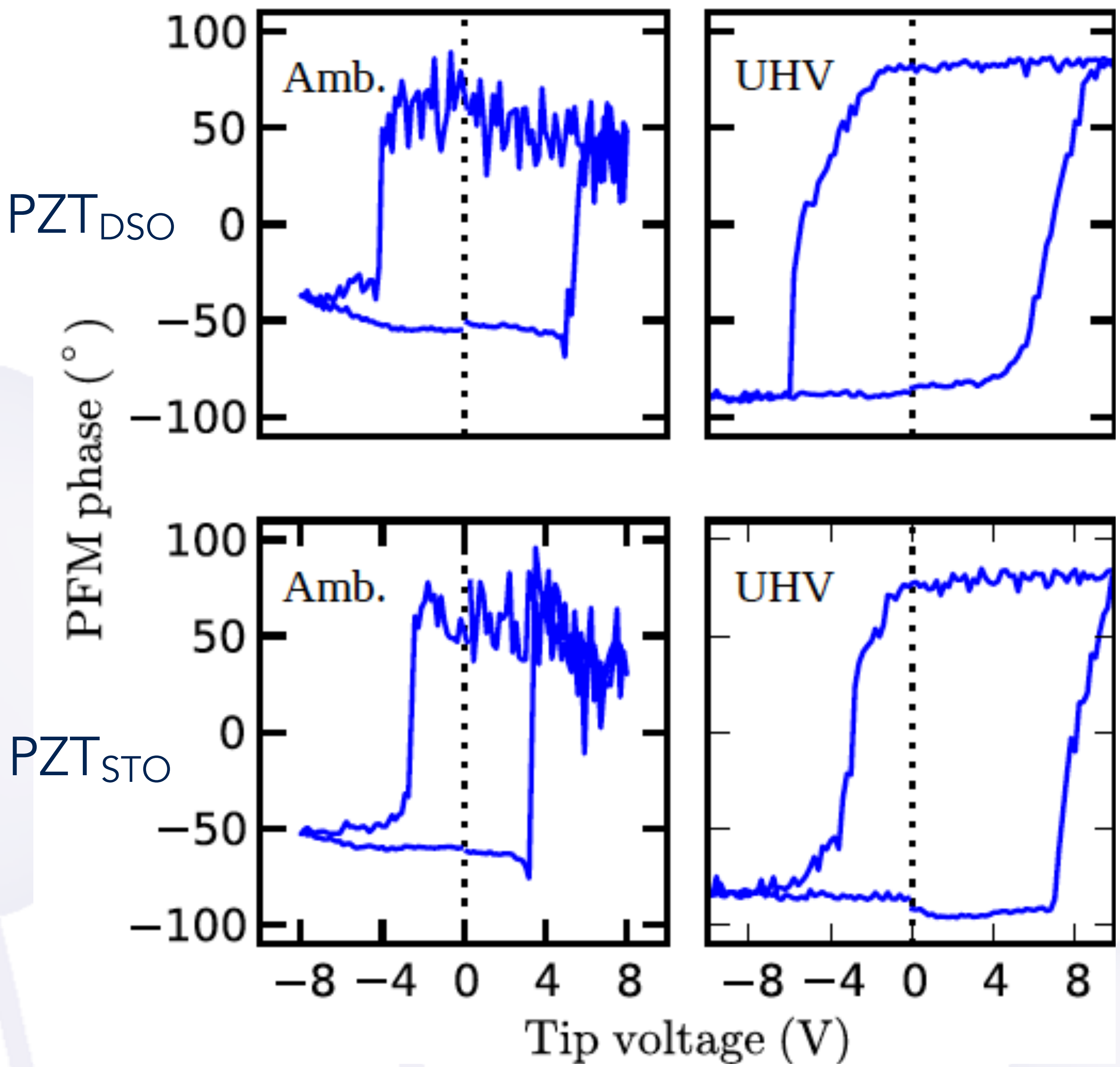

Measurements in ambient

Measurements in UHV after short sample bakeout at 100°C

Defect pinning vs screening by surface adsorbates

ambient PZT_{DSO} | ambient PZT_{STO}

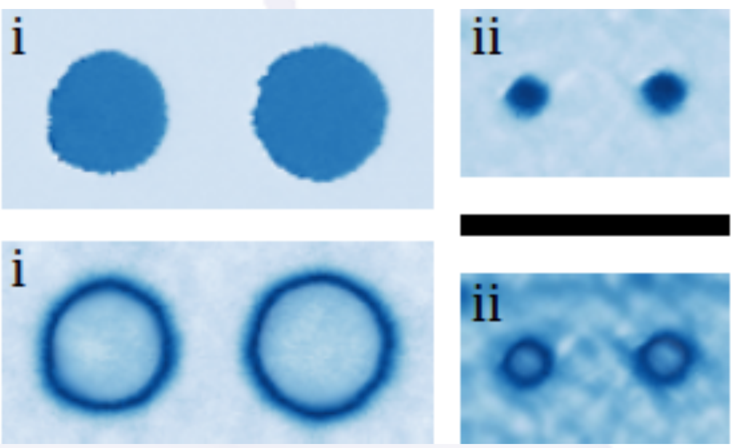

UHV PZT_{DSO} | UHV PZT_{STO}

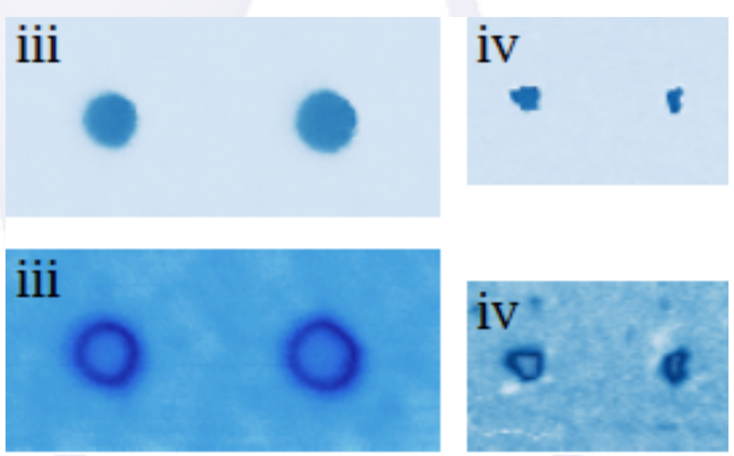

extracting dynamics

$$v(t_{n+1}) = \frac{r(t_{n+1}) - r(t_n)}{t_{n+1} - t_n}$$

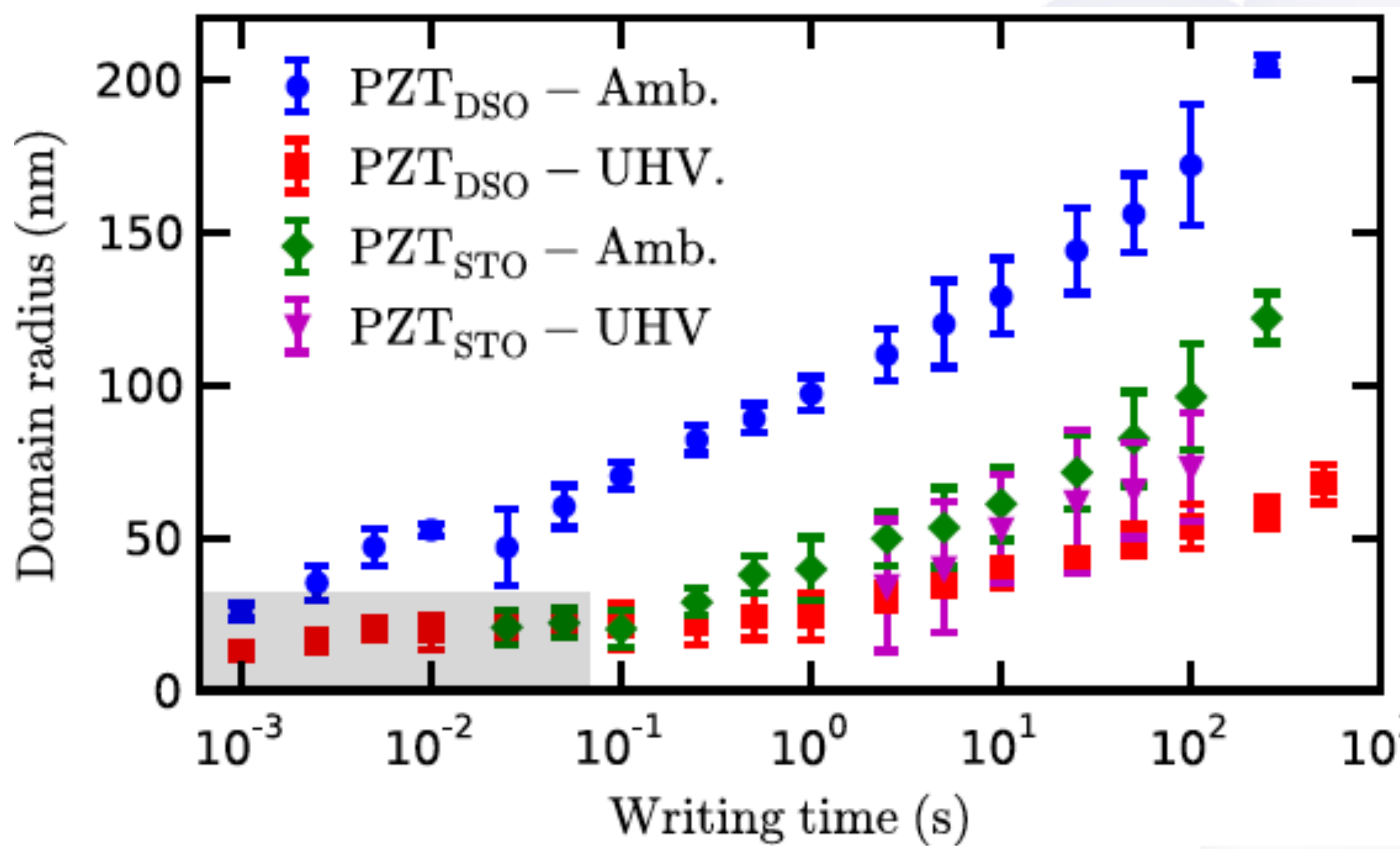

Slower domain growth in UHV

Smooth domain walls at ambient conditions

Increased roughness in more disordered films in UHV

Domain wall creep in UHV and ambient

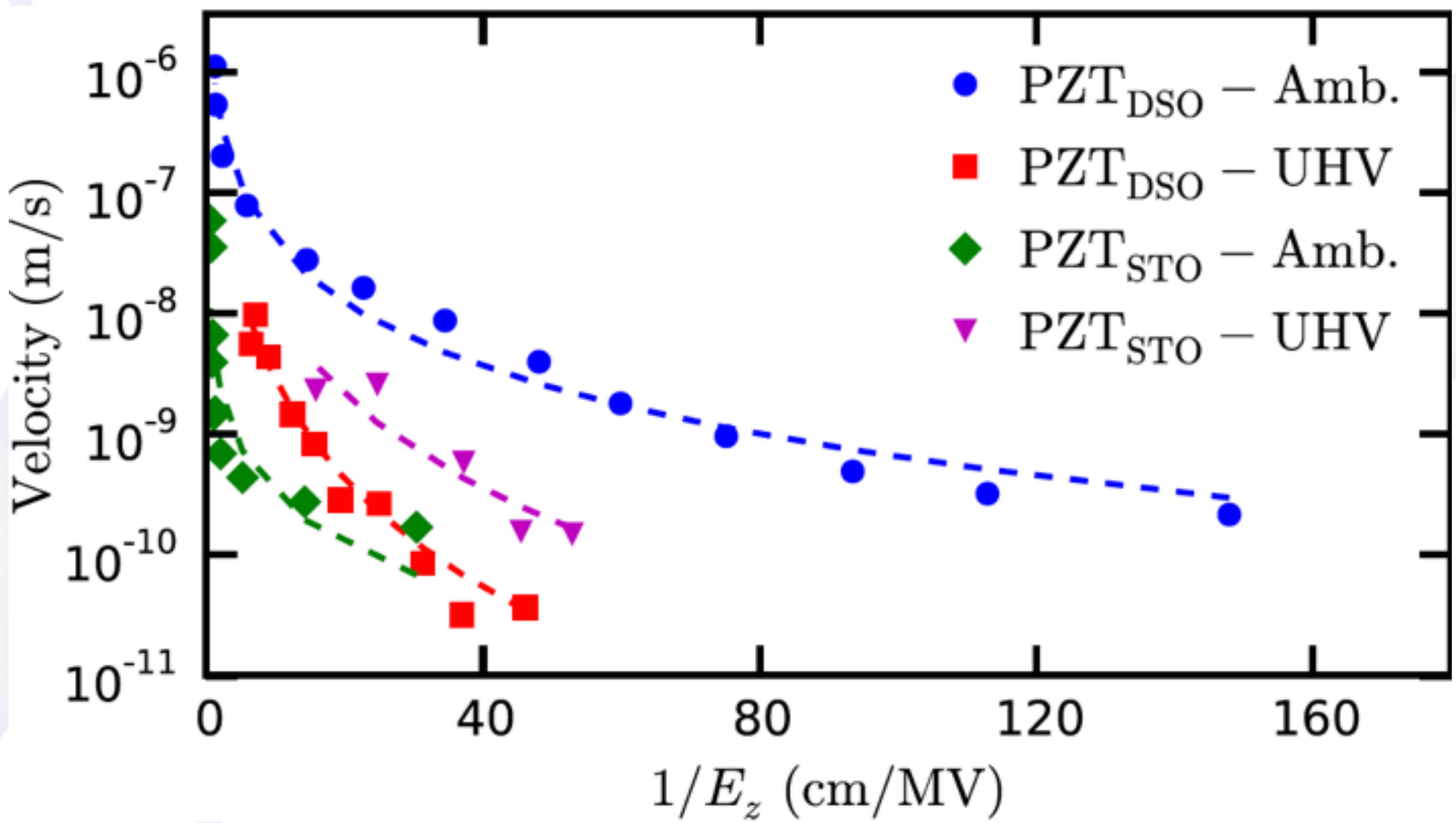

Surface water NOT essential for subcritical domain wall dynamics (suggested by Brugère et al., JAP 110, 052016 (2011))

Domain wall roughness in UHV and ambient

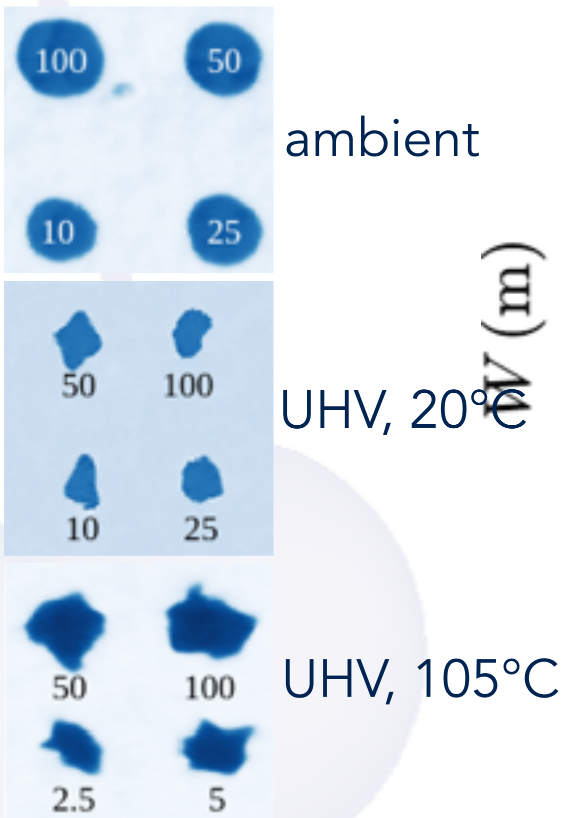

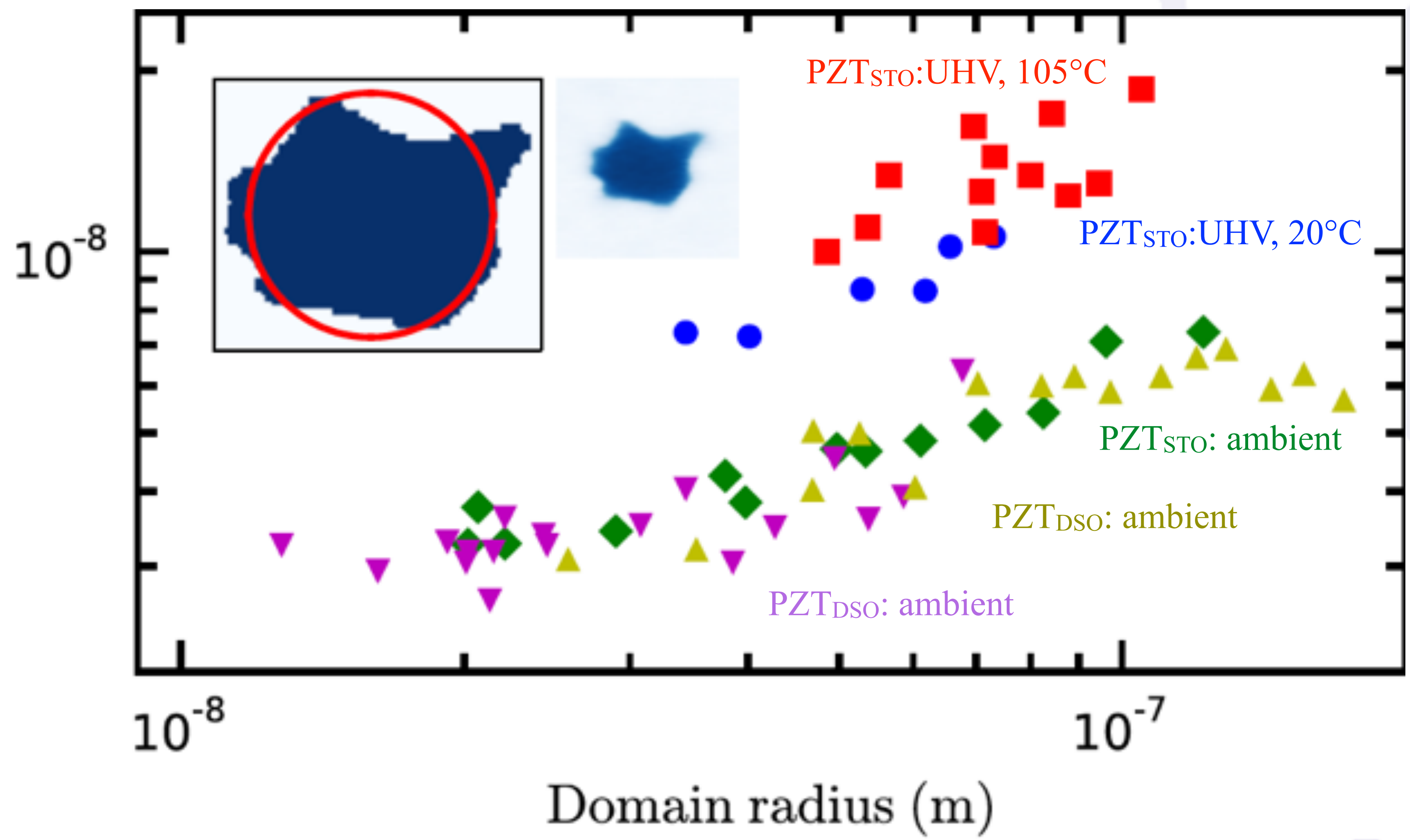

$$w(r) = \sqrt{\left\langle \left[u(z) - \langle u \rangle_r \right]^2 \right\rangle_r} \sim r^{\zeta}$$

Higher domain wall roughness in UHV for films with more defects

Numerical switching simulations in GLD framework confirm observations

Sebastian Bustingorry

$$f(\boldsymbol{R}) = \alpha\left(-\frac{P^2}{2} + \frac{P^4}{4}\right) + \beta\frac{|\Delta P|^2}{2} + \gamma\int \frac{PP'}{|\boldsymbol{R}-\boldsymbol{R}'|^3}d\boldsymbol{R}' - e(\boldsymbol{R},t)P + \sqrt{T}\eta$$

double-well potential barrier height

$$\alpha = \alpha_0(1 + \Delta\xi)$$

random-bond disorder strength

domain wall energy

dipolar interaction

less screening = higher dipolar term

electric field

$$e(\boldsymbol{R},t) = e_0/|\boldsymbol{R}|$$

temperature

square lattice

start from monodomain configuration

apply a field at center for a given time

let domain relax

Bustingorry et al., JPCM 33, 354001 (2021)

Rougher domains and slower growth in the presence of disorder

Surface water screening of dipolar interactions is important

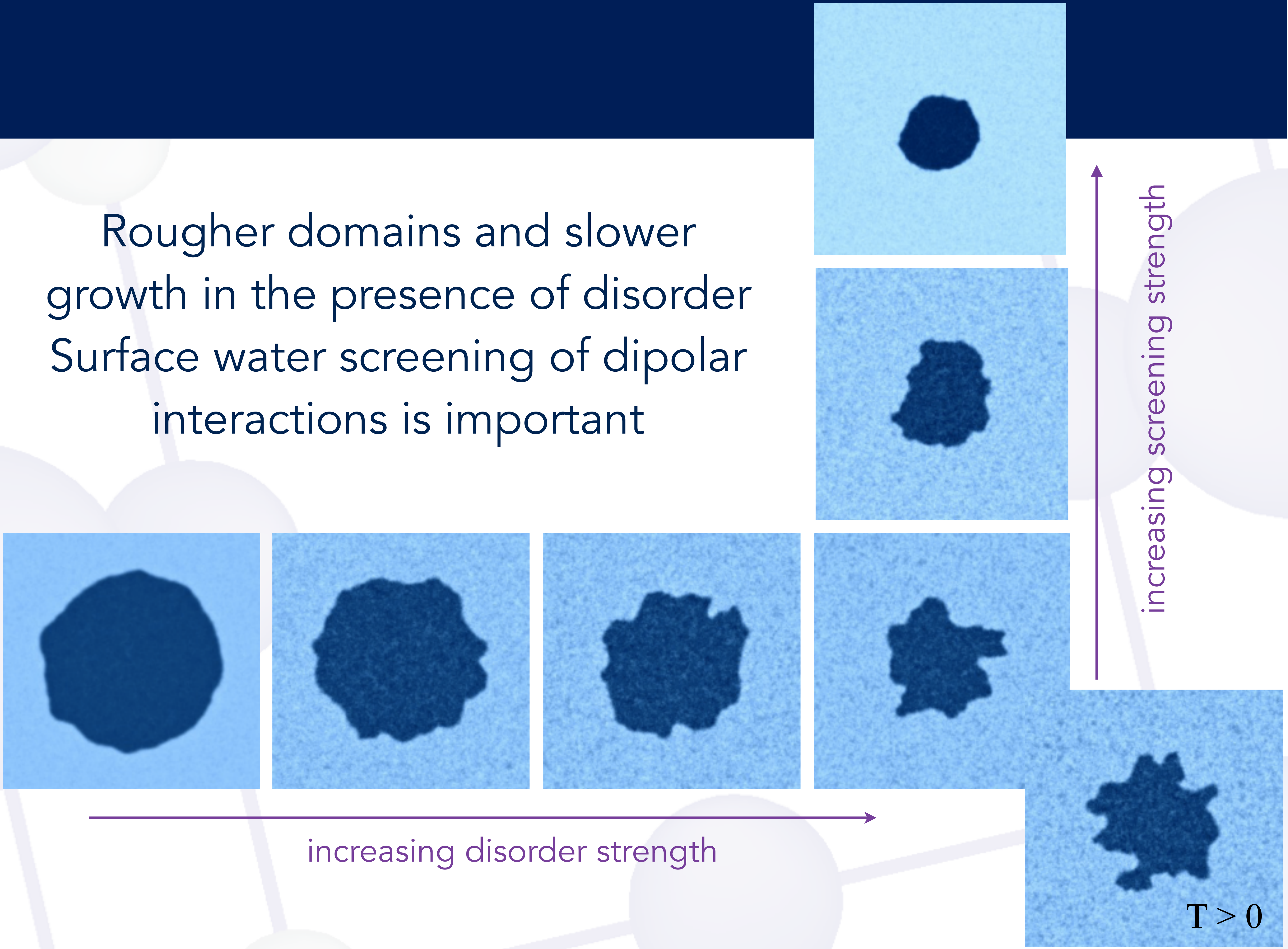

Complex polarisation textures at the nanoscale

Flux-closure domains and superdomains in thin films, single crystal and superlattices

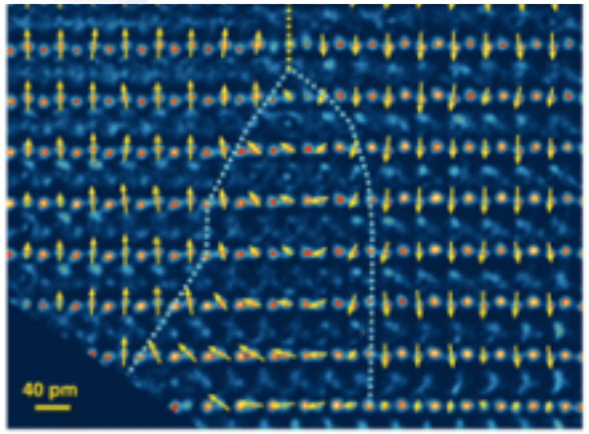

Jia et al, Science 331, 1420 (2011)

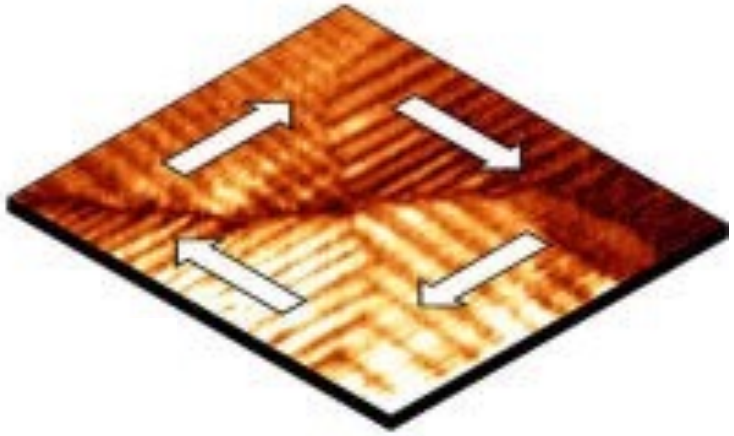

McQuaid et al, Nano Lett. 14(8) (2014)

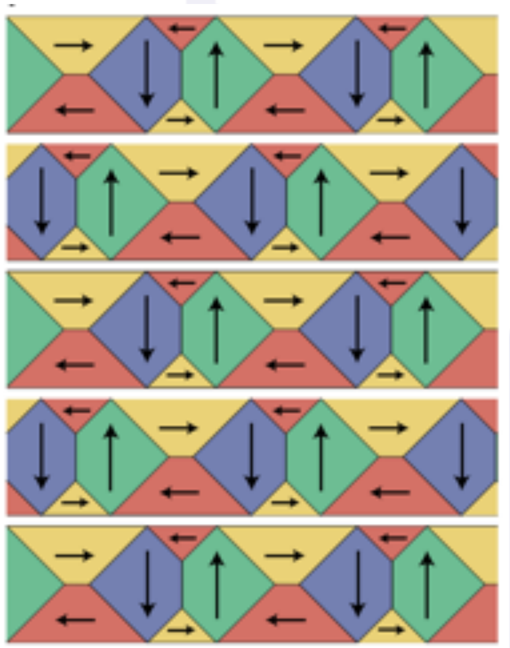

Hadjimichael et al, Nat. Mat. (2021)
Tang et al, Science 348, 6234 (2015)

Polar vortices

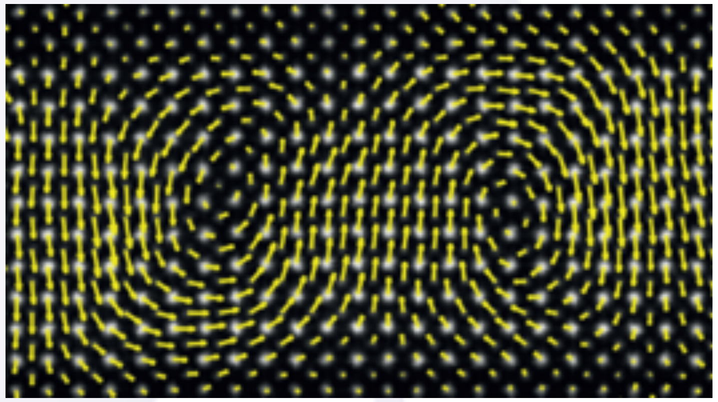

Yadav et al, Nat. 530, 198-201 (2016)
Li et al., Nat. Comm. 8, 1468 (2017)
Li et l., Nat 592, 376 (2021)
Hong et al., Nano LEtt. 21, 3533 (2021)

Bubble domain zoology

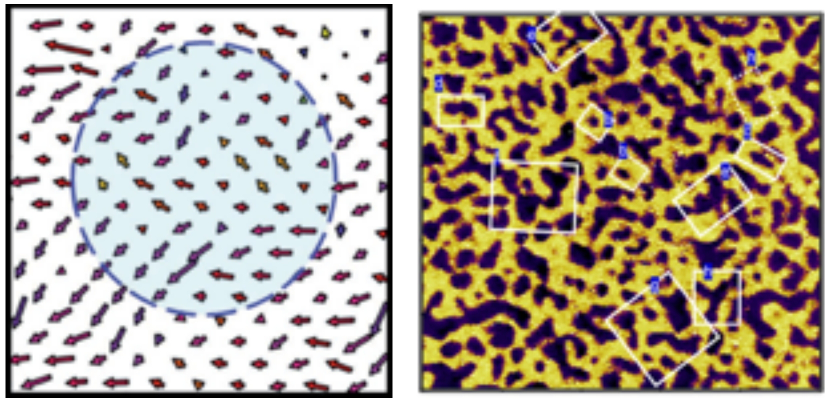

Zhang et al, Adv. Mat. 29, 46 (2017)
Nahas et al., Nat. Comm 11, 5779 (2020)
Govinden et al., PRM 5, 124205 (2021)

Skyrmions

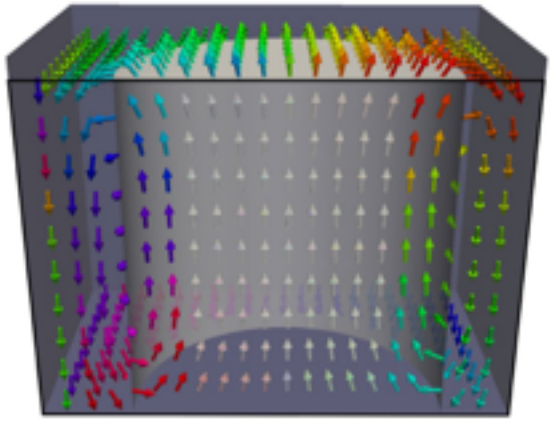

Das et al, Nature 568 (2019)
Gonçalves et al, Sci. Adv. 5, eaau7023 (2919)

Complex polarisation patterns arise as an interplay between strain and electrostatic boundary conditions

Pinned elastic interfaces in biology

"can you use this physics description to look at our wound healing profiles?"

Steven Brown

Elisabeth Agoritsas

wound healing

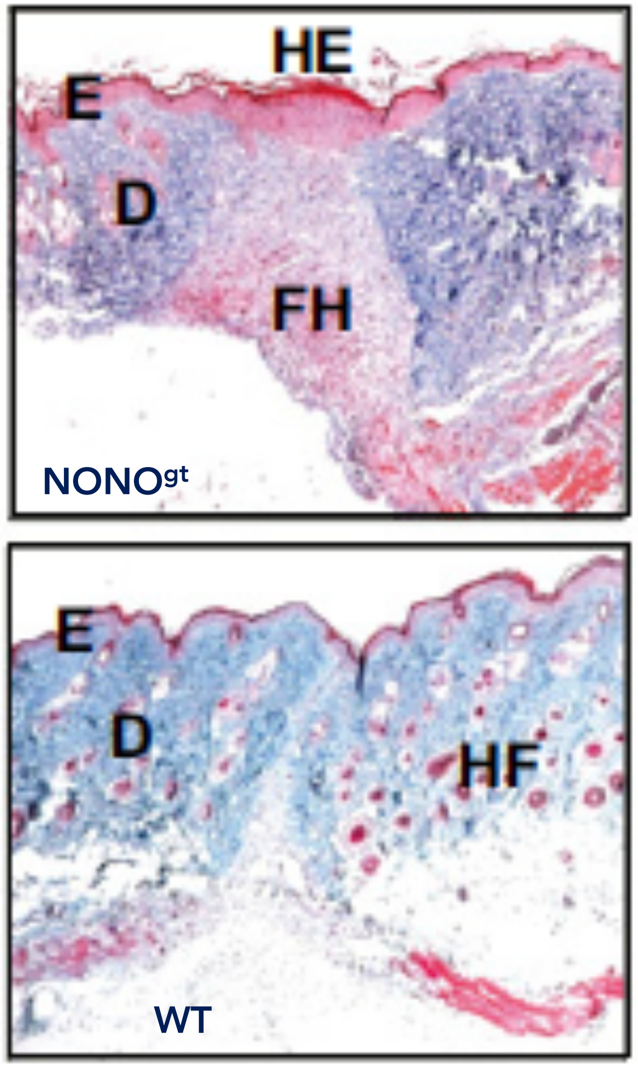

Kowalska et al, PNAS 110, 1592 (2013)

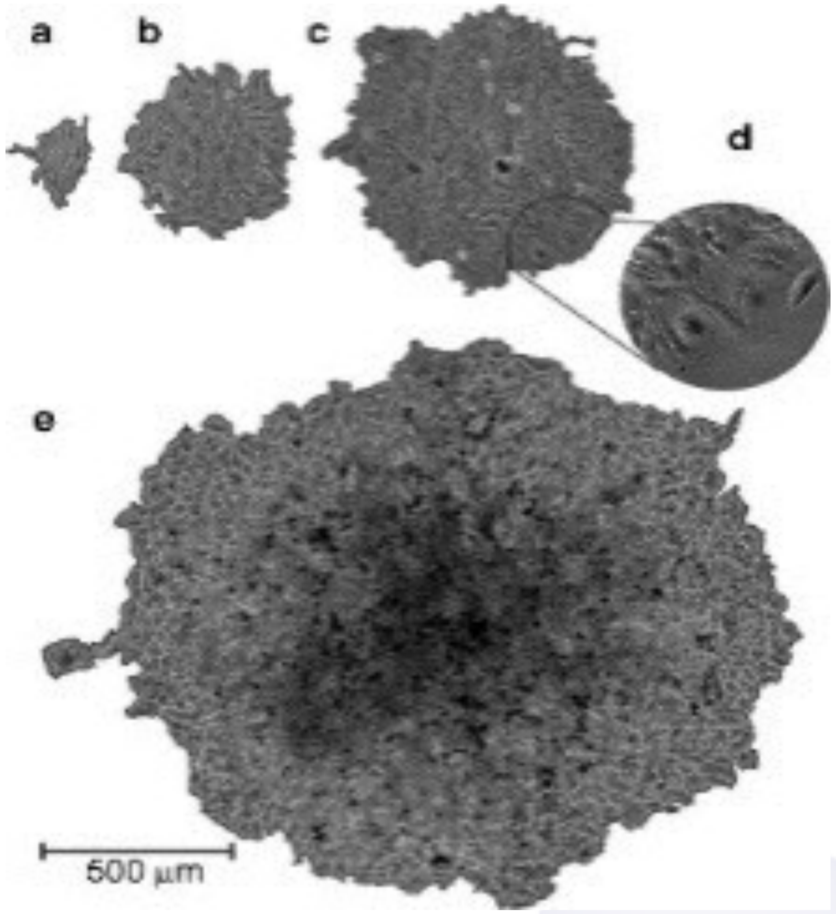

Muzzio et al., J. Biol. Phys. 40, 285 (2014)

Bacterial colony edges and epithelial cell fronts present universal scaling laws in morphology and dynamics characteristic of glassy systems

Vicsek et al., Phys. A 167, 315 (1990)
Fleury and Watanabe, C. R. Biologies 325, 571 (2002)
Callaghan et al., J. Stat. Phys. 122, 909 (2006)
Trepat et al., Soft Matter 4, 1750 (2008)
Bonachela et al., J. Stat. Phys. 144, 303 (2011)
Chiou et al., PLOS Comp. Biol. 8, e1002512 (2012)

Mapping forces in moving epithelial cell fronts

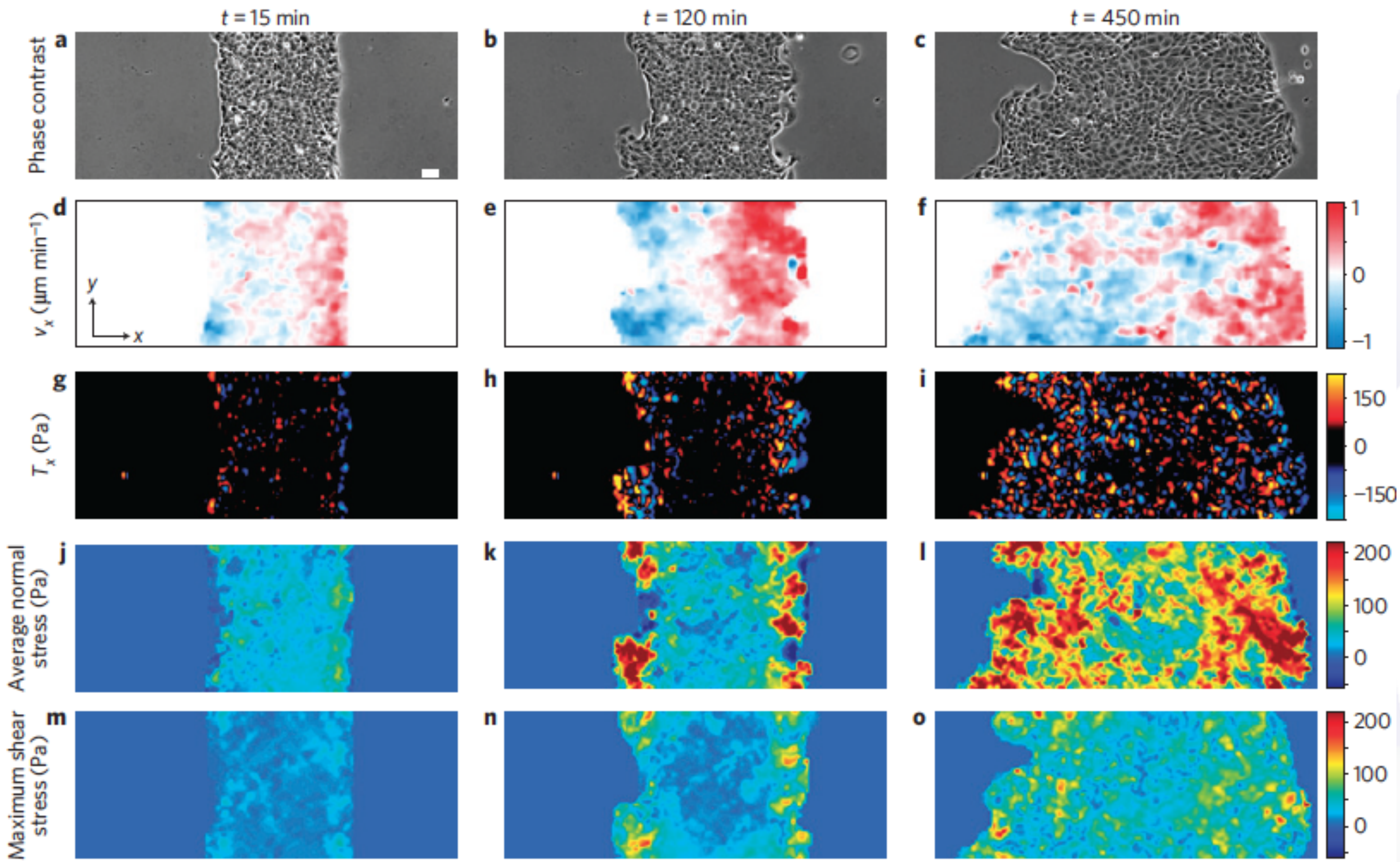

Trepat et al, Nat. Phys. 8, 628 (2012)

Dickinson et al., J. Math. Biol. 31, 563 (1993)
Callaghan et al., J. Stat. Phys. 122, 909 (2006)
Khain et al., J. Stat. Phys. 128, 209 (2007)

Trepat et al, Nat. Phys. 5, 426 (2009)
Vedula et al., Nat. Comm. 6, 6111 (2015)

Tembe et al., Nat. Mat. 10, 469 (2011)
Kim et al., Nat. Mat. 12, 856 (2013)

Controlling cell colony geometry and dynamics

Vicsek et al., Phys. A 167, 315 (1990)
Huergo et al., PRE 82, 031903 (2010)
Huergo et al., PRE 84, 021917 (2011)

Effects of sol vs gel medium

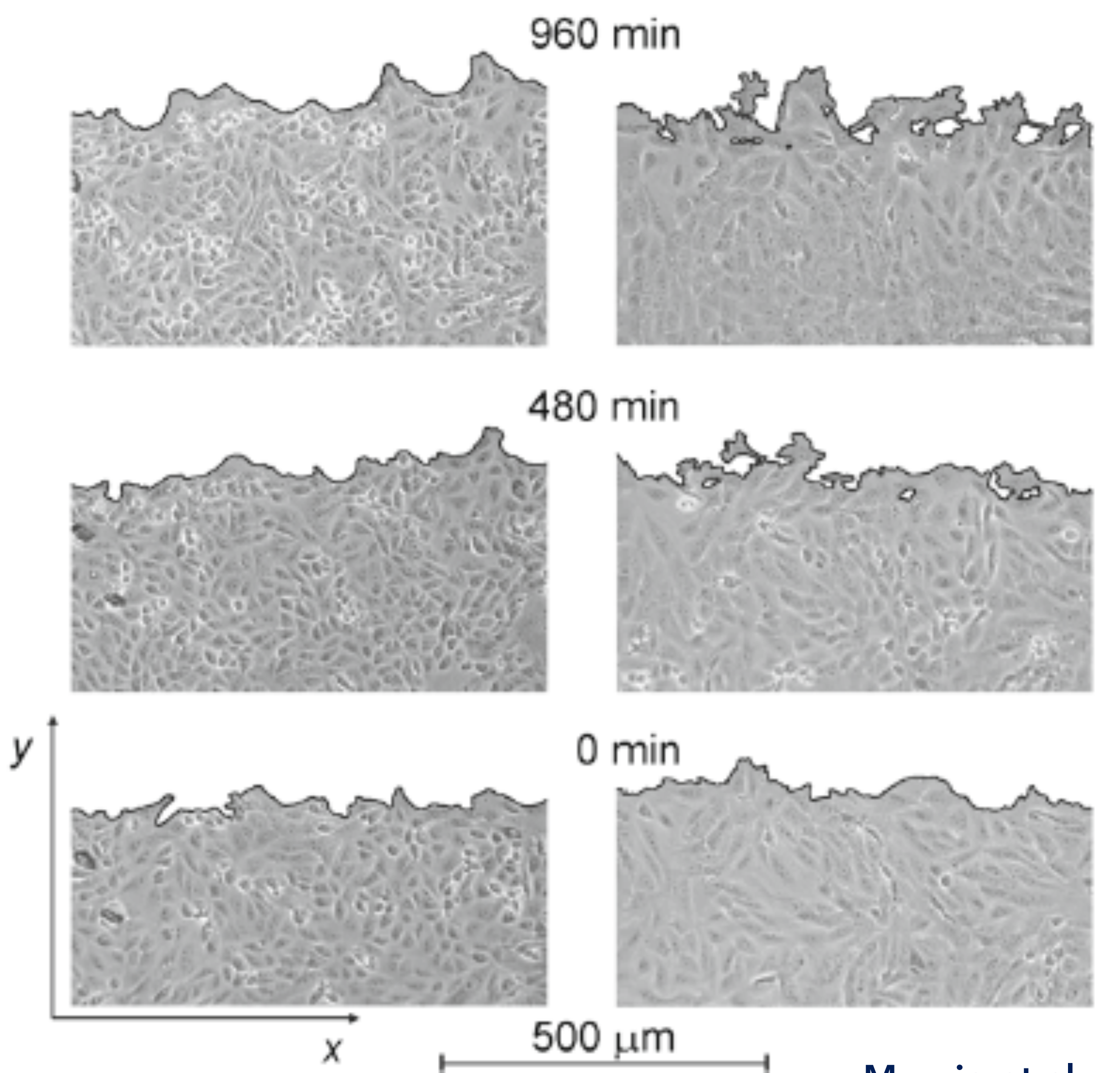

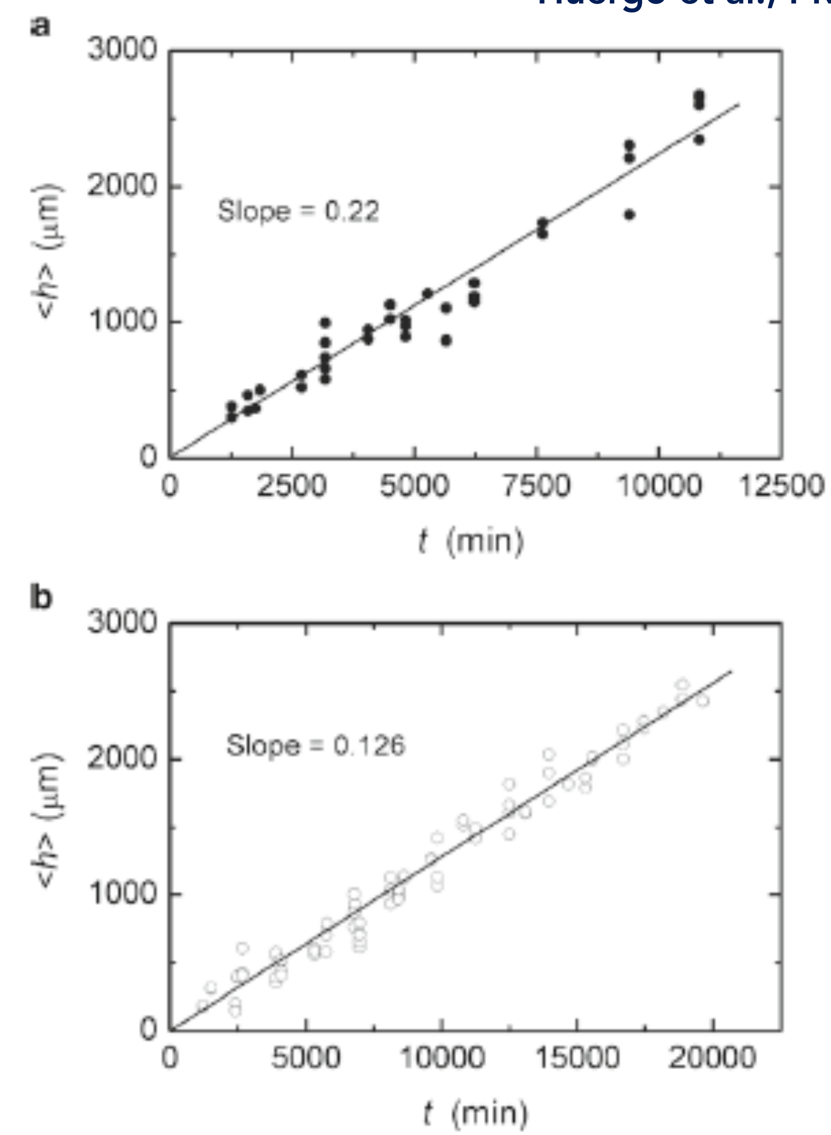

Muzzio et al., J. Biol. Phys 42, 477 (2016)

Can the "physics" (roughness scaling, dynamics) tell us useful information about the biological processes during front growth?

Can we correlate the roughness scaling and dynamic behaviour with specific interactions governing front behaviour from sub-cellular to multicellular level?

cell communication
in proliferating front

chemical

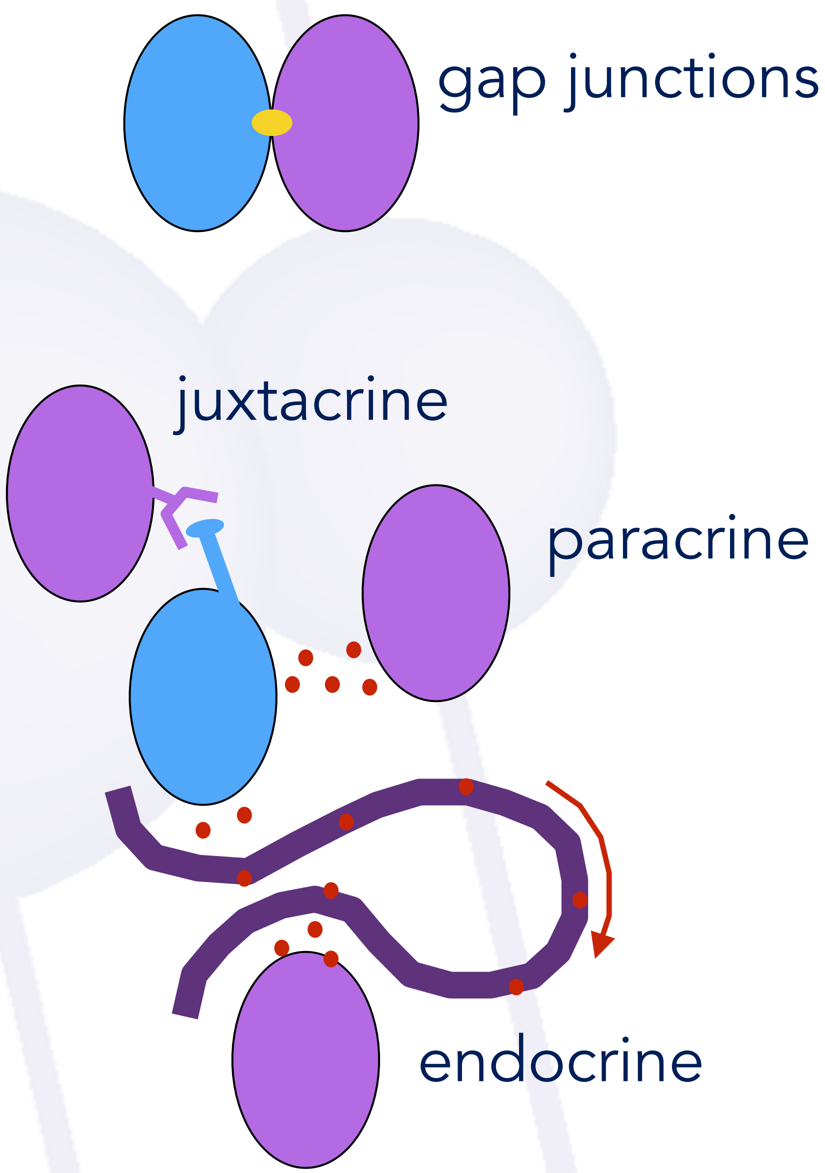

mechanical

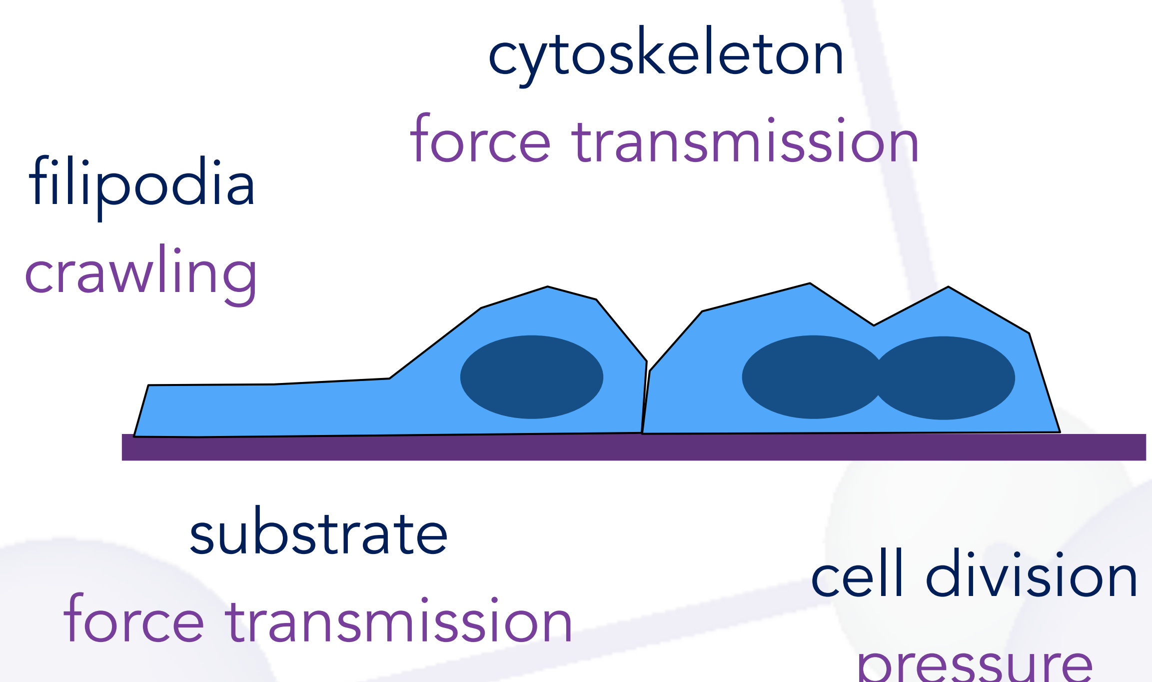

Can we correlate the roughness scaling and dynamic behaviour with specific interactions governing front behaviour from sub-cellular to multicellular level?

geometry

what is the roughness / scaling
- evolution
- lengthscale/regime crossovers

dynamics

what is the front displacement / speed
- global vs. local effects
- circadian/clock effects

inhibitor effects

cytochalasin B - cytoskeleton/lamellipodia/cytokinetics
colchicine - microtubules/spindle/mitosis
meclofenamic acid (MFA) - gap junctions
forskolin - cAMP levels

Experimental setup (physicists doing biology)

Benedikt Ziegler

Guillaume Rapin

scratch assay: silicon insert liftoff from plate of confluent epithelial RATI cells, ideal 1D front model system

cytoplasm and nuclei staining, GFP labelling

fluorescence microscopy of front at 4 hour intervals

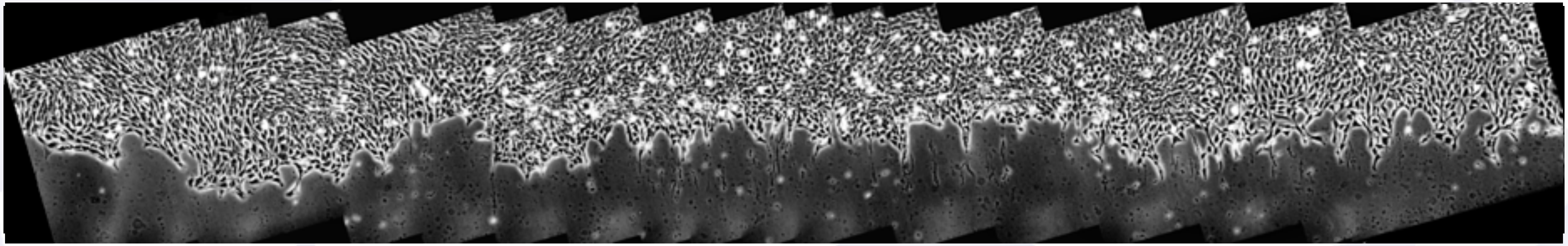

Measuring cell front roughness and dynamics

panorama of stitched front images 6.0 cm

identifying continuous front as largest subdomain

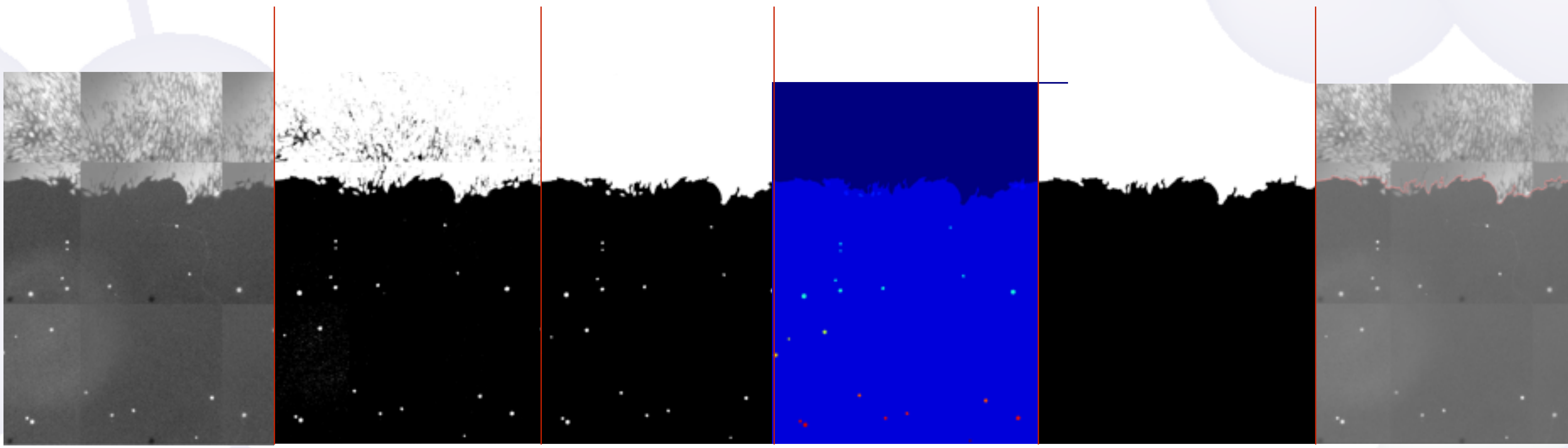

binarisation and noise cleaning

extracting front position for analysis

Front proliferation under control conditions


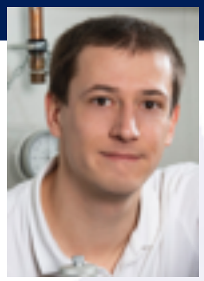

Nirvana Caballero

Guillaume Rapin

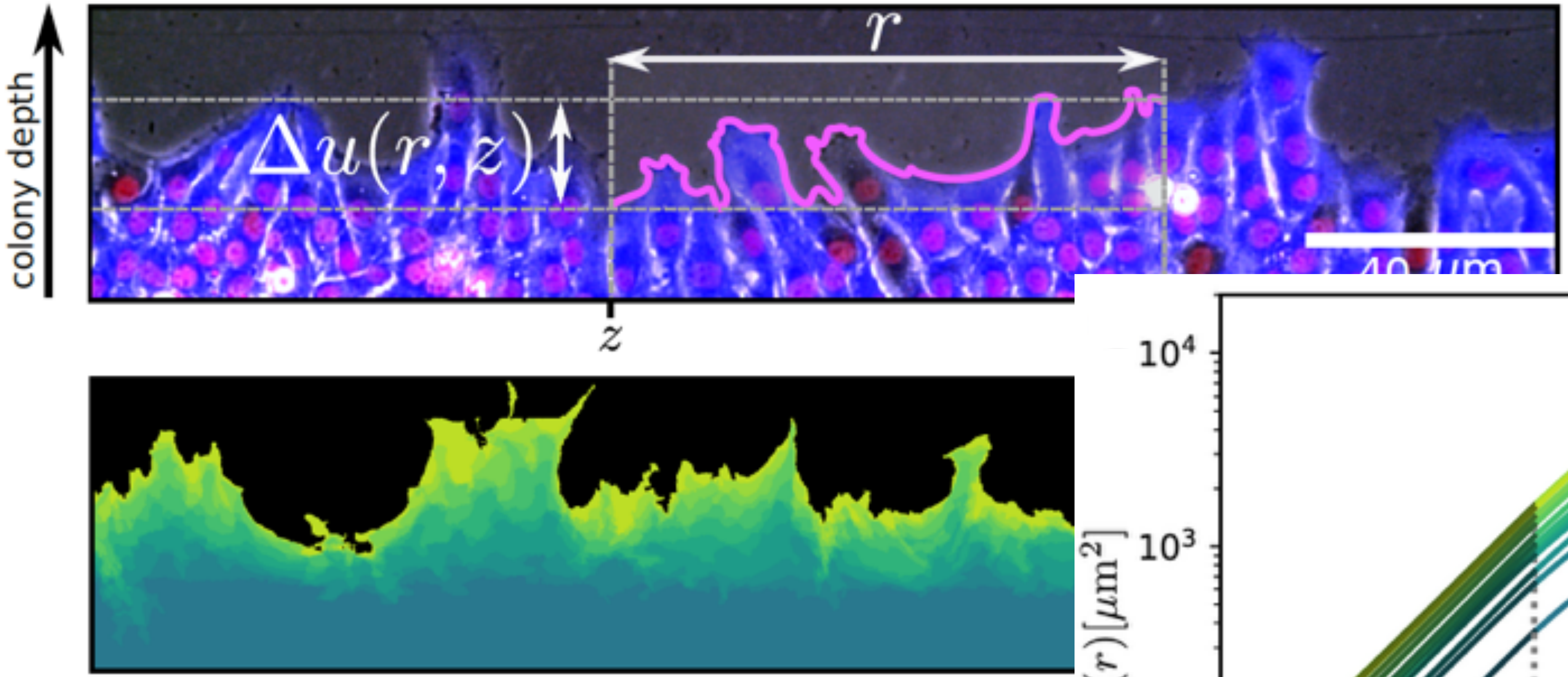

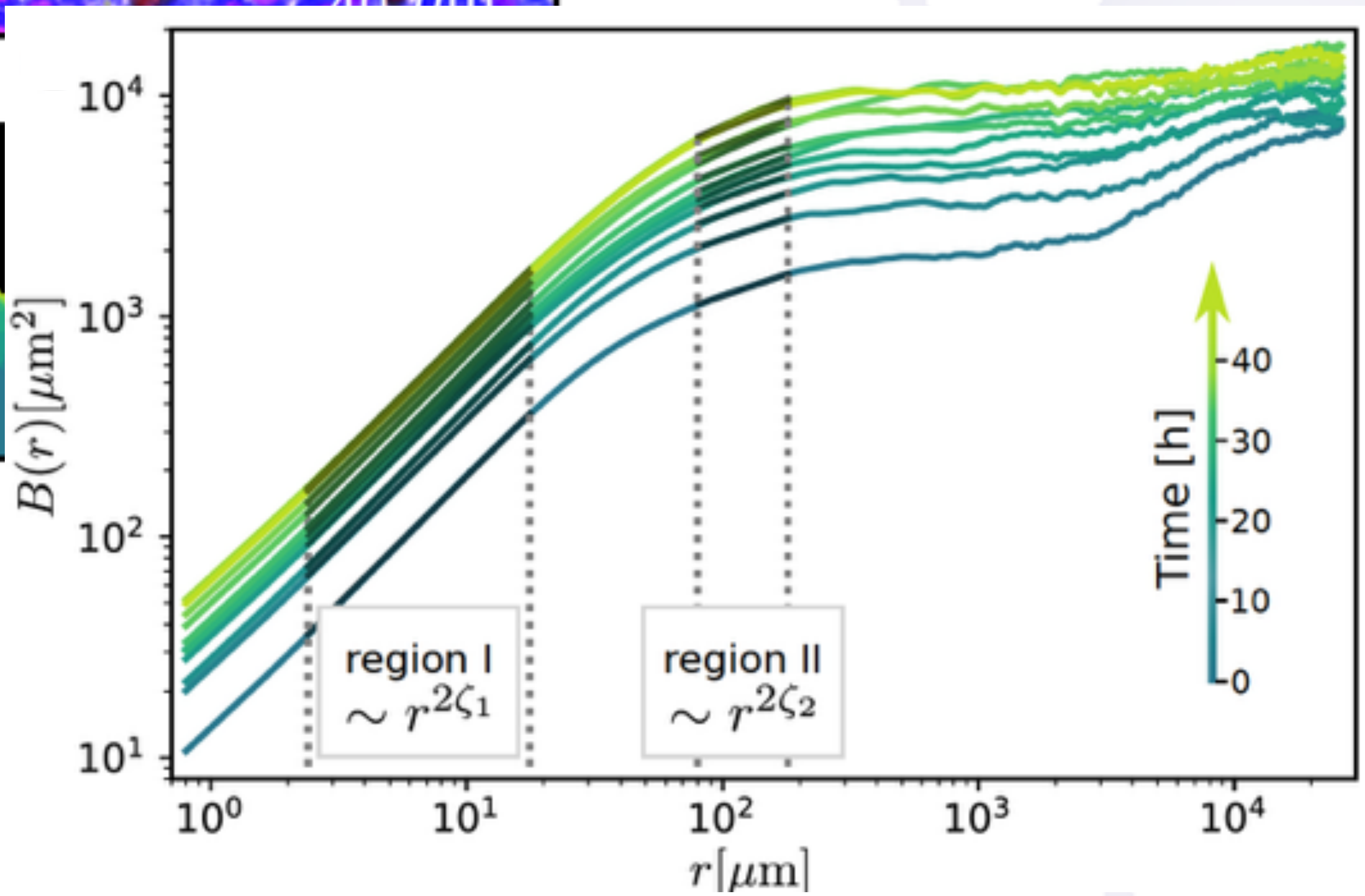

Rapin, Caballero et al. npj Sci. Rep. 11, 8869 (2021)

Saturation of front roughness at high length scales

Roughness scaling with ζ~0.2 at few-cell lengthscales

Roughness scaling with ζ~0.6 at sub-cell lengthscales

Targeting different interactions using inhibitors

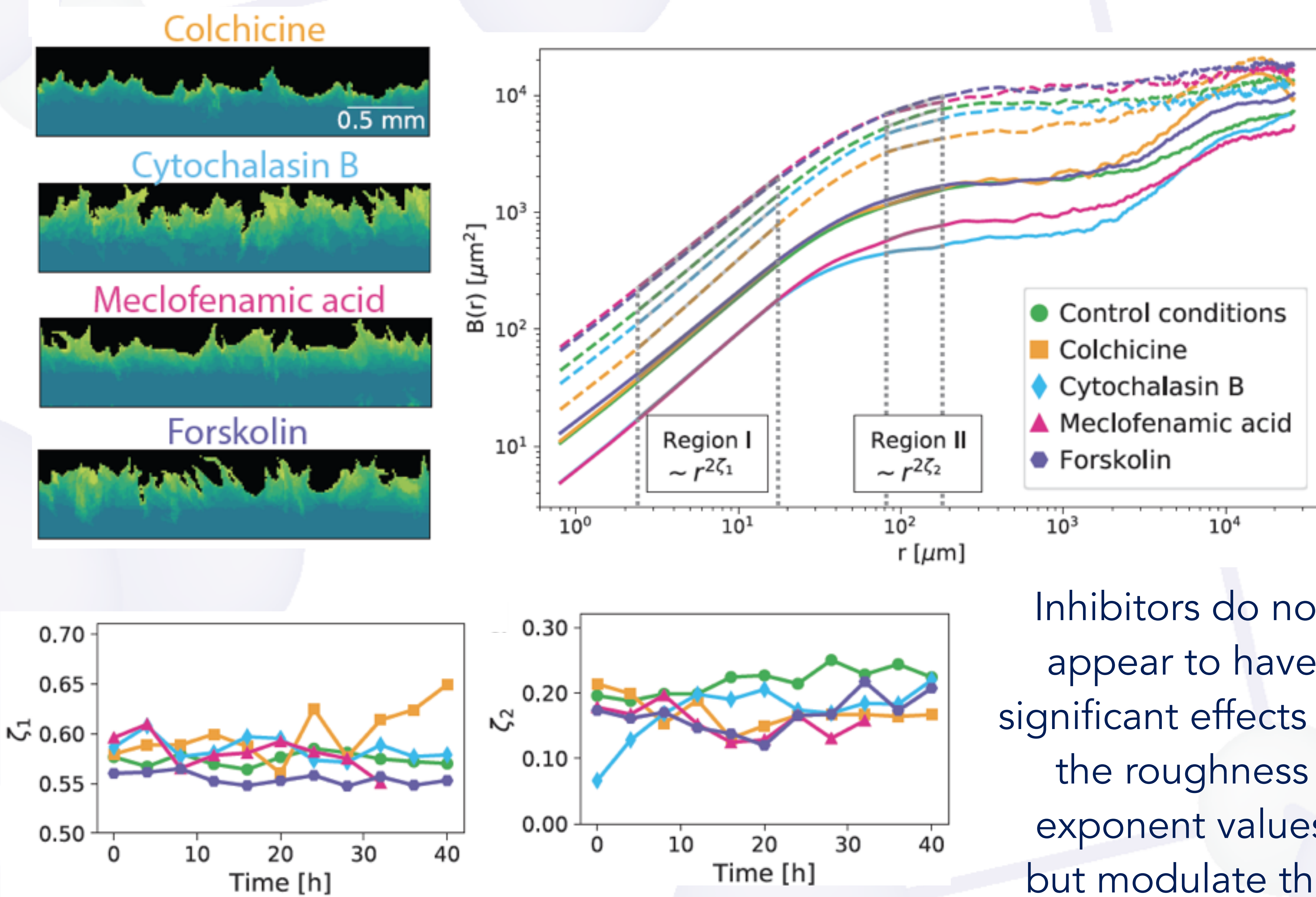

Inhibitors do not appear to have significant effects on the roughness exponent values but modulate the roughness itself

Rapin, Caballero et al. npj Sci. Rep. 11, 8869 (2021)

Targeting different interactions using inhibitors

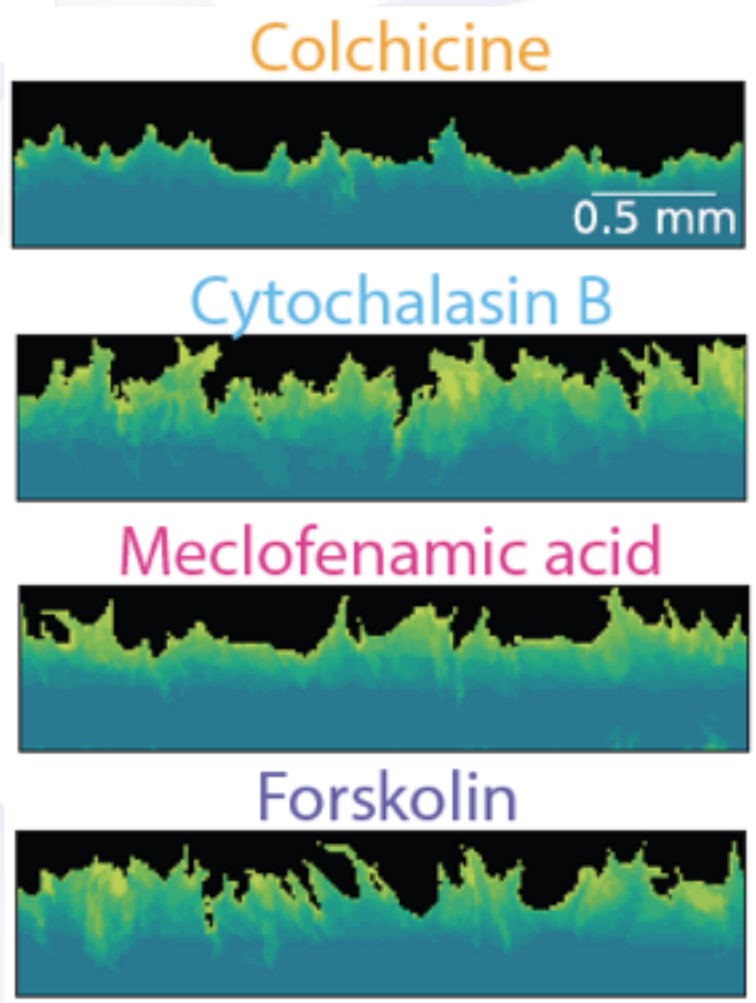

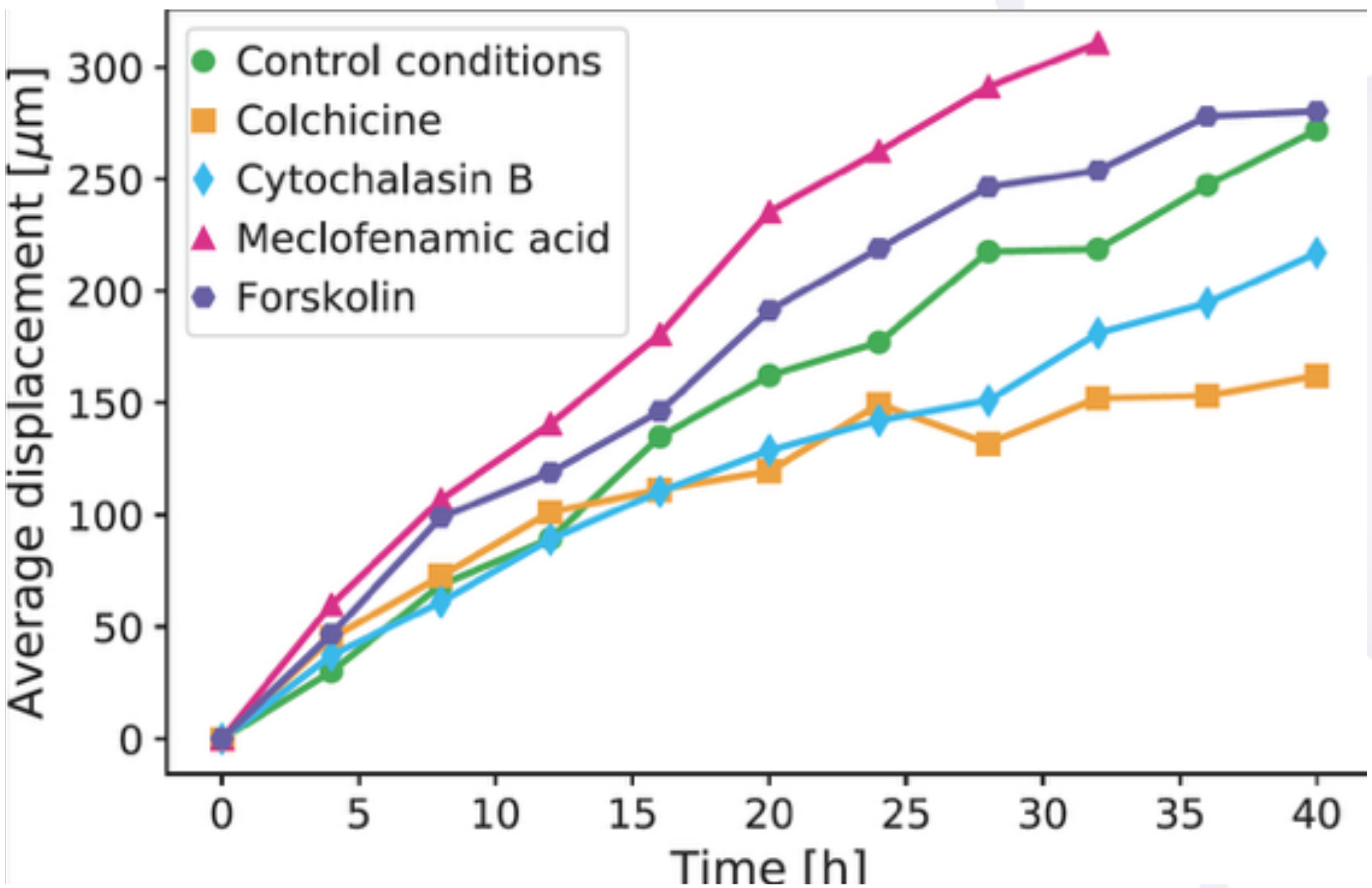

Inhibiting cell division by colchicine and disrupting cell motility/ cytoskeleton via cytochalasin-B significantly slows front motion and decreases roughening, while MFA inhibition of gap junctions and forskolin activation of c-AMP accelerate front motion and increase roughening

Rapin, Caballero et al. npj Sci. Rep. 11, 8869 (2021)

Comparison with numerical simulations

Aziza Merzouki Bastien Chopard

$$H = \sum_{\text{all cells } \alpha} \frac{1}{2} K_\alpha \left(A_\alpha - A_\alpha^0\right)^2 + \sum_{\text{all cells } \alpha} \frac{1}{2} \Gamma_\alpha L_\alpha^2 + \sum_{\text{all edges } e_{ij}} \Lambda_{i,j} L_{i,j}$$

Merzouki et al, Soft Matter 12, 4745 (2016)

epicells.unige.ch

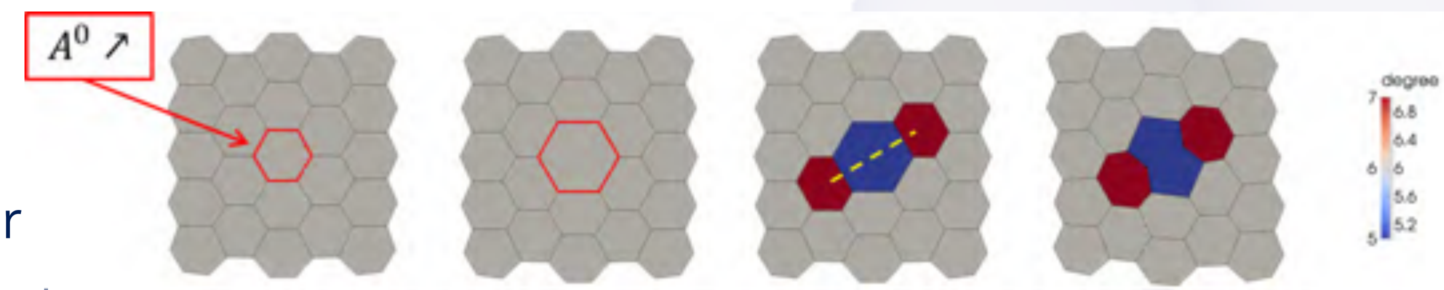

2D vertex model of confluent cell layer incorporates cell area elasticity, cell perimeter contractility and intercell line tension, developed to model mechanical properties of epithelial sheet

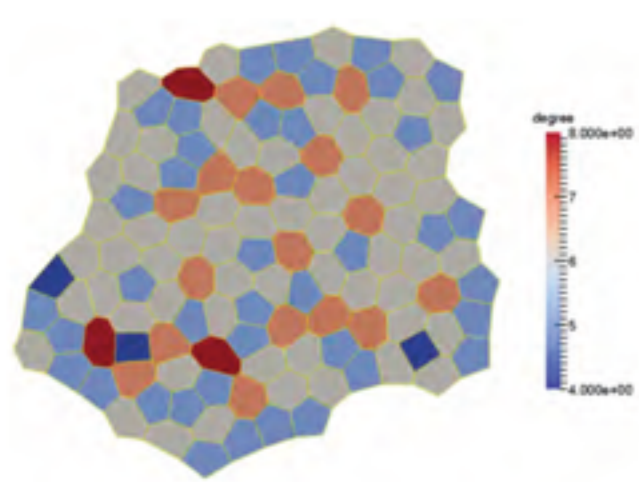

- set original vertex positions, minimise H
- probability of cell growth at adjustable rate up to fixed threshold
- probability of cell division based on random / oldest first/biggest first choice, always along shortest edge-edge axis
- adjustable elastic constraints set boundary conditions (wall vs. medium)
- miminise H, iterate

Comparison with numerical simulations

Iaroslav Gaponenko

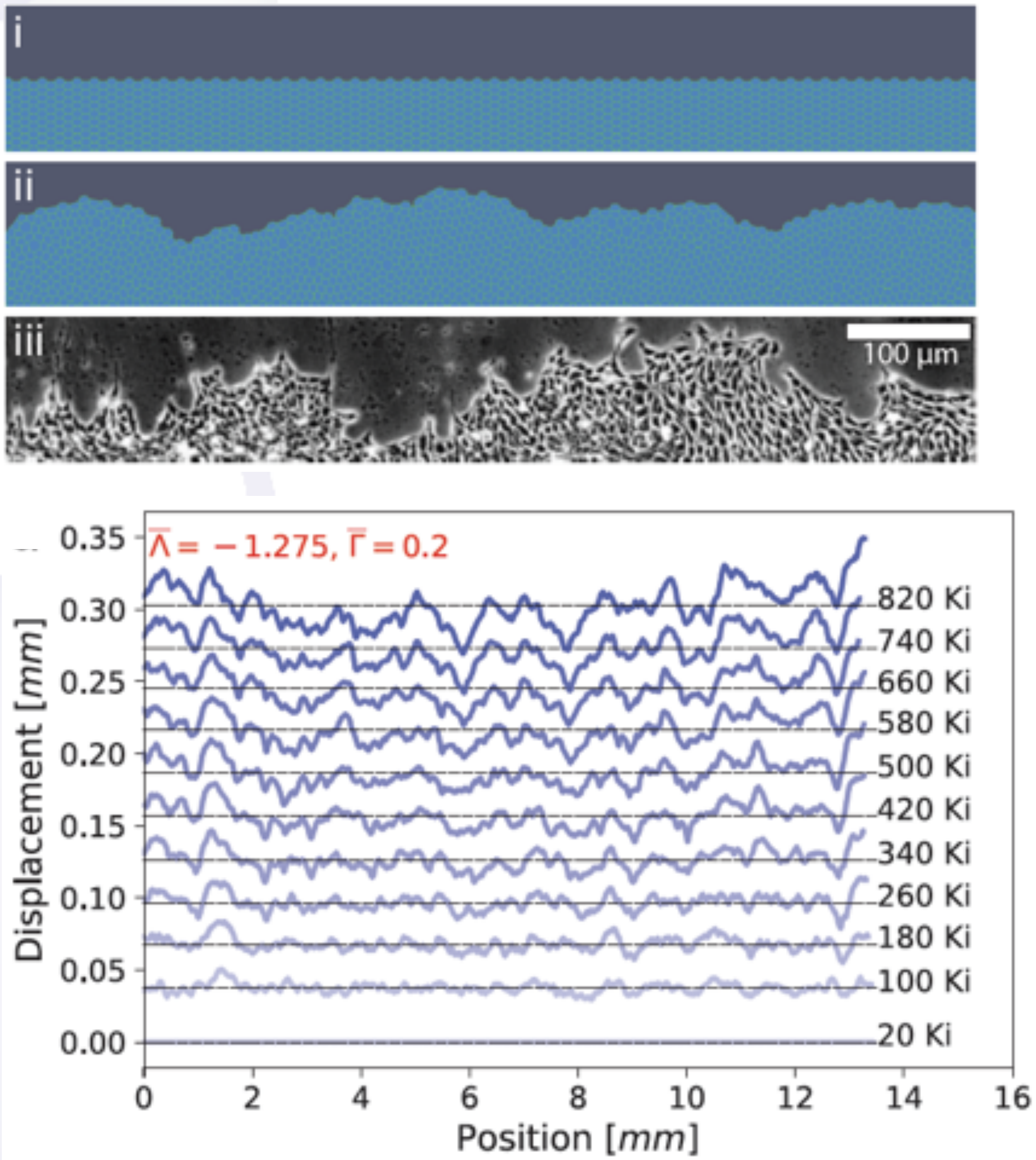

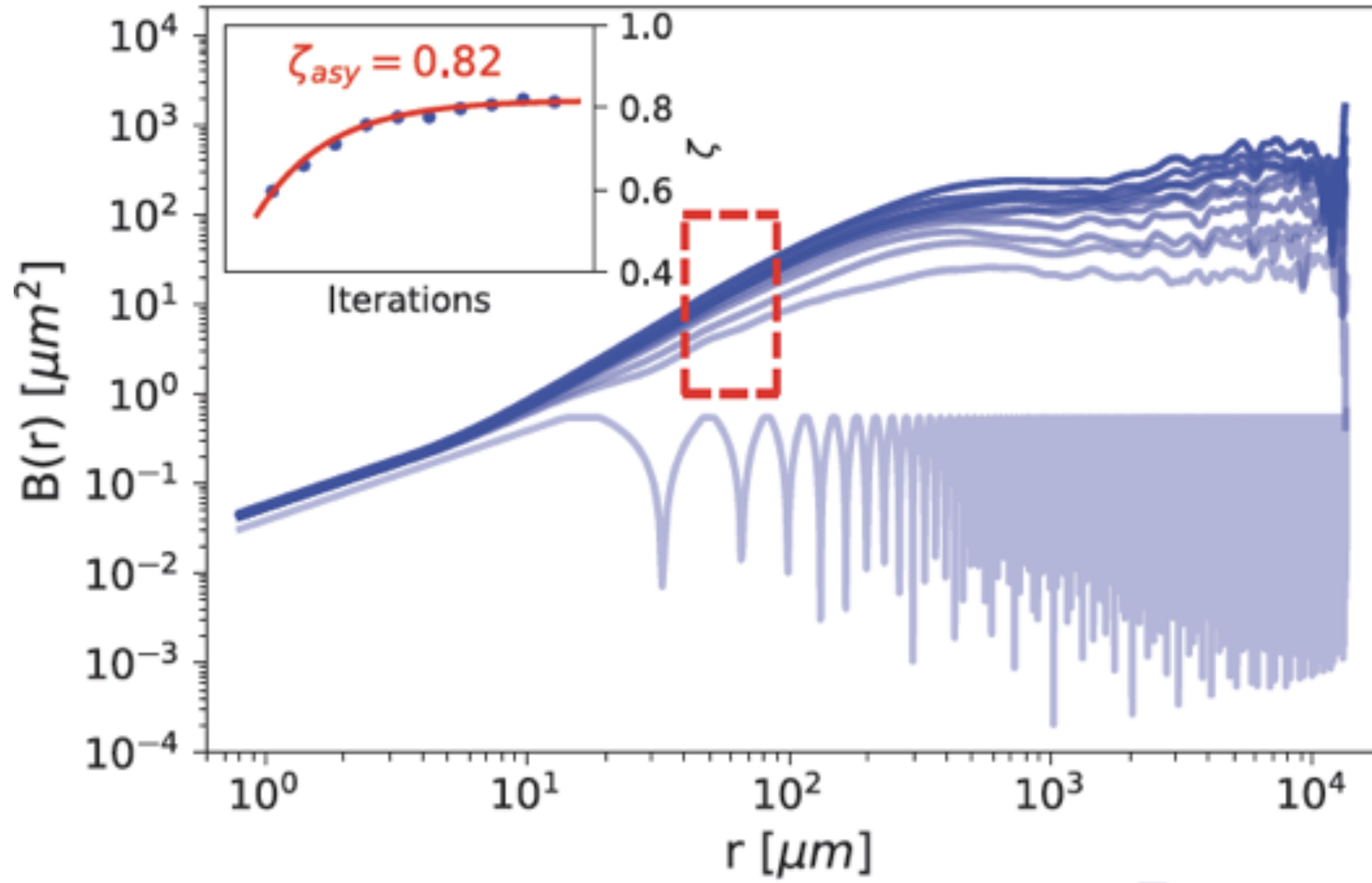

Tissue relevant information as well as cell front position and roughness can be extracted from each simulation run

Mapping out a roughness "phase diagram"

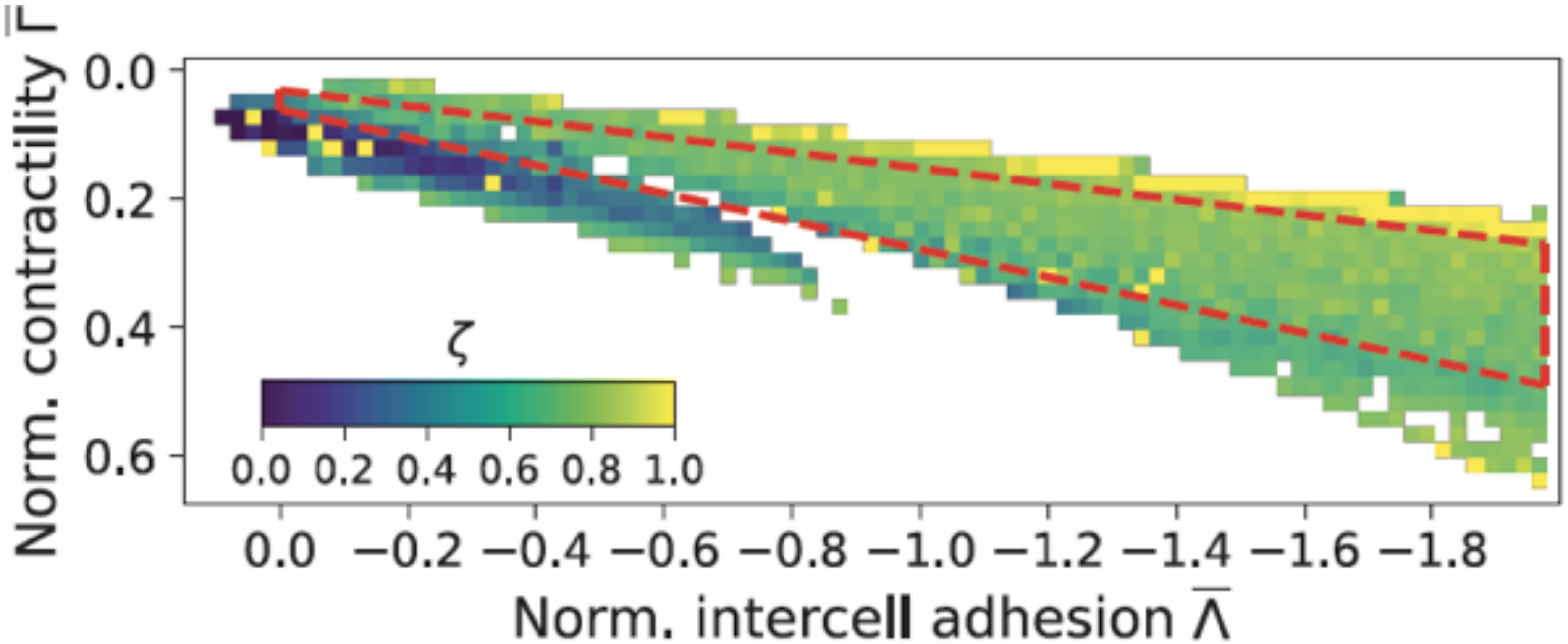

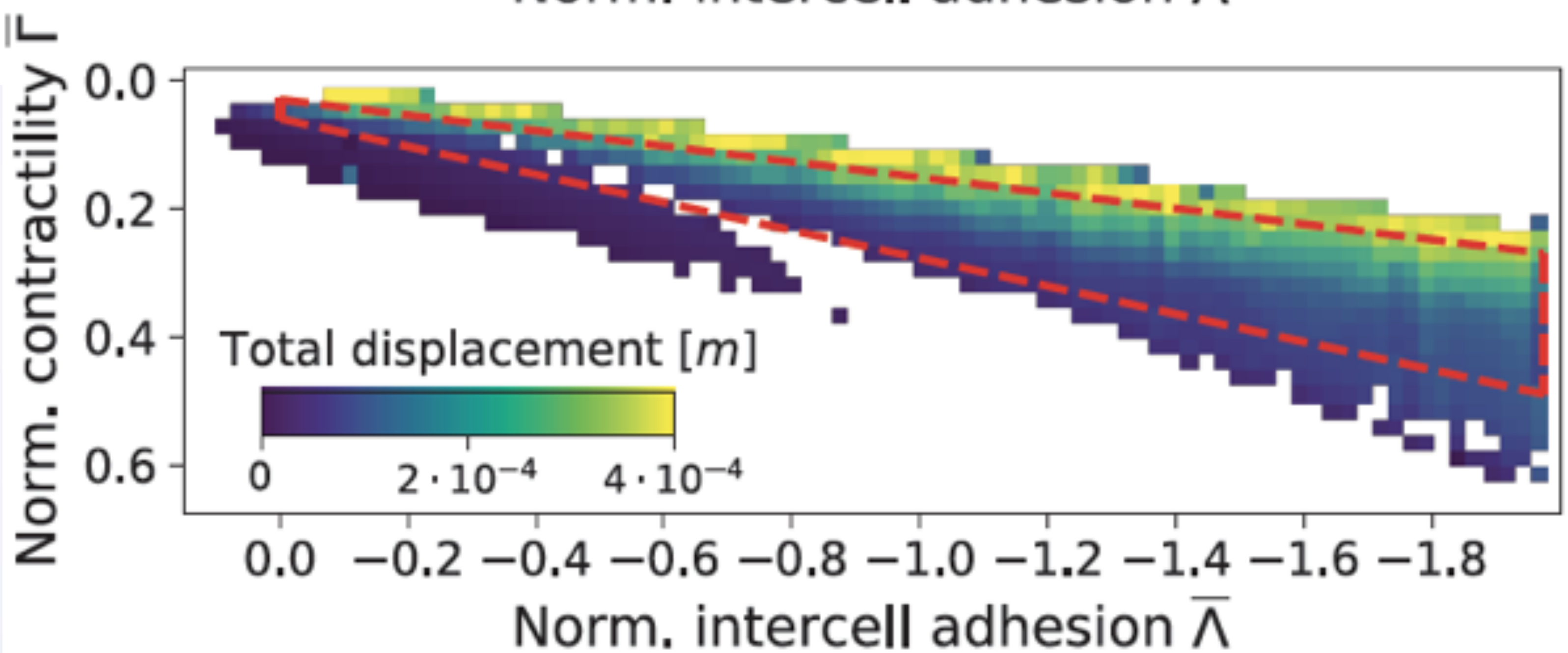

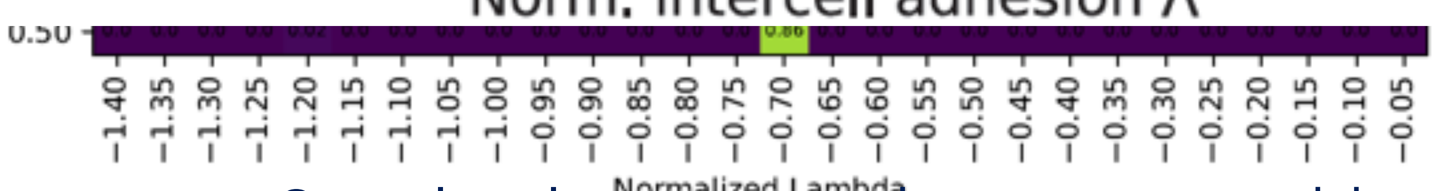

key parameter for simulation viability is ratio between normalised cell perimeter contractility and intercell line tension

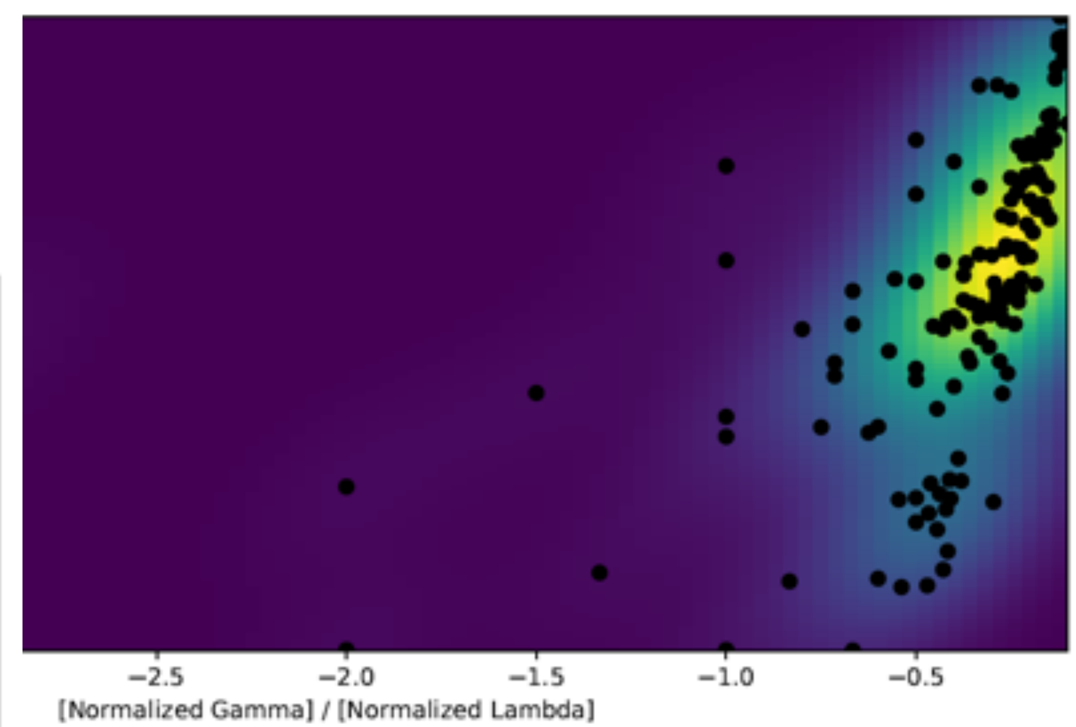

ζ values ranging from 0.4 - 1.0, with optimum of around 0.65

Rapin, Caballero et al. npj Sci. Rep. 11, 8869 (2021)

Simple elasticity and nearest neighbour interactions do not reproduce the lower zeta values /second power law scaling regime

Perspectives

- compare epithelial cell fronts from known pathological and prolific wound healing phenotypes

Spiny mice: *Acomys*

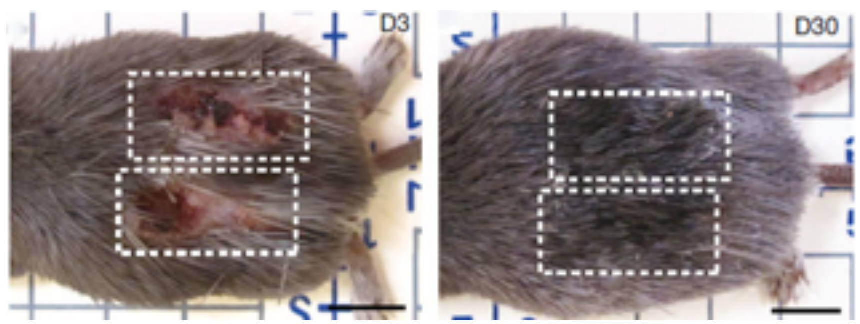

Seifert et al, Nat. 489, 561 (2012)

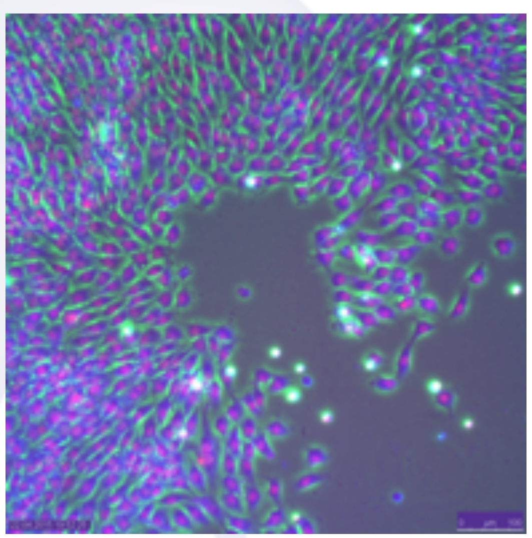

- explore effects of varying front curvature, cell size, clock gene mutations, substrate mechanics

- use measurements of cell front roughness to suggest potential interaction at play in wound healing mutations of unknown origin

Thank you !

Iaroslav Gaponenko
Philippe Tückmantel
Nirvana Caballero
Ralph Bulanadi

Kumara Cordero
Christian Weymann
Guillaume Rapin
Loïc Musy

Jill Guyonnet
Cédric Blaser

Benedikt Ziegler
Sophia Ehrensperger

Jambunathan Karthik, Lane W. Martin — UC Berkeley
Steven Brown — UniZH
Aziza Merzouki, Bastien Chopard — UniGE
Salia Cherifi-Hertel — IPCM, Strasbourg
Alejandro Kolton, Sebastian Bustingorry — Centro Atomico Bariloche
Thierry Giamarchi — UniGE

We gratefully acknowledge financial support from:

UNIVERSITÉ DE GENÈVE
FACULTÉ DES SCIENCES
Département de physique de la matière quantique

FNSNF

Fondation Ernst et Lucie Schmidheiny

Société Académique de Genève